


5-2-2018

Identification and spatiotemporal dynamics of tuna (Family: Scombridae; Tribe: Thunnini) early life stages in the oceanic Gulf of Mexico

Nina Pruzinsky

Nova Southeastern University, np720@nova.edu

Follow this and additional works at: https://nsuworks.nova.edu/occ_stuetd

 Part of the [Marine Biology Commons](#), and the [Oceanography and Atmospheric Sciences and Meteorology Commons](#)

Share Feedback About This Item

NSUWorks Citation

Nina Pruzinsky. 2018. *Identification and spatiotemporal dynamics of tuna (Family: Scombridae; Tribe: Thunnini) early life stages in the oceanic Gulf of Mexico*. Master's thesis. Nova Southeastern University. Retrieved from NSUWorks, . (472)
https://nsuworks.nova.edu/occ_stuetd/472.

This Thesis is brought to you by the HCNSO Student Work at NSUWorks. It has been accepted for inclusion in HCNSO Student Theses and Dissertations by an authorized administrator of NSUWorks. For more information, please contact nsuworks@nova.edu.

Thesis of
Nina Pruzinsky

Submitted in Partial Fulfillment of the Requirements for the Degree of

Master of Science

M.S. Marine Biology

Nova Southeastern University
Halmos College of Natural Sciences and Oceanography

May 2018

Approved:
Thesis Committee

Major Professor: Tracey Sutton

Committee Member: David Kerstetter

Committee Member: Jay Rooker

HALMOS COLLEGE OF NATURAL SCIENCES AND OCEANOGRAPHY

IDENTIFICATION AND SPATIOTEMPORAL DYNAMICS OF TUNA (FAMILY:
SCOMBRIDAE; TRIBE: THUNNINI) EARLY LIFE STAGES IN THE OCEANIC
GULF OF MEXICO

By

Nina M. Pruzinsky

Submitted to the Faculty of
Halmos College of Natural Sciences and Oceanography
in partial fulfillment of the requirements for
the degree of Master of Science with a specialty in:

Marine Biology

Nova Southeastern University

May 2, 2018

Thesis of
Nina M. Pruzinsky

Submitted in Partial Fulfillment of the Requirements for the Degree of

Masters of Science:
Marine Biology

Nova Southeastern University
Halmos College of Natural Sciences and Oceanography

May 2, 2018

Approved:

Thesis Committee

Major Professor : _____

Tracey Sutton, Ph.D.

Committee Member : _____

David Kerstetter, Ph.D.

Committee Member : _____

Jay Rooker, Ph.D.

ABSTRACT

Fishes within the family Scombridae (i.e. tunas, mackerels and bonitos) are of high ecological and economic value, as they are heavily targeted by commercial and recreational fisheries. In coastal and open-ocean environments, adults are high-level predators, while larvae and juveniles serve as prey for numerous species. Much is known about the distribution and abundance of adult tunas, but high taxonomic uncertainty and limited knowledge regarding the distributional patterns of larval and juvenile tunas have led to an “operational taxonomic unit” gap in our understanding of tuna ecology. Scombrids were collected across the Gulf of Mexico (GoM, hereafter) during seven research cruises from 2010-2011, as part of the NOAA-supported Offshore Nekton Sampling and Analysis Program, and during five research cruises from 2015-2017, as a part of the GOMRI-supported Deep Pelagic Nekton Dynamics of the Gulf of Mexico Consortium. In this thesis, species composition, distribution, and abundance of tunas collected from the surface to 1500 m depth are characterized in relation to depth, time of year, and physical oceanographic features. A synthesis of the morphological characteristics used to identify the taxonomically challenging larval and juvenile stages of tunas is presented, along with length-weight regressions to fill the data gap on the growth patterns of these early life stages. A total of 945 scombrid specimens were collected, representing 11 of the 16 species that occur in the GoM. The dominant species included: *Euthynnus alletteratus* (Little Tunny), *Thunnus atlanticus* (Blackfin Tuna), *Auxis thazard* (Frigate Mackerel), and *Katsuwonus pelamis* (Skipjack Tuna). Evidence of sampling gear selectivity was observed, with a MOCNESS (rectangular, research-sized trawl) collecting larvae predominantly, and a large, high-speed rope trawl catching only juveniles. Scombrids were collected primarily in the upper 200 m of the water column. Species-specific environmental preferences and seasonality were identified as the main drivers of tuna spatial distributions across the epipelagic GoM. Integrating aspects of scombrid ecology in neritic and oceanic environments improves management and conservation efforts for this highly important taxon.

Keywords: early life stages, oceanic Gulf of Mexico, tuna ecology

ACKNOWLEDGEMENTS

I would like to thank my major advisor, Dr. Tracey Sutton, for his wisdom, knowledge, patience, and much needed humor! Joining Dr. Sutton's Oceanic Ecology Lab as a research assistant was a great decision. Through lab and thesis work, I was spoiled by learning about the processes and organisms not only in the deep sea, but at the surface as well. Working for and learning from Dr. Sutton on an everyday basis was an incredible and fortunate experience.

I would like to thank my other committee members, Drs. Dave Kerstetter and Jay Rooker, for providing their insight and expertise on tuna throughout my thesis project. I want to extend an additional thanks to Dr. Rosanna Milligan for not only keeping me sane in our office on a daily basis, but for also increasing my knowledge on statistics. Thank you, April Cook, for teaching me all of the ins and outs of running a database. Also, a special thanks to Aki Shiroza for his generosity with his time and knowledge on identifying larval tuna.

I would like to thank my other labmates in the Oceanic Ecology Lab, both past and present: Kendall Lord, Alex Marks, Mike Novotny, Matt Woodstock, Natalie Slayden, Drew Mertzlufft, and Kris Ramkissoon. We have had endless laughs throughout the years both in the lab and at conferences. You are like a second family to me. Also, thanks to Mr. Doug Dahms, my high school AP Ecology teacher and friend, who introduced me to the wonders of the ocean and peaked my interest in marine biology.

Lastly, I would like to thank my family for their continuous love, support, and encouragement as I worked toward becoming a marine biologist. Thank you to my parents for believing in me. I could not have done this without you.

This project was supported by Gulf of Mexico Research Initiative (GOMRI) through the DEEPEND Consortium. Additional support was provided by: a Research Grant from the Southern Florida Chapter of the Explorers Club, Inc., a Graduate Student Travel Grant from the American Society of Ichthyologists and Herpetologists, and a Pan Student Government Association Professional Development Grant from Nova Southeastern University.

TABLE OF CONTENTS

ABSTRACT.....	i
ACKNOWLEDGEMENTS.....	ii
TABLE OF CONTENTS.....	iii
LIST OF TABLES.....	v
LIST OF FIGURES.....	vii
1. INTRODUCTION.....	1
1.1. Global importance of scombrid fishes.....	1
1.2. Systematics of the Family Scombridae.....	3
1.3. Scombrid biology and ecology.....	4
1.4. The biophysical milieu: major oceanographic features of the Gulf of Mexico.....	6
1.5. Statement of problem.....	9
1.6. Objectives.....	10
2. METHODS.....	12
2.1. Scombrid sample collection and processing.....	12
2.1.1. MOCNESS sampling, 2011 and 2015-2017.....	12
2.1.2. High-speed rope trawl sampling, 2010-2011.....	15
2.2. Morphological and genetic taxonomy.....	16
2.3. Species composition and spatiotemporal distribution analyses.....	18
2.3.1. Generalized additive models/presence-absence models.....	20
3. RESULTS.....	22
3.1. Larval and juvenile scombrid taxonomy.....	22
3.1.1. Genetic analyses.....	22
3.1.2. Morphological analyses.....	25
3.2. Larval and juvenile scombrids faunal composition and ecology.....	48
3.2.1. Assemblage structure.....	48
3.3. Length-weight regressions of larval and juvenile scombrids in the northern Gulf of Mexico.....	54
3.4. Variation in the morphometrics of juvenile <i>Euthynnus alletteratus</i> and <i>Thunnus atlanticus</i>	56
3.5. Spatiotemporal distributions of larval and juvenile scombrid fishes in the northern Gulf of Mexico.....	59
3.5.1. Vertical distributions and diel catch rates.....	59

3.5.2. Horizontal distributions of larval and juvenile scombrids in the northern Gulf of Mexico.....	67
3.5.3. Seasonal distributions.....	92
4. DISCUSSION.....	97
4.1. Larval and juvenile scombrid taxonomy.....	97
4.1.1. Genetic analyses.....	97
4.1.2. Morphological analyses.....	98
4.2. Larval and juvenile scombrids faunal composition and ecology.....	102
4.2.1. Assemblage structure.....	102
4.3. Length-weight regressions of larval and juvenile scombrids in the northern Gulf of Mexico.....	106
4.4. Variation in the morphometrics of juvenile <i>Euthynnus alletteratus</i> and <i>Thunnus atlanticus</i>	108
4.5. Spatiotemporal distributions of larval and juvenile scombrid fishes in the northern Gulf of Mexico.....	110
4.5.1. Variations in vertical distributions.....	110
4.5.2. Diel catch rates.....	111
4.5.3. Seasonal and horizontal distributions of larval and juvenile scombrids in the northern Gulf of Mexico.....	112
4.6. Caveats and suggestions for future research.....	121
5. CONCLUSION.....	123
APPENDIX.....	125
REFERENCES.....	132

LIST OF TABLES

Table 1. Summary of the seven surveys conducted by the ONSAP (three M/V <i>Meg Skansi</i> and four FRV <i>Pisces</i> surveys) and the five surveys by the DEEPEND Consortium (R/V <i>Point Sur</i>) in the GoM; MOC10 = 10-m ² MOCNESS, HSRT = High-speed rope trawl. No. of Samples indicates the amount of quantitative tows per cruise. The gray line designates the separation of gear types.....	16
Table 2. Summary of the life stage and size range of the genetically identified specimens separated by cruise series.....	23
Table 3. Meristics of genetically identified juvenile scombrids.....	24
Table 4. Summary of morphometric ratios for genetically identified specimens. The ratios (presented as percentages) were compared to standard length (mm) and are presented by size class (0-50, 50-100, 100-150, and 150-200 mm SL). N represents the number of specimens collected for each species. Informative ratios are highlighted.....	26
Table 5. Summary of morphometric ratios for genetically identified specimens. The ratios (presented as percentages) were compared to head length (mm) and are presented by size class (0-10, 10-20, 20-30, 30-40, 40-50 mm HL). N represents the number of specimens collected for each species. Informative ratios are highlighted.....	27
Table 6. Quick reference chart for identifying larvae in the Tribe Thunnini.....	28
Table 7. Diagnostic key for identifying genera/species in the Tribe Thunnini using known meristics.....	28
Table 8. Standardized abundance (No. ind. 10 ⁻⁶ m ⁻³), rank, and frequency of occurrence (F _O) of each species collected during the three cruise series. F _O is listed as percent of trawls in which taxon was collected. Dashes indicate no collections.....	50
Table 9. Counts and size range of scombrid specimens caught during the MOCNESS 2011 survey. Dashes indicate no collections.....	51
Table 10. Counts and size range of scombrid specimens caught during the MOCNESS 2015-2017 survey. Dashes indicate no collections.....	52
Table 11. Counts and size range of scombrid specimens caught during the high-speed rope trawl 2010-2011 survey. Dashes indicate no collections.....	53
Table 12. Sampling effort (number of tows) based on day (D) vs. night (N) sampling, depth (m), and cruise series.....	59
Table 13. Standardized abundance (No. ind. 10 ⁻⁶ m ⁻³) and frequency of occurrence (F _O) of scombrid larvae and juveniles collected in the epipelagic zone of the GoM using a MOCNESS trawl. F _O is listed as percent of trawls in which a taxon was collected. Samples were separated based on day (D) and night (N) sampling. Dashes indicate no collections.....	65

Table 14. AIC values and degrees of freedom (df) of each GAM tested for the family Scombridae, and the species *Euthynnus alletteratus*, *Thunnus atlanticus*, and *Auxis thazard*. The best models with the lowest AIC score are bolded..... 75

Table 15. AIC values of GAMs with dropping one explanatory variable for (a) Scombridae, (b) *Euthynnus alletteratus*, (c) *Thunnus atlanticus*, and (d) *Auxis thazard*. The full models' AIC values are highlighted in gray and are referred to as "none." Important explanatory variables are bolded 78

Table 16. AIC values of the presence-absence models with dropping one explanatory variable for (a) Scombridae, (b) *Euthynnus alletteratus*, (c) *Thunnus atlanticus*, and (d) *Auxis thazard*. The full model's AIC values are highlighted in gray and are referred to as "none." Important explanatory variables are bolded 82

LIST OF FIGURES

Figure 1. NOAA Gulf of Mexico Data Atlas map of the essential fish habitats for the highly migratory <i>Thunnus thynnus</i> (Cooper 2011), emphasizing the lack of knowledge on juvenile distributions.....	11
Figure 2. MOCNESS 2011 stations sampled aboard the M/V <i>Meg Skansi</i>	13
Figure 3. MOCNESS 2015-2017 stations and cruise tracks for cruises (a) DP01, (b) DP02, (c) DP03, (d) DP04, and (e) DP05, relative to the SEAMAP/ONSAP station grid. Stations were sampled aboard the R/V <i>Point Sur</i>	14
Figure 4. High-speed rope trawl 2010-2011 stations sampled aboard the FRV <i>Pisces</i>	15
Figure 5. Identifiable characteristics of larval scombrids. Features include: (A-B) snout length, (B-C) eye diameter, (A-D) head, (D-E) trunk, (D-G) body, (E-F) tail, and (F-G) caudal peduncle (edited from Nishikawa & Rimmer 1987).	17
Figure 6. Morphometrics used to analyze the genetically identified juvenile specimens. Black represents features that were measured, blue represents features that were counted, and red represents features that were both measured and counted.	18
Figure 7. Correlation of standard length (SL) and head length (HL) from genetically identified juveniles.....	25
Figure 8. Images of (a) larval <i>Auxis rochei</i> , (b) juvenile <i>Auxis rochei</i> , (c) larval <i>Auxis thazard</i> , and (d) juvenile <i>Auxis thazard</i>	30
Figure 9. Ratio of interdorsal length to head length vs. head length for all genetically identified juvenile specimens.....	31
Figure 10. Ratio of interdorsal length to first dorsal length vs. standard length for all genetically identified juvenile specimens.	31
Figure 11. Ratio of interdorsal length to standard length vs. standard length for all genetically identified juvenile specimens.	32
Figure 12. Ratio of upper jaw length to head length vs. head length for all genetically identified juvenile specimens.....	32
Figure 13. Images of (a) larval and (b and c) juvenile <i>Euthynnus alletteratus</i>	34
Figure 14. Ratio of eye diameter to snout length vs. standard length for genetically identified juvenile specimens, including <i>Acanthocybium solandri</i> , <i>Euthynnus alletteratus</i> , and all <i>Thunnus</i> spp.	34
Figure 15. Ratio of eye diameter to head length vs. head length for genetically identified juvenile specimens, including <i>Acanthocybium solandri</i> , <i>Euthynnus alletteratus</i> , and all <i>Thunnus</i> spp.	35

Figure 16. Ratio of snout length to head length vs. head length for genetically identified juvenile specimens, including <i>Acanthocybium solandri</i> , <i>Euthynnus alletteratus</i> , and all <i>Thunnus</i> spp.	35
Figure 17. Images of (a) larval and (b) juvenile <i>Katsuwonus pelamis</i>	37
Figure 18. Images of (a) larval and (b) juvenile <i>Thunnus albacares</i>	39
Figure 19. Images of (a) larval, and (b and c) juvenile <i>Thunnus atlanticus</i>	41
Figure 20. The (a) left and (b) right lobes of a liver from a genetically identified <i>Thunnus atlanticus</i> specimen (42.5 mm SL), preserved in 99% ethanol.	41
Figure 21. Images of (a and b) larval and (c) juvenile <i>Thunnus thynnus</i>	43
Figure 22. Image of a larval <i>Sarda sarda</i>	44
Figure 23. Image of a juvenile <i>Scomber colias</i>	45
Figure 24. Images of (a) larval and (b) juvenile <i>Acanthocybium solandri</i>	46
Figure 25. Image of a larval <i>Scomberomorus cavalla</i>	47
Figure 26. Standardized abundances from the three cruise series.	49
Figure 27. Size-frequency plot of larval and juvenile scombrids, color-coded by cruise series.	49
Figure 28. Length-weight regressions of all species/taxa collected during the three cruise series.	55
Figure 29. Ratio of head length (HL) to standard length (SL) vs. standard length for genetically identified juvenile <i>Euthynnus alletteratus</i> and <i>Thunnus atlanticus</i> specimens.	57
Figure 30. Ratio of snout length (SN) to head length (HL) vs. head length for genetically identified juvenile <i>Euthynnus alletteratus</i> and <i>Thunnus atlanticus</i> specimens.	57
Figure 31. Ratio of upper jaw length (UPJL) to head length (HL) vs. head length for genetically identified juvenile <i>Euthynnus alletteratus</i> and <i>Thunnus atlanticus</i> specimens.	58
Figure 32. Ratio of eye diameter (ED) to head length (HL) vs. head length for genetically identified juvenile <i>Euthynnus alletteratus</i> and <i>Thunnus atlanticus</i> specimens.	58
Figure 33. Vertical distribution of larval and juvenile scombrids collected during the MOCNESS 2011 survey.	60

Figure 34. Vertical distribution of scombrids collected during the MOCNESS 2015 – 2017 survey.....	62
Figure 35. Standardized abundances collected in quantitative shallow tows separated by day vs. nighttime sampling.	66
Figure 36. A heat map of <i>Euthynnus alletteratus</i> standardized abundances in the epipelagic zone collected during the day time in 2011 using the MOCNESS. White indicates that no individuals were collected. Abundances range from blue (1 ind. 10^{-6} m^{-3}) to red (550 ind. 10^{-6} m^{-3}).....	69
Figure 37. A heat map of <i>Euthynnus alletteratus</i> standardized abundances in the epipelagic zone collected at night in 2011 using the MOCNESS. White indicates that no individuals were collected. Abundances range from blue (1 ind. 10^{-6} m^{-3}) to red (550 ind. 10^{-6} m^{-3}).70	
Figure 38. A heat map of <i>Thunnus atlanticus</i> standardized abundances in the epipelagic zone collected during the day time in 2011 using the MOCNESS. White indicates that no individuals were collected. Abundances range from blue (1 ind. 10^{-6} m^{-3}) to red (550 ind. 10^{-6} m^{-3}).....	71
Figure 39. A heat map of <i>Thunnus atlanticus</i> standardized abundances in the epipelagic zone collected at night in 2011 using the MOCNESS. White indicates that no individuals were collected. Abundances range from blue (1 ind. 10^{-6} m^{-3}) to red (550 ind. 10^{-6} m^{-3}).72	
Figure 40. A heat map of <i>Auxis thazard</i> standardized abundances in the epipelagic zone collected during the day time in 2011 using the MOCNESS. White indicates that no individuals were collected. Abundances range from blue (1 ind. 10^{-6} m^{-3}) to red (550 ind. 10^{-6} m^{-3}).....	73
Figure 41. A heat map of <i>Auxis thazard</i> standardized abundances in the epipelagic zone collected at night in 2011 using the MOCNESS. White indicates that no individuals were collected. Abundances range from blue (1 ind. 10^{-6} m^{-3}) to red (550 ind. 10^{-6} m^{-3}).....	74
Figure 42. Scombridae negative binomial residuals.	76
Figure 43. <i>Euthynnus alletteratus</i> negative binomial residuals.	76
Figure 44. <i>Thunnus atlanticus</i> negative binomial residuals.....	77
Figure 45. <i>Auxis thazard</i> negative binomial residuals.	77
Figure 46. Term plots for Scombridae abundances in relation to (a) water body with LCOW as Loop Current Origin Water, CW as Common Water, and INT as Intermediate/Mixed Water, and (b) diel cycle.	78
Figure 47. Term plots and standardized abundances for <i>Euthynnus alletteratus</i> in relation to (a and b) Julian date, (c and d) minimum salinity, and (e and f) distance to the nearest 200-m isobath.....	79

Figure 48. Term plots and standardized abundances of *Thunnus atlanticus* in relation to (a and b) Julian date, (c and d) minimum salinity, and (e and f) diel cycle. 81

Figure 49. (a) Term plot and (b) standardized abundances of *Auxis thazard* in relation to diel cycle, showing a dominance in nighttime samples. 81

Figure 50. Term plots of Scombridae in relation to (a) Julian date and (b) water mass... 82

Figure 51. Term plots of: *Euthynnus alletteratus* in relation to (a) Julian date, (b) minimum salinity, and (c) distance to 200-m isobath; *Thunnus atlanticus* in relation to (d) Julian date and (e) minimum salinity; and *Auxis thazard* in relation to (f) diel cycle. 83

Figure 52. A heat map of *Thunnus* spp. standardized abundances in the epipelagic zone collected during the day using the high-speed rope trawl from 2010-2011. White indicates that no individuals were collected. Abundances range from blue (1 ind. 10^{-6} m^{-3}) to red (550 ind. 10^{-6} m^{-3}). 86

Figure 53. A heat map of *Thunnus* spp. standardized abundances in the epipelagic zone collected at night using the high-speed rope trawl from 2010-2011. White indicates that no individuals were collected. Abundances range from blue (1 ind. 10^{-6} m^{-3}) to red (550 ind. 10^{-6} m^{-3}). 87

Figure 54. A heat map of *Euthynnus alletteratus* standardized abundances in the epipelagic zone collected during the day using the high-speed rope trawl from 2010-2011. White indicates that no individuals were collected. Abundances range from blue (1 ind. 10^{-6} m^{-3}) to red (550 ind. 10^{-6} m^{-3}). 88

Figure 55. A heat map of *Euthynnus alletteratus* standardized abundances in the epipelagic zone collected at night using the high-speed rope trawl from 2010-2011. White indicates that no individuals were collected. Abundances range from blue (1 ind. 10^{-6} m^{-3}) to red (550 ind. 10^{-6} m^{-3}). 89

Figure 56. A heat map of *Katsuwonus pelamis* standardized abundances in the epipelagic zone collected during the day using the high-speed rope trawl from 2010-2011. White indicates that no individuals were collected. Abundances range from blue (1 ind. 10^{-6} m^{-3}) to red (550 ind. 10^{-6} m^{-3}). 90

Figure 57. A heat map of *Katsuwonus pelamis* standardized abundances in the epipelagic zone collected at night using the high-speed rope trawl from 2010-2011. White indicates that no individuals were collected. Abundances range from blue (1 ind. 10^{-6} m^{-3}) to red (550 ind. 10^{-6} m^{-3}). 91

Figure 58. Seasonal occurrence of the top three most-abundant scombrid species, (a) *Euthynnus alletteratus*, (b) *Thunnus atlanticus*, and (c) *Auxis thazard*, collected during the MOCNESS 2011 survey. 93

Figure 59. Seasonal occurrence of (a) *Euthynnus alletteratus* and (b) all other scombrids collected during the MOCNESS 2015 - 2017 survey. 94

Figure 60. Seasonal occurrence of the top three most-abundant scombrid taxon (a) *Thunnus* spp., (b) *Euthynnus alletteratus*, and (c) *Katsuwonus pelamis* collected during the high-speed rope trawl 2010-2011 survey. Only months with quantitative samples were included.
..... 96

1. INTRODUCTION

1.1. Global importance of scombrid fishes.

Scombridae (i.e. the tunas, mackerels, and bonitos) are high-level predators in tropical to temperate waters worldwide (Matthews et al. 1977). In many coastal and oceanic ecosystems, scombrids exhibit top-down control in pelagic food webs (Polovina et al. 2009). In addition to their ecological significance, larger scombrids are economically important, as they are targeted and valued for their meat. Smaller tunas are often caught as incidental catch in commercial fisheries and are used recreationally as bait to catch larger pelagic fishes. It is well-established that overexploitation has directly affected scombrid species-specific population dynamics and stock sizes (IUCN 2018).

Massive overfishing with purse seines, longlines, and traps has led to global population declines of scombrids, on average by 60% over the past half century (Juan-Jordá et al. 2011). Abundances of *Thunnus albacares* (Yellowfin Tuna), *T. obesus* (Bigeye Tuna), and *T. thynnus* (Atlantic bluefin tuna) have been decreasing in areas such as the GoM, where their populations are considered to be depleted or fully exploited (Majkowski 2007, Juan-Jordá et al. 2011). As a result of increasing fishing pressures, several species have been placed on the International Union for Conservation of Nature (IUCN) Red List of Threatened Species since 1994. On a global scale, *T. obesus* is listed as vulnerable, *T. alalunga* (Albacore) and *T. albacares* are near threatened, and *T. thynnus* is endangered. More specifically in the GoM, *T. obesus* is listed as near-threatened and *T. thynnus* remains categorized as endangered. Moreover, *T. thynnus*, a heavily targeted species whose populations have been driven close to extinction (IUCN 2018), is only considered a “species of concern” under the Endangered Species Act (ESA). A petition to list *T. thynnus* as endangered under the ESA had been previously submitted to the federal government in 2010 by the Convention on Biological Diversity in order to promote their protection (Center for Biological Diversity 2010).

Due to their high economic value and ecological importance, several research programs have been created in order to understand and monitor the population dynamics of adult and larval scombrids. Tagging studies of adult tunas of the Tribe Thunnini have collected valuable information regarding their movement and stock structure (Scott et al.

1990, Block et al. 2005, Rooker et al. 2007). The National Oceanic and Atmospheric Administration's (NOAA) Southeast Fisheries Science Center established a large-scale tagging program in the 1980s off the southeastern coast of the United States, now known as the Cooperative Tagging Center (CTC). Cumulatively in the western North Atlantic, 40743 releases were made between 1954 and 2005 (Scott et al. 1990, Rooker et al. 2007). Due to the enormous commercial interest in *T. thynnus*, several initiatives involving both scientists and recreational fishermen have been created to promote scientific research and conservation of this endangered species. For example, the Tag-A-Giant Foundation electronically tags large *T. thynnus* to gather data regarding their migrations, behaviors, and environmental preferences in both the Atlantic Ocean and Pacific Ocean (Block et al. 1998, Gunn & Block 2001, Wilson et al. 2005, Marcek et al. 2016).

Management and conservation efforts require information on the population dynamics of early life stages in addition to spawning adults. Thus, ichthyoplankton surveys have been conducted since 1982 by the NOAA National Marine Fisheries Service (NMFS) Southeast Area Monitoring and Assessment Program (SEAMAP) in order to describe spawning times and abundance of eggs and larvae found in epipelagic zone of the northern GoM. SEAMAP focuses on developing an annual index of larval abundance for the western population of *T. thynnus* to use for international management (Richards et al. 1984, Habtes et al. 2014).

Declines in large-tuna fisheries are expected to directly affect and increase fishing pressures on small tunas (e.g., *T. atlanticus* and *Euthynnus alletteratus*). Small tunas (maximum of 110 cm fork length (FL), Collette 2010) typically receive less attention, as there are currently no federal management plans or stock assessments for these species (ICCAT 2016b). *Thunnus atlanticus* and *E. alletteratus* are not included in the Highly Migratory Species (HMS) management plan implemented by the NMFS (NMFS 2006) and are listed as least concern under the IUCN Red List (IUCN 2018). As a result, limited knowledge regarding their basic ecology, biology, and distribution and abundance patterns has hindered the ability to manage small tuna species that may be heavily fished in the future. Thus, understanding the ecology of early life stages of both large and small

scombrids will improve the assessment and management of their populations on local, regional, and global scales.

1.2. Systematics of the Family Scombridae.

Tunas, mackerels, and bonitos historically belonged to the order Perciformes (suborder Scombroidei: family Scombridae). However, recent taxonomic revisions now place scombrids in the order Scombriformes (Eschmeyer et al. 2018). Recent uncertainties regarding the evolutionary origin of the family Scombridae have hindered the understanding of interrelationships within the teleost radiation Percomorpha, more specifically the suborder Scombroidei (Miya et al. 2013). Dating back to the group's original definition by Regan (1909), the taxonomic limits within Scombroidei remain unclear (Collette et al. 1984, Johnson 1986, Block et al. 1993, Orrell et al. 2006).

Scombroidei originally included six families: Sphyrænidae (barracudas), Gempylidae (snake mackerels), Trichiuridae (cutlassfishes), Scombridae (tunas, mackerels, and bonitos), Xiphiidae (swordfish), and Istiophoridae (billfishes). However, molecular studies (Block et al. 1993, Orrell et al. 2006) questioned the relationship between scombrids and billfishes, as more recent studies suggest that the latter are more closely related to flatfishes, jacks, and remoras (Near et al. 2012). As of this writing, the Scombroidei comprises three families: Gempylidae, Trichiuridae, and Scombridae. Xiphiidae and Istiophoridae now belong to the suborder Xiphoidei, and Sphyrænidae to the suborder Sphyrænoidei (Eschmeyer et al. 2016). As the suborder Scombroidei represents a polyphyletic group, ongoing molecular studies show that Scombridae, along with Trichiuridae and Gempylidae, form a monophyletic group with 12 other perciform families: Pomatomidae (bluefish), Bramidae (pomfrets), Arripidae (Australian salmon), Chiasmodontidae (swallowers), Stromateidae (butterfishes), Icosteidae (ragfish), Scombrolabracidae (longfin escolar), Centrolophidae (medusafishes), Nomeidae (driftfishes), Caristiidae (manefishes), Ariommatidae (ariommatids), and Tetragonuridae (squaretails) (*sensu* Miya et al. 2013). Although these are non-scombroid fishes, they all possess similarities in their pelagic ecology, such as long-distance migrations (Yagishita et al. 2009). While there is strong morphological heterogeneity among these 15 families, Miya et al. (2013) suggested that they represent an undetected adaptive radiation in the

pelagic realm from a deep-sea ancestor that began after the Cretaceous-Paleogene mass extinction. Betancurr et al. (2013) hypothesized that these 15 families belong to a new order, Scombriformes. The debate regarding the classification of scombrids remains unresolved and requires further analysis.

The family Scombridae, a group of ecologically, morphologically and physiologically specialized epipelagic fishes, consists of 51 species in 15 genera worldwide. Scombridae is further divided into two subfamilies, Gasterochismatinae and Scombrinae. *Gasterochisma melampus* (Richardson, 1845), also known as the butterfly kingfish, is the only species in the subfamily Gasterochismatinae and is confined in southern temperate waters (Collette & Nauen 1983). The subfamily Scombrinae further divides into four tribes, which include: Thunnini (tunas), Sardini (bonitos), Scombrini (mackerels), and Scomberomorini (Spanish mackerels). Each of these four tribes are represented among the 16 species in eight genera of the family Scombridae found in the GoM: Thunnini with nine species: *Auxis rochei* (Bullet Mackerel), *Auxis thazard*, *E. alletteratus*, *Katsuwonus pelamis*, *Thunnus alalunga*, *T. albacares*, *T. atlanticus*, *T. obesus*, and *T. thynnus*; Sardini with one species: *Sarda sarda* (Atlantic Bonito); Scombrini with one species: *Scomber colias* (Atlantic Chub Mackerel); and Scomberomorini with five species: *Acanthocybium solandri* (Wahoo), *Scomberomorus brasiliensis* (Serra), *Scomberomorus cavalla* (King Mackerel), *Scomberomorus maculatus* (Spanish Mackerel), and *Scomberomorus regalis* (Cero) (Collette & Nauen 1983, Richards 2005).

1.3. Scombrid biology and ecology.

Scombrids are robust, elongate and streamlined pelagic fishes. Some are recognized among the largest and fastest predators in the oceans (Collette 1978). They are characterized by having a pair of caudal keels in the middle of their slender caudal peduncle at the caudal fin base and at least four finlets (typically seven to ten) behind the dorsal and anal fins. Their small dorsal and ventral finlets minimize turbulence, helping the fish propel its body forward. Their fusiform bodies and lunate tail also minimize drag as they rapidly swim through the water (Collette 1978, Collette & Nauen 1983, Schulze-Haugen et al. 2003). Additionally, their first dorsal and anal fins can fold into grooves and the pectoral

and pelvic fins into depressions in the body, allowing the fishes to prolong their high-speed swimming (Collette & Nauen 1983).

Their morphological characteristics allow tunas to travel at high speeds and far distances, compared to other pelagic fishes (Collette & Nauen 1983). Seasonal migrations over long distances for feeding or reproduction are common in scombrid species. For example, *T. alalunga* and *T. thynnus* form large schools to migrate from temperate feeding waters to low-latitude waters for spawning (Richards 1975). However, *K. pelamis* and *T. albacares* remain in warm waters year-round.

Their global distributions depend on species-specific thermal tolerances. Tropical tunas can be found in waters greater than 18 °C, and temperate tunas can be found in water temperatures as cold as 10 °C (Brill 1994). This definition is flexible, as *T. obesus* is considered a tropical tuna despite its largest and most valuable fishery being in the Grand Banks (ICCAT 2016a). Their unique physiology allows them to tolerate a broad thermal niche, ranging from 3 to 31 °C waters (Carey & Lawson 1973). However, their endothermic ability to tolerate high temperatures can reduce their cardiac function (Blank et al. 2004). Therefore, the physiological abilities of some adult species are challenged during the warmer spring and summer spawning seasons in the GoM, when water temperatures approach or exceed 31 °C. In response to high sea surface temperatures (SSTs), some adult tunas, such as *T. thynnus*, are found at colder, deeper mesopelagic depths between 500 and 1000 m (ICCAT 2016a). In contrast, other thunnine species (e.g., *T. albacares* and *T. atlanticus*) rarely encounter mesopelagic depths (ICCAT 2016a).

Scombrids spawn in warm, open-ocean waters in the GoM, as high temperatures improve the development of eggs and larvae and in turn increase their growth rates (Miyashita et al. 2000). All scombrid species are oviparous, with the majority spawning buoyant, pelagic eggs (Richards 2005). The annual batch fecundities of most tunas range from 2 to 70 million eggs (Collette 1978, Collette & Nauen 1983), with the higher annual batch fecundities reported for *K. pelamis* (7 to 76 million) and other small tunas (Collette & Nauen 1983, ICCAT 2016a). Spawning behavior is species-specific, and varies from directed spawning within a season (e.g., *T. thynnus*; (Richards 1975) to more protracted or year-round spawning (e.g., *T. albacares*; (Richards 2005). However, Lutcavage et al.

(1999) also found through electronic tagging and experiments in captivity that *T. thynnus* might spawn once every two or three years. Most tuna species spawn in waters with surface temperature greater than 24 °C. As rapidly growing species, these pelagic fishes typically reach maturity after 2 to 5 years (Collette 1978, Collette & Nauen 1983), but it can extend to 8 years, as exhibited by the western population of *T. thynnus* (ICCAT 2016a).

While the distribution of adult tunas is adequately understood (ICCAT 2016a), the distributions of tuna early life stages (more specifically, juveniles) have not been sufficiently characterized. Lindo-Atichati et al. (2012) identified that larval *E. alletteratus*, *Auxis thazard*, and *Thunnus* spp. distributions were associated with different mesoscale oceanographic features. Muhling et al. (2010) found that *T. thynnus* larvae were rarely collected within the Loop Current and anticyclonic rings, but preferred oligotrophic conditions. Moreover, *Thunnus* spp. distributions were found to be driven by SST and salinity and were associated with anticyclonic regions and the Loop Current (Rooker et al. 2013, Cornic & Rooker 2018, Cornic et al. 2018). While a few studies have been conducted on the spatial distributions of tuna larvae (Richards et al. 1984, Muhling et al. 2013), there is limited knowledge regarding the distributional patterns of juvenile tunas in the GoM.

1.4. The biophysical milieu: major oceanographic features of the Gulf of Mexico.

The GoM is a semi-enclosed oceanic ecosystem that connects the Caribbean Sea to the Atlantic Ocean by water entering through the Yucatan Channel and exiting through the Straits of Florida. Encompassing 4000 km of coastline and reaching a maximum depth of 3750 m (McEachran & Fechhelm 1998), the GoM can be divided into two distinct areas: the eastern and western GoM. The eastern side encompasses the Loop Current and its frontal zone, while the western GoM experiences fluctuating mesoscale eddies that pinch off the anticyclonic Loop Current.

The circulation in the eastern GoM is dominated by the Loop Current, which transports more than 25 million m³ s⁻¹ of water at 2.5 m s⁻¹ throughout the GoM. This warm current enters the GoM through the Yucatan Channel. As the current flows to the center of the GoM, it makes an anticyclonic (clockwise) turn before the water exits through the Straits of Florida and becomes the Florida Current. Ultimately, the warm water serves as

the primary source of the Gulf Stream. Furthermore, the current's pattern is controlled by the topography of the eastern GoM basin. The Loop Current is typically confined between Campeche Bank and the Florida Shelf, with its core closer to the bank on the west (Capurro & Reid 1972). However, the northern and western extensions of the Loop Current have strong seasonal and annual variability, which alter the current's location, flow patterns, temperature, and hydrographic features (Molinari 1980, Nakata et al. 2000).

The boundary of the Loop Current is a highly dynamic region with meanders and strong convergence and divergence zones that generate cyclonic and anticyclonic eddies (Olson & Backus 1985). In the eastern GoM, the anticyclonic flow of the Loop Current favors the formation of frontal zones due to differences in water density between the current and the surrounding ocean waters. Along the eastern boundaries (frontal zone) of the Loop Current, meanders create cold "tongues" (large isolated perturbations 400 km or more in size of cold water) extending from the warm Loop Current (Vukovich et al. 1979). As these cold tongues pinch off of the Loop Current into circular currents of water, eddies are created. Vukovich and Maul (1985) discovered that cold-core, cyclonic (counterclockwise) eddies form in the center of these cold tongues on or near the frontal boundary of the Loop Current. The Loop Current frontal eddies are 80 to 120 km in diameter, and they experience a vertical flow from the lower layers upward towards the divergent surface layer in the eddy's center, known as active cyclonic upwelling (Bane et al. 1981). Upwelling in the eddy's center brings cold, nutrient-rich water from depth to the surface, and it enhances primary and secondary production (Bakun 2006). Therefore, the cyclonic eddies and frontal zone in the eastern GoM are associated with high productivity (Olson 1991).

Anticyclonic eddies are also prominent oceanographic features created by the Loop Current. After the Loop Current extends into higher latitudes in the GoM, which it does quasi-seasonally, the retraction of the current towards the south in the spring generates large rapidly rotating anticyclonic, warm-core eddies. These large, mesoscale eddies, which can reach diameters of 300 to 400 km and depths of 1000 m, propagate westward at about 4 km d^{-1} (Elliott 1982, Dietrich & Lin 1994) until they diminish along the western GoM shelf between a few days up to possibly a year later (Elliott 1982). Water converges toward the center of the anticyclonic eddies, creating a local high and downwelling in their

centers. The centers of downwelling, anticyclonic cores can serve as areas of enhanced retention, especially for buoyant particles (Olson 1991).

The Mississippi River, the largest river in North America, drains 41% of the adjoining United States into the GoM (Van der Leeden 1990). Turbid, low-density plumes extend from the river into the coastal waters, making a clear front. Plumes and fronts change the physical oceanography, distribution of plankton, variation in nutrient inputs, and primary and secondary production (Le Fevre 1986, Grimes & Kingsford 1996). Specifically, the Mississippi River empties large quantities of nutrients into the GoM, creating a zone of high primary productivity at the shallow water near the river's mouth. Large filaments of nutrients can be driven to the shelf edge and offshore by eddies. Anthropogenic inputs of nitrogen, as well as changes in the river channel morphology and land use, have increased the nitrate concentrations leaving the Mississippi River. Phosphorous concentrations have increased around the mouth of the Mississippi River as well, extending from Mobile Bay westward to longitude 91°W (Riley 1937, Turner & Rabalais 1991). Increases in nitrate and phosphorous levels have led to an increase in primary production of organic carbon in the GoM ecosystem (Turner & Rabalais 1991, Dinnel & Bratkovich 1993).

Higher primary production supports higher concentrations of microzooplankton (mostly copepod nauplii) and macrozooplankton productivity (Dagg & Whitley 1991, Grimes & Finucane 1991) in the Mississippi River Plume region. Zooplankton promote higher ichthyoplankton concentrations by offering rich trophic resources that can be utilized for growth. Larval and juvenile fishes (e.g., *T. atlanticus*, *T. albacares*, and *E. alletteratus*) prey upon macrozooplankton (Grimes & Finucane 1991), while other fish species (e.g., *Scomberomorus cavalla* and *Scomberomorus maculatus*) prey primarily upon larval fishes (De Vries et al. 1990, Grimes & Finucane 1991). Copepod nauplii and various microzooplankton also act as critical components of other larval fish diets (Peterson & Ausubel 1984, Grimes & Finucane 1991). These enhanced food resources sustain larval and small juvenile fish assemblages (Grimes & Finucane 1991) in the Mississippi River Plume, offering ideal conditions for growth, survival and recruitment of local fishes, such as tunas (e.g., *T. atlanticus*, *T. albacares*, *E. alletteratus*, and *Scomberomorus cavalla*) and

other ichthyoplankton (e.g., *Leiostomus xanthurus*, *Brevoortia patronus*, and *Chloroscombrus chrysurus*, Grimes & Finucane 1991). In turn, the Mississippi River Plume significantly influences larval fish distributions, feeding patterns, and recruitment.

1.5. Statement of problem.

It is difficult to differentiate larval and juvenile scombrid stages, since there is not a clearly marked metamorphosis between these stages. Adult characteristics usually develop gradually and separately, which makes distinguishing the two early life history stages challenging. However, Matsumoto et al. (1971) reported that once a larva develops the full complement of fin spines and rays, all of its vertebrae ossify, and its anal opening moves back near the anal fin origin, the larval stage ends and the individual is considered a juvenile. Scombrids typically develop these characteristics when they grow to about 10 to 13 mm SL (Matsumoto et al. 1971). This definition is generally accepted among larval tuna specialists (Matsumoto et al. 1971, Boehlert & Mundy 1994), and it will be the definition for the purpose of this thesis.

Genetic barcoding studies have revealed misidentifications of larval and juvenile tunas when using morphology-based taxonomy, largely due to the lack of defined characters (Puncher et al. 2015). Diagnostic keys are available for larvae between 3 and 12 mm standard length (SL) (Nishikawa & Rimmer 1987, Richards 2005); however, larger larvae and smaller juveniles lack morphological descriptions. Due to high taxonomic uncertainty of this size range, the ecological and biological aspects of large larvae and smaller juvenile are lacking, which prevents adding this cohort in a life history model. Smaller juvenile tuna assemblages in the GoM remain inadequately described due to limited sampling across their wide range of coastal and oceanic habitats, as small juveniles are agile enough to avoid small sampling nets and too small to be collected using conventional fishing gear.

Information on the spatiotemporal distribution and abundance data of this cohort provides insight into scombrid recruitment patterns. Thus, understanding the biological information of small juveniles of these commercially important species will provide new data for fisheries management efforts and will increase our understanding of juvenile

habitat and spawning areas that can be protected from exploitation. In turn, the lack of data on these important life history stages (larger larvae and smaller juveniles) can make managing adult populations problematic. In summary, incomplete taxonomy, lack of knowledge regarding the ecology of scombrid early life stages, and the dearth of large-scale sampling efforts of juvenile tunas relative to larvae and adults in the GoM have impeded our base knowledge of these keystone taxa.

1.6. Objectives.

The initial goal of this study was to synthesize the known early life stage taxonomy and supplement current information regarding juvenile taxonomy. A combination of genetic analyses and morphological characteristics (meristic counts and body measurements) was used to compare and identify qualitative morphological differences among scombrid genera and/or species found in the GoM. The taxonomic synthesis was then applied to larval and juvenile specimens to address the ecological knowledge gap of tuna early life stages (specifically juveniles) in the GoM. The primary goal of this study was to characterize the faunal composition, abundance, and spatiotemporal distribution of tuna early life stages with respect to depth, time of year, and physical oceanographic features in the GoM.

The samples collected in 2010-2011 and 2015-2017 represent one of the few juvenile tuna time-series datasets of its kind (larger larvae and smaller juveniles collected with large, rectangular midwater trawls). The Offshore Nekton Sampling and Analysis Program (ONSAP) sampled over a 10-month interval from December 2010 to September 2011, while the Deep Pelagic Nekton Dynamics of the Gulf of Mexico (DEEPEND) Consortium sampled in the spring (April to May) and late summer (August) each year between 2015 and 2017. Such large-scale surveys taken over seasonal cycles across multiple years are extremely rare in oceanic ecosystems. Moreover, multiple gear types were used during the two programs. During ONSAP and DEEPEND sampling, a multiple-net rectangular trawling system was used to sample larvae and smaller juveniles in a quantitative, discrete-depth fashion. This system allowed for precise vertical distribution determination, primarily of larvae and smaller juveniles. Additionally during ONSAP, a second gear type, a large, dual-warp pelagic trawl, allowed for the collection of more and

larger scombrid specimens, specifically larger juveniles. As opposed to larval scombrids, juvenile individuals are a rarity in collections, which makes this dataset a significant contribution to global scombrid research. From a modeling perspective, juveniles are important, as they are the cohort that have survived the high-mortality gauntlet experienced by larvae (Anonymous 1984, ICCAT 2016a).

Advancements in the identification processes of larval and juvenile tunas can improve our knowledge of these critical life stages and enhance conservation methods for the taxon. This study provided quantitative data on the assemblage structure of tuna early life stages, which is useful for population dynamics and essential habitat models. Figure 1 depicts the lack of juvenile data currently available in the GoM for the essential habitat of the highly migratory *T. thynnus*. Through this thesis, additional essential habitats and preferences of several juvenile tuna species were identified. This thesis identified the assemblage structure of scombrid early life stages in the GoM and characterized the primary drivers (location, oceanography, and seasonality) of this assemblage structure.

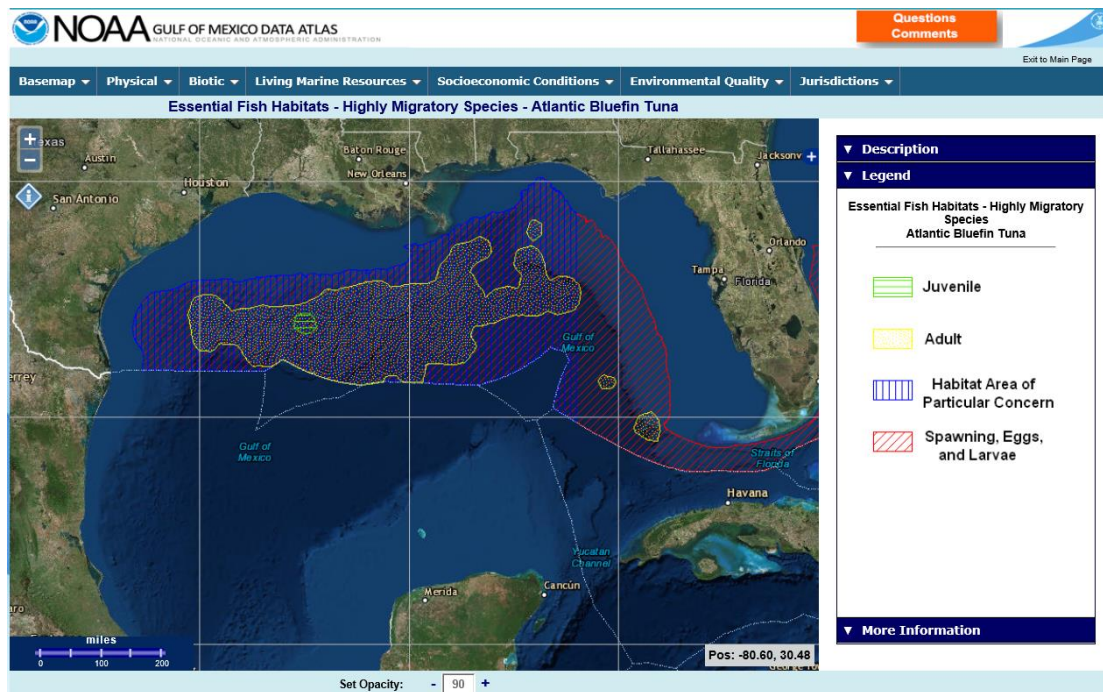


Figure 1. NOAA Gulf of Mexico Data Atlas map of the essential fish habitats for the highly migratory *Thunnus thynnus* (Cooper 2011), emphasizing the lack of knowledge on juvenile distributions.

2. METHODS

2.1. *Scombrid sample collection and processing.*

Larval and juvenile scombrids were collected in the northern GoM during seven research cruises in 2010-2011, as part of the NOAA-supported ONSAP, and during five research cruises from 2015-2017, as a part of the DEEPEND Consortium research program. Specimens were identified to the lowest taxonomic level possible. The ONSAP was created to assess the damage imposed on the deep-water invertebrates and fishes in the GoM from the *Deepwater Horizon* oil spill (DWHOS) in April - September, 2010. The ONSAP sampling was conducted on two research vessels, the M/V *Meg Skansi* and the NOAA FRV *Pisces*. From 2015-2017, the DEEPEND Consortium continued sampling on the R/V *Point Sur* visiting the same stations as ONSAP (Figure 2). All station's bottom depths were greater than 1000 m, and the maximum sampling depth was 1500 m. Two different types of sampling gear were utilized in these surveys: a discrete-depth sampling gear known as a Multiple Opening/Closing Net and Environmental Sensing System (MOCNESS) in 2011 and from 2015-2017, and a larger, commercial-sized, pelagic sampling gear known as high-speed rope trawl from 2010-2011. The analyses in this thesis will be grouped based on gear type.

2.1.1. *MOCNESS sampling, 2011 and 2015-2017.*

The M/V *Meg Skansi 6* (MS6), *Meg Skansi 7* (MS7), and *Meg Skansi 8* (MS8) cruises used a 10-m² mouth area, 3-mm mesh MOCNESS to sample the designated stations from January 28 to March 30, 2011 (MS6), April 14 to June 30, 2011 (MS7), and July 18 to September 30, 2011 (MS8). Samples in each survey were collected across a 46-station grid (Table 1, Figure 2, Appendix Table 1). The MOCNESS, a six-net discrete-depth sampling system (Wiebe et al. 1985), surveyed specific depth strata in the water column from the surface down to 1500 m depth, with deployments centered around solar noon and night. The net depth intervals were from 0 to 200 m, 200 to 600 m, 600 to 1000 m, 1000 to 1200 m, and 1200 to 1500 m. A Tsurumi-Seiki-Kosakusho (T.S.K.) magnetically sensed flowmeter determined the water filtered by each net, which was used to standardize the abundance per unit of effort (no. individuals 10⁻⁶ m⁻³). This cruise series will be referred to as the MOCNESS 2011 survey, hereafter.

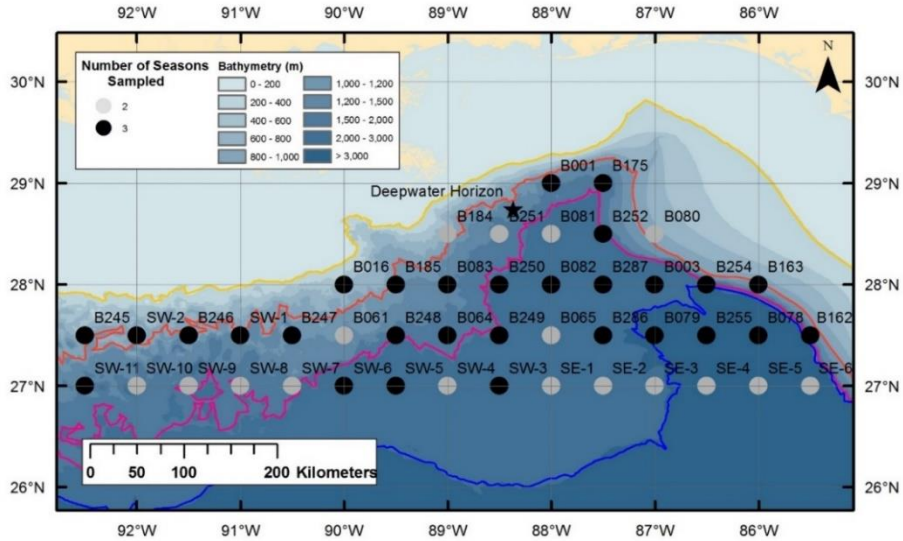


Figure 2. MOCNESS 2011 stations sampled aboard the M/V *Meg Skansi*.

The DEEPEND cruises on the R/V *Point Sur* utilized the same size MOCNESS (10-m² mouth area with a 3-mm mesh) previously used during the MOCNESS 2011 series. Select stations (Appendix Table 1) were sampled from 2015-2017 during the spring (April to May; Figure 3a, c, and e) and late summer (August; Figure 3b and d; Table 1). The sampling was centered around the approximate minimum and maximum outflow from the Mississippi River. This cruise series is referred to as the MOCNESS 2015-2017 survey, hereafter.

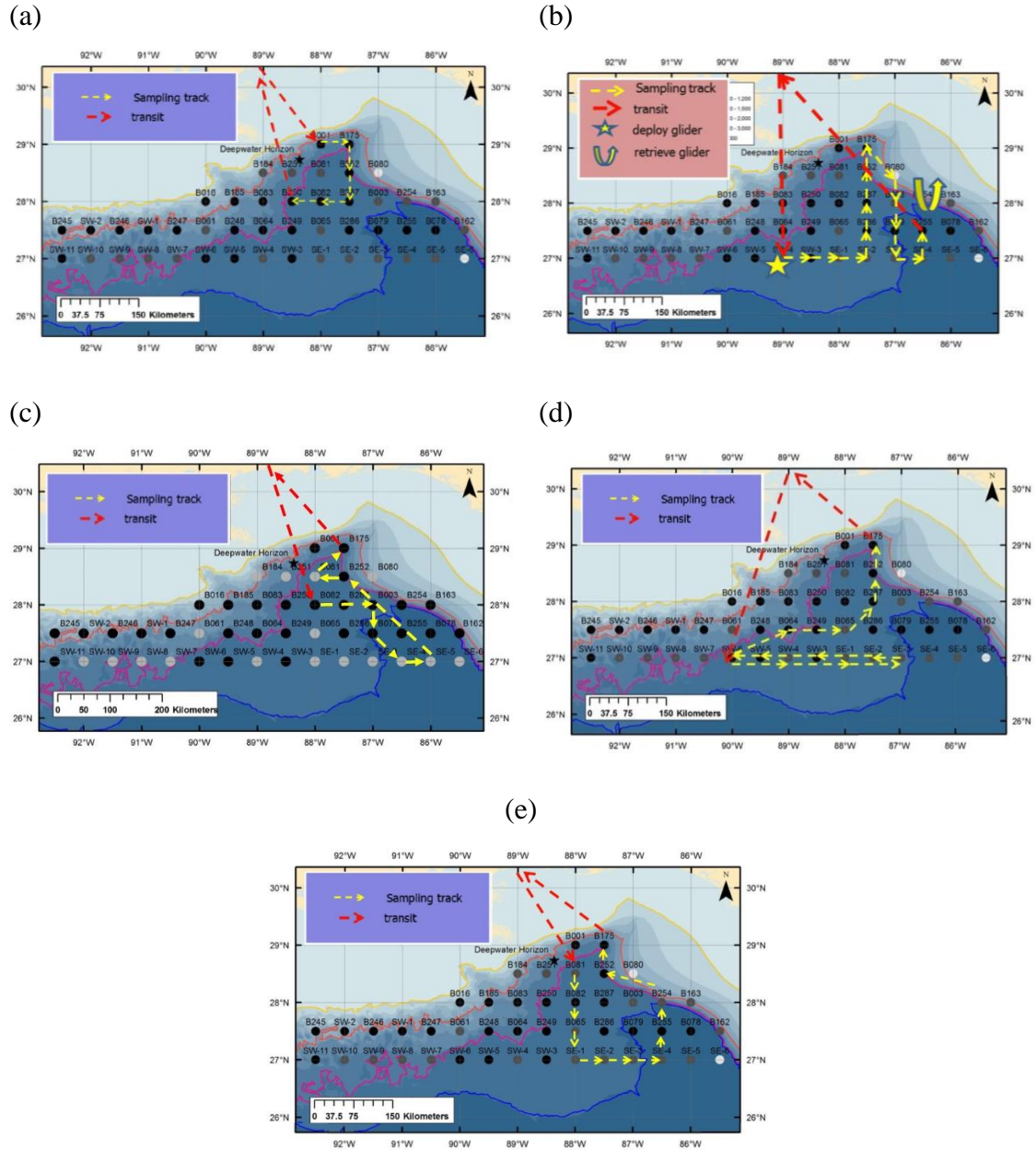


Figure 3. MOCNESS 2015-2017 stations and cruise tracks for cruises (a) DP01, (b) DP02, (c) DP03, (d) DP04, and (e) DP05, relative to the SEAMAP/ONSAP station grid. Stations were sampled aboard the R/V *Point Sur*.

2.1.2. High-speed rope trawl sampling, 2010-2011.

The NOAA FRV *Pisces* 8 (PC8), *Pisces* 9 (PC9), *Pisces* 10 (PC10), and *Pisces* 12 (PC12) cruises utilized a commercial-sized, high-speed rope trawl with a 165-m² mouth and a graded mesh (3.2-m to 19-mm) to survey the water column. The net sampled from the surface to depth and back to the surface in an oblique “V” without closing, during both day and night, in two patterns: “shallow” (0-700 m) and “deep” (0-1500 m) (Table 1). Sampling occurred from December 2 to December 19, 2010 (PC8), March 23 to April 6, 2011 (PC9), June 23 to July 13, 2011 (PC10), and September 8 to September 27, 2011 (PC12) at a subset of the previously mentioned MOCNESS stations (Figure 4, Appendix Table 1). This cruise series will be referred to as the high-speed rope trawl 2010-2011 survey, hereafter.

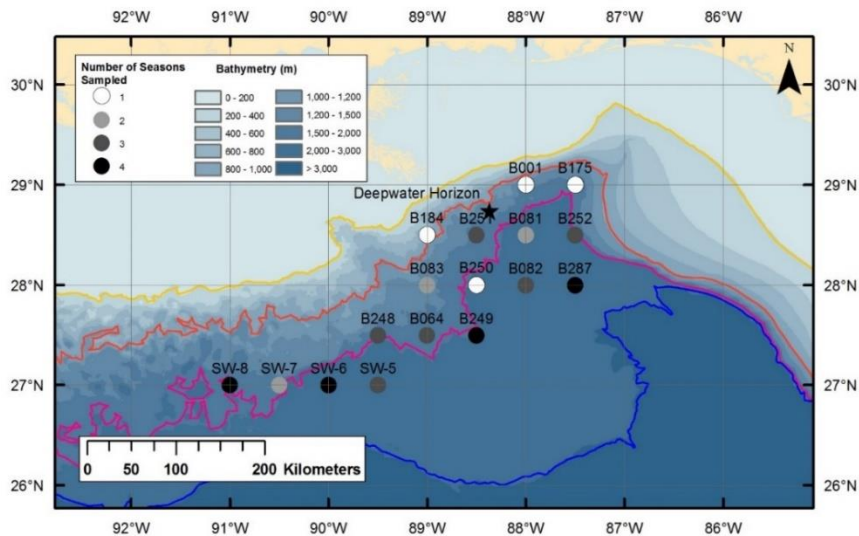


Figure 4. High-speed rope trawl 2010-2011 stations sampled aboard the FRV *Pisces*.

Samples collected across all cruise series were fixed in 10% buffered formalin:seawater onboard and later were transferred to 70% ethanol:water. Several specimens were frozen or preserved in 99% ethanol:water for genetic analyses. In addition to initial sample processing on board each ship, the fish taxonomic identifications and quantitative analyses were completed in the Oceanic Ecology Laboratory at the Halmos College of Natural Sciences and Oceanography at Nova Southeastern University (NSU). SL in millimeters and weight in grams were recorded for each individual.

Table 1. Summary of the seven surveys conducted by the ONSAP (three M/V *Meg Skansi* and four FRV *Pisces* surveys) and the five surveys by the DEEPEND Consortium (R/V *Point Sur*) in the GoM; MOC10 = 10-m² MOCNESS, HSRT = High-speed rope trawl. No. of Samples indicates the amount of quantitative tows per cruise. The gray line designates the separation of gear types

Cruise	Dates	Gear Type	No. of Samples	Combined Volumes (m³)
MS6	January 28 - March 30, 2011	MOC10	211	8077563.70
MS7	April 14 - June 30, 2011	MOC10	302	10362542.90
MS8	July 18 - September 30, 2011	MOC10	377	11616293.50
DP01	May 1- 8, 2015	MOC10	34	1179842.00
DP02	August 8 - 21, 2015	MOC10	95	2880308.00
DP03	April 30 – May 14, 2016	MOC10	75	2239905.80
DP04	August 5 – 19, 2016	MOC10	112	2674249.30
DP05	May 1 -11, 2017	MOC10	74	3278176.60
PC8	December 2 - 19, 2010	HSRT	22	89419063.84
PC9	March 23 - April 6, 2011	HSRT	3	11714434.26
PC10	June 23 - July 13, 2011	HSRT	42	98686682.90
PC12	September 8 - 27, 2011	HSRT	48	106376488.60

2.2. Morphological and genetic taxonomy.

Larval and juvenile scombrid specimens were identified to the lowest taxonomic level possible. Body shape, myomere counts, and pigmentation (Figure 5) were the key morphological characteristics examined to correctly identify each larva; however, pigmentation can migrate or disappear following preservation, which complicated the identification process. Overall, larval scombrid descriptions are relatively well known, with the exception of *Scomberomorus brasiliensis*, which was not identified in this study. However, larvae in the Tribe Thunnini are the most difficult larvae to identify, specifically those in the genus *Thunnus* (Richards 2005). Quality Assurance/Quality Control were conducted with leading scombrid taxonomic experts, Dr. John Lamkin (NOAA NMFS, Miami) and Aki Shiroza, M.S. (NOAA NMFS, Miami), in order to ensure the accuracy of larval specimen identifications.

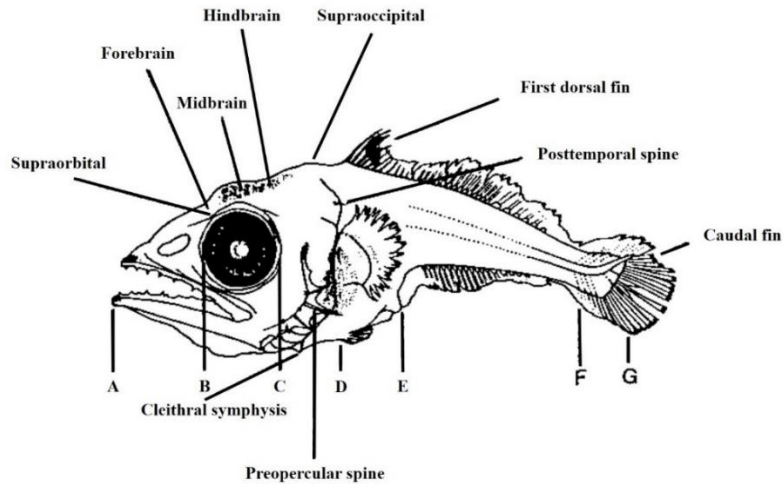


Figure 5. Identifiable characteristics of larval scombrids. Features include: (A-B) snout length, (B-C) eye diameter, (A-D) head, (D-E) trunk, (D-G) body, (E-F) tail, and (F-G) caudal peduncle (edited from Nishikawa & Rimmer 1987).

In order to confirm our identifications and help correctly identify the challenging and poorly described scombrid species (namely juveniles), genetic barcoding (COI gene region) of a range of specimens was conducted in collaboration with Drs. Mahmood Shivji and Andrea Bernard (NSU, Conservation Biology and Genetics Laboratory). Genetic barcoding facilitates species identifications and enables identifications where morphological characteristics cannot be applied (e.g., for undescribed juvenile scombrids) (Ward et al. 2009). A total of 70 larval and juvenile scombrids were taken for genetic barcoding from the high-speed rope trawl 2010-2011 survey (PC10 and PC12) and MOCNESS 2015-2017 survey (DP02, DP03, and DP04). These genetically confirmed individuals were used to produce voucher specimens for each species and used to identify morphological characteristics that are unique to the currently undescribed juvenile scombrid species.

Genetic analyses additionally provided validation for morphometric analyses. A total of 13 morphometric variables were used for juvenile morphometric analyses (Figure 6). Measurements were obtained for SL, head length (HL), upper jaw length, snout length, eye diameter, pelvic fin, and interdorsal length. Finlets and caudal fin rays were counted and assisted in species identifications. The first dorsal, second dorsal, pectoral, and anal fins were measured and fin elements (spines and rays) were counted. All measurements were taken with a digital caliper to the nearest 0.01 millimeter. Gill rakers were pulled from the largest genetically identified specimens of each species in order to determine the size

at which adult gill raker counts are obtained. Livers were also examined for *Thunnus* spp. to help with species identifications.

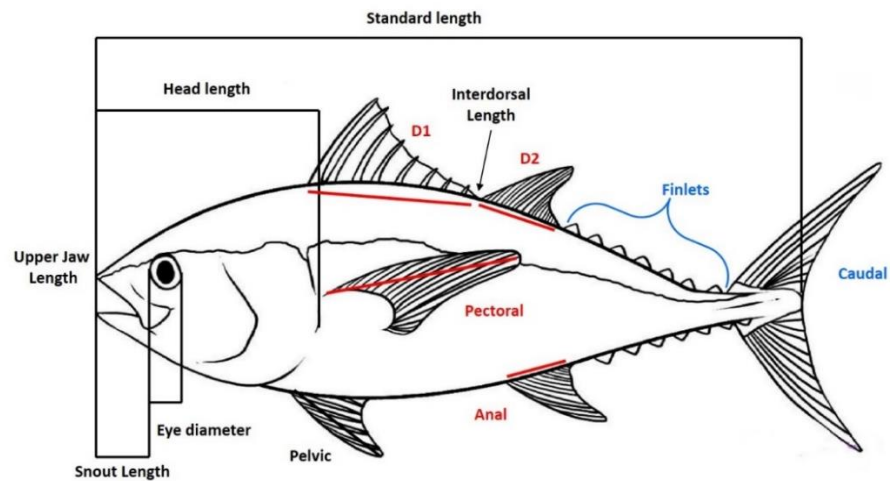


Figure 6. Morphometrics used to analyze the genetically identified juvenile specimens. Black represents features that were measured, blue represents features that were counted, and red represents features that were both measured and counted.

The ratio of measured morphometric features were expressed in relation to SL and/or to HL in order to demonstrate how the ratio changes ontogenetically (as an individual grows). Investigating these ratios helped determine if morphometric features grow isometrically and elucidated the combination of variables that best identify scombrid specimens. Principal component analysis and discriminant analysis could not be used in this study due to an inadequately small sample size per species. Therefore, descriptive statistics of all measurements and ratios were recorded for all possible species. Curvilinear (power) regressions of various body parts were plotted against SL or HL for the two species with the largest sample size (i.e. *Euthynnus alletteratus* and *Thunnus atlanticus*) in order to analyze the differences in growth patterns between the two species. All data and statistical analyses were conducted with R and R Studio (Version 1.1.442, R Foundation for Statistical Computing).

2.3. Species composition and spatiotemporal distribution analyses.

Faunal composition was determined for all three cruise series (MOCNESS 2011, high-speed rope trawl 2010-2011, and MOCNESS 2015-2017). Assemblage abundances were calculated using quantitative samples. Standardized abundances were calculated by

dividing the sum of the raw count of individuals by the sum of the volume of water filtered. Percent frequency of occurrence per species was determined by cruise series. Comparisons between gear type and SL was investigated using a non-parametric Kruskal-Wallis test. Length-weight regressions were created for all scombrid species. Ratio plots of *E. alletteratus* and *T. atlanticus* were analyzed in order to identify differences in growth patterns. Seasonal abundances were determined for the three most-abundant taxon groups for each cruise series in order to gain a better understanding of the GoM habitat as spawning and nursery grounds.

Diel vertical distributions of scombrids species were determined using the standardized abundances for each species per depth interval by day and night. Standardized abundances and percent frequency of occurrence per species were further investigated in the epipelagic zone for both MOCNESS surveys, as the majority of specimens were caught in the upper 200 m of the water column. The differences between day and night abundance estimates in the top 200 m for the entire family and the top four species from the MOCNESS 2011 cruises were analyzed with a two-sample non-parametric Mann-Whitney Wilcox t-test to determine if the catch rates of scombrids was affected by time of day (specifically, light environment).

Both generalized additive models (GAMs) and presence-absence models were created for the most-abundant species collected in the epipelagic zone during the MOCNESS 2011 cruise series. These models are further described in the following section. Presence-absence models were constructed using binomial distributions in order to further investigate the results produced by the GAMs. Presence-absence models were used to determine whether the chances of catching a given scombrid (e.g., family Scombridae, *E. alletteratus*, *T. atlanticus*, and *Auxis thazard*) were greater under specific environmental conditions (i.e. previously identified using GAMs). A more detailed description of the GAMs and presence-absence models are included below.

Spatial maps of the horizontal distributions of the most-abundant larval and juvenile scombrids, apportioned by diel cycle (day vs. night), were created using R and R Studio. The patterns in the standardized abundances were visually compared with chlorophyll *a* concentrations, minimum salinity levels, bathymetry, and sea surface height anomaly

(SSHA). Seasonal occurrences were used to identify spawning patterns and potential areas of increased recruitment in the GoM.

2.3.1. Generalized additive models/presence-absence models.

GAMs were developed in R in order to examine the spatiotemporal distributions of scombrids in the GoM. GAMs allow for non-linear relationships between response and multiple explanatory variables using additive smoothing functions (Zuur 2009). The family Scombridae and the three most-abundant scombrid species caught during the MOCNESS 2011 survey were analyzed using GAMs. Scombrids were collected in higher abundances in the epipelagic zone; therefore, individual species abundances were compared solely in the upper 200 m of the water column in the models. Due to the small sample size during the MOCNESS 2015-2017 survey and oblique tow sampling during the high-speed rope trawl 2010-2011 survey, GAMs were not constructed with these data.

Scombrid densities were modeled by including counts (integer values) as dependent variables with volume as an offset term and several environmental (categorical and numerical) variables as the independent variables. Therefore, in order to create a model that described which covariates were associated with scombrid densities, collinearity was tested. A pair-plot or pairwise scatterplot was used to compare covariates. SST and Julian date were collinear. Thus, one of the collinear variables (e.g., SST) was dropped in order to create a model without covariance. The inclusion of variables that appeared to covary in the pair-plots were verified using the variance inflation factors (Zuur et al. 2010).

As a result of comparing the covariates using a pair-plot, the original dataset was reduced and the full model consisted of five explanatory variables, which included: minimum salinity of the epipelagic zone, distance to the nearest 200-m isobath, water mass, Julian date (2011), and diel cycle (day vs. night). Minimum salinity values, indicative of coastal runoff and riverine input, were collected from the MOCNESS sensors. Distance to the nearest 200-m isobath, which related to coastal influence, was calculated in R with the *marmap* package (Pante & Simon-Bouhet 2013). Water mass of the sample denoted either Loop Current Origin Water (LCOW), Gulf Common Water (CW), or Mixed Water (MIX) and was based on the mean temperature between 200 and 600 m, following Johnston et al. (submitted) and Milligan (unpub. data). Water mass classifications were used as a

simplified factor that related to SSHA, which was too complex to fit the model. Diel cycle was used to investigate differential catch patterns exhibited during the day and at night. Day samples referred to deployments centered around solar noon, while night samples were centered around solar midnight. The full model is defined as:

$$\text{counts} = \text{minimum salinity} + \text{distance to the nearest 200-m isobath} + \text{water mass} \\ + \text{Julian date} + \text{diel cycle} + \text{offset}(\log(\text{volume})).$$

In order to create a GAM to determine whether scombrid densities were affected by the five explanatory variables, the appropriate distribution of the response variable, which was represented as integer or count data, was determined and the terms were selected. The distributions of the response variables (i.e. Poisson, negative binomial, zero-inflated Poisson, and zero-inflated negative binomial) were compared by investigating the residuals, Akaike information criterion (AIC) values, and degrees of freedom (Zuur 2009). The lowest AIC values and degrees of freedom indicated the best model (distribution) for describing scombrid abundances in this study (Zuur et al. 2010). Due to the high amount of zeros in the dataset (Zuur 2009), zero-inflation distribution models were included in the distribution comparisons. The Penalized Beta-splines (pb) smoother was used with a fine-scaled, mixed model focusing between 50 and 200 and a log link. The pb smoother is a P-spline smoother that uses singular value decomposition to fit the model and estimates the smoothing parameters using different local (performance iteration) methods (Eilers & Marx 1996, Eilers et al. 2015).

Term selection was conducted by dropping one explanatory variable at a time and comparing the AIC values of the reduced models to the full model's AIC value. If the difference between the full and reduced models' AIC values (dAIC) was: 1) less than 2, the models were considered to be equivalent, 2) between 2 and 4, the explanatory variable marginally affected scombrid abundance, and 3) greater than 4, the explanatory variable was an important determinant of scombrid densities (Zuur 2009). If dropping a term resulted in a negative dAIC, the model fit was improved (the AIC value of the reduced model was lower than the full model) and the variable was removed. A positive dAIC indicated that dropping the variable weakened the model fit (higher AIC value), and the variable was retained.

3. RESULTS

3.1. Larval and juvenile scombrid taxonomy.

A total of 945 scombrid larvae and juveniles were collected during the MOCNESS 2011, MOCNESS 2015-2017, and high-speed rope trawl 2010-2011 surveys. Overall, 68.6% of individuals were identified fully to species, 30.7% to genus only, and 0.7% to the family Scombridae only.

3.1.1. Genetic analyses.

Mitochondrial CO1 Sequence Basic Local Alignment Search Tool (BLAST) was used to genetically identify scombrid specimens. Eight species from five genera were genetically identified, apportioned between the two survey types. A total of 28 specimens were collected using the high-speed rope trawl during PC10 and PC12 cruises and were preserved frozen. All specimens were juveniles, ranging from 15.0 – 124.8 mm SL. The smallest genetically identified scombrid collected using the high-speed rope trawl was *Thunnus albacares* (15.0 mm SL), while the largest was *T. thynnus* (124.8 mm SL). Additionally, 42 specimens were collected for genetic analyses from the MOCNESS 2015-2017 survey during DP02, DP03, and DP04 cruises and preserved in 99% Ethanol. These specimens ranged in size from 8.2 – 87.8 mm SL, with a larger *Euthynnus alletteratus* (175.2 mm SL) collected using a dip net. The smallest and largest genetically identified scombrids from 2015 to 2017 were both *E. alletteratus*. Table 2 presents a summary of the genetically identified specimens. Table 3 shows the frequency of occurrence of countable meristic features (e.g., fin rays and finlets) from the genetically identified juvenile specimens.

Table 2. Summary of the life stage and size range of the genetically identified specimens separated by cruise series

Species	High-speed rope trawl 2010-2011		MOCNESS 2015-2017		Total	Size range (mm SL)
	Larvae	Juveniles	Larvae	Juveniles		
<i>Euthynnus alletteratus</i>	-	2	11	20	33	8.2 - 175.2
<i>Thunnus atlanticus</i>	-	12	4	1	17	8.3 - 121.7
<i>Thunnus albacares</i>	-	4	1	-	5	9.0 - 18.3
<i>Auxis rochei</i>	-	4	-	-	4	75.4 - 108.4
<i>Auxis thazard</i>	-	2	-	2	4	17.8 - 87.8
<i>Katsuwonus pelamis</i>	-	2	1	-	3	12.0 - 32.5
<i>Thunnus thynnus</i>	-	1	2	-	3	10.0 - 124.8
<i>Acanthocybium solandri</i>	-	1	-	-	1	47.0
Total per Life History Stage/Cruise	-	28	19	23	70	8.2 - 175.2

Table 3. Meristics of genetically identified juvenile scombrid

	First Dorsal Fin										Second Dorsal Fin						Anal Fin				
	10	11	12	13	14	15	16	17	23	10	11	12	13	14	15	16	11	12	13	14	15
<i>Acanthocybium solandri</i>									1				1							1	
<i>Auxis rochei</i>	1	1	1							2		2					2		2		
<i>Auxis thazard</i>		1	3							1	2	1					1	1		1	
<i>Euthynnus alletteratus</i>						5	11	4			1	10	10				1	8	5	6	1
<i>Katsuwonus pelamis</i>						1	1								1	1				1	1
<i>Thunnus albacares</i>					4										4				1	2	
<i>Thunnus atlanticus</i>				3	9	1							2	11					1	10	1
<i>Thunnus thynnus</i>				1									1						1		
Total	1	2	4	4	13	7	12	4	1	3	3	13	11	3	16	1	4	9	11	20	3

	Pectoral Fin											Caudal Fin						Top Finlets			Bottom Finlets		
	23	24	25	26	27	28	30	31	32	34	35	46	47	48	49	50	51	7	8	9	7	8	9
<i>Acanthocybium solandri</i>	1										1								1			1	
<i>Auxis rochei</i>	2		2										4					4		4			
<i>Auxis thazard</i>	1	2											3				1	2		3			
<i>Euthynnus alletteratus</i>			3	3	8	7						6	8	7			1	17	3	18	3		
<i>Katsuwonus pelamis</i>															1	1		2		2			
<i>Thunnus albacares</i>								1					2		1		1	2		3			
<i>Thunnus atlanticus</i>						2	2	3	1	1		2	3	5	2	1	1	11		11			
<i>Thunnus thynnus</i>								1								1		1			1		
Total	4	2	5	3	8	7	2	3	4	1	1	1	8	20	12	4	3	4	39	4	41	4	1

3.1.2. Morphological analyses.

The following paragraphs describe the key morphological characteristics used to identify larval and juvenile scombrids found in the GoM. The taxonomic results comprised a synthesis of existing knowledge based on: 1) the available literature, predominately (Nishikawa & Rimmer 1987, Richards 2005), 2) personal communications with Dr. John Lamkin and Aki Shiroza, M.S. (NOAA NMFS, Miami, Florida), and 3) original data presented herein. The meristics of the 16 scombrid species found in the GoM are included in the Appendix Table 2, in order to improve the identification process (Richards 2005).

The ratio of measured morphometric features of the genetically verified juvenile specimens were expressed in relation to SL and/or to HL. An r^2 value of 0.997 illustrated the tight correlation of HL and SL, suggesting that either can be used as a ratio base (Figure 7). The juvenile descriptions were based on and compared to morphometric ratios that were previously described for adult scombrids (Matsumoto et al. 1971, Hammond & Cupka 1975, ICCAT 2016a). For example, Hammond and Cupka (1975) identified the large gap between the first and second dorsal fins of *Auxis* spp. that is approximately 80% of the HL. A summary of the important morphometric ratios (represented as percentages) is listed by species and separated into size classes in Table 4 and 5.

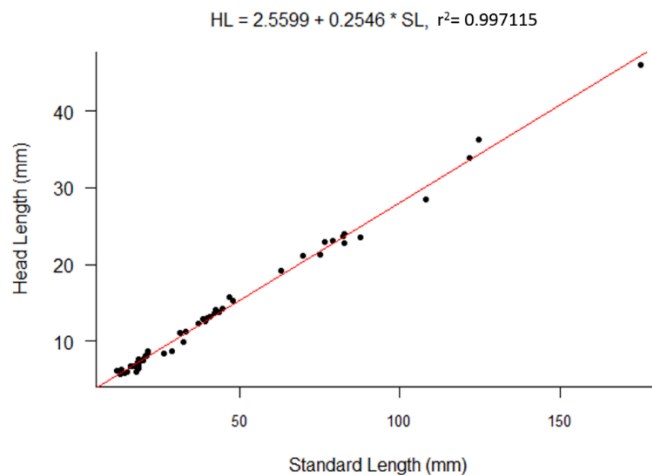


Figure 7. Correlation of standard length (SL) and head length (HL) from genetically identified juveniles

Table 4. Summary of morphometric ratios for genetically identified specimens. The ratios (presented as percentages) were compared to standard length (mm) and are presented by size class (0-50, 50-100, 100-150, and 150-200 mm SL). N represents the number of specimens collected for each species. Informative ratios are highlighted

Species	N	Interdorsal Length: First Dorsal Fin Length			Interdorsal Length: SL			Eye Diameter: Snout Length			
		0-50	50-100	100-150	0-50	50-100	100-150	0-50	50-100	100-150	150-200
<i>Acanthocybium solandri</i>	1	7	-	-	2	-	-	50	-	-	-
<i>Auxis rochei</i>	4	-	103-111	130	-	16-17	19	-	62-72	74	-
<i>Auxis thazard</i>	4	71-82	84	-	13	14	-	90-91	67	-	-
<i>Euthynnus alletteratus</i>	22	2-4	4-7	-	1	1-2	-	58-85	56-61	-	56
<i>Katsuwonus pelamis</i>	2	4-6	-	-	1-2	-	-	87	-	-	-
<i>Thunnus albacares</i>	4	4-5	-	-	1	-	-	100-122	-	-	-
<i>Thunnus atlanticus</i>	13	3-6	-	7	1	-	2	88-138	-	79	-
<i>Thunnus thynnus</i>	1	-	-	5	-	-	1	-	-	94	-

Table 5. Summary of morphometric ratios for genetically identified specimens. The ratios (presented as percentages) were compared to head length (mm) and are presented by size class (0-10, 10-20, 20-30, 30-40, 40-50 mm HL). N represents the number of specimens collected for each species. Informative ratios are highlighted

(a)	Species	N	Interdorsal Length: HL					Upper Jaw Length: HL				
			0-10	10-20	20-30	30-40	40-50	0-10	10-20	20-30	30-40	40-50
	<i>Acanthocybium solandri</i>	1	-	7	-	-	-	-	55	-	-	-
	<i>Auxis rochei</i>	4	-	-	56-71	-	-	-	-	37-38	-	-
	<i>Auxis thazard</i>	4	28-42	-	52	-	-	42-43	-	39	-	-
	<i>Euthynnus alletteratus</i>	22	1-2	1-5	4-6	-	-	54-62	47-51	45-47	-	43
	<i>Katsuwonus pelamis</i>	2	4-5	-	-	-	-	49-61	-	-	-	-
	<i>Thunnus albacares</i>	4	2-3	-	-	-	-	48-56	-	-	-	-
	<i>Thunnus atlanticus</i>	13	2-3	2-3	-	6	-	46-59	47-51	-	45	-
	<i>Thunnus thynnus</i>	1	-	-	-	4	-	-	-	-	41	-

(b)	Species	N	Eye Diameter: HL					Snout Length: HL				
			0-10	10-20	20-30	30-40	40-50	0-10	10-20	20-30	30-40	40-50
	<i>Acanthocybium solandri</i>	1	-	22	-	-	-	-	44	-	-	-
	<i>Auxis rochei</i>	4	-	-	19-21	-	-	-	-	28-31	-	-
	<i>Auxis thazard</i>	4	27-32	-	20	-	-	28-32	-	29	-	-
	<i>Euthynnus alletteratus</i>	22	24-28	19-27	18-19	-	17	38-44	31-35	32	-	31
	<i>Katsuwonus pelamis</i>	2	29	-	-	-	-	33	-	-	-	-
	<i>Thunnus albacares</i>	4	31-35	-	-	-	-	28-33	-	-	-	-
	<i>Thunnus atlanticus</i>	13	30-40	29-34	-	23	-	29-35	26	-	29	-
	<i>Thunnus thynnus</i>	1	-	-	-	23	-	-	-	-	25	-

3.1.2.1. Thunnini (tunas).

Thunnine larvae are the most difficult to identify to species-level. Large heads, triangular guts, and large jaws are distinguishable features of this tribe. Tunas also have relatively short bodies and typically lack pigmentation compared to other oceanic larvae. The first dorsal fin develops before the second dorsal fin, preopercular spines are present, and a supraoccipital crest is absent. Myomeres of thunnine larvae exceed 38, with all *Thunnus* spp. having 39 myomeres. Similar to the larvae, thunnine juveniles are poorly described and difficult to identify, with *Thunnus* being the most problematic genus. Reference tools for identifying larval thunnine specimens are presented in Table 6 and juveniles in Table 7, followed by a detailed synopsis of species-specific morphological descriptions.

Table 6. Quick reference chart for identifying larvae in the Tribe Thunnini

Genus/Species	Forebrain pigment present?	Cleithral symphysis pigment present?	Further identification
<i>Euthynnus alletteratus</i>	Yes	Yes	-
<i>Katsuwonus pelamis</i>	Yes	No	-
<i>Auxis</i> spp.	No	Yes	No lateral midline pigment (<i>A. rochei</i>) vs. lateral midline pigment (<i>A. thazard</i>)
<i>Thunnus</i> spp.	No	No	Investigate pigmentation patterns further

Table 7. Diagnostic key for identifying genera/species in the Tribe Thunnini using known meristics

Key to Thunnine Species/Genera	
1a. Pectoral fin rays ≥ 30 (30-36)	<i>Thunnus</i> spp.
1b. Pectoral fin rays < 30	2
2a. First dorsal fin ≤ 12 fin rays (10-12)	<i>Auxis</i> spp.
2b. First dorsal fin > 12 fin rays.....	3
3a. Second dorsal fin < 14 fin rays (11-13).....	<i>Euthynnus alletteratus</i>
3b. Second dorsal fin ≥ 14 fin rays (14-16).....	<i>Katsuwonus pelamis</i>

Auxis spp. – Bullet and Frigate Mackerel

Pigmentation patterns differentiate *Auxis rochei* (Risso, 1810) and *Auxis thazard* (Lacepède, 1800). Primary characteristics for identifying *A. rochei* include: pigmentation on the cleithral symphysis, a row of pigmentation on the dorsal and ventral margins of tail, and the lack of pigmentation on the forebrain (Figure 8a). Pigmentation is also located on their midbrain, hindbrain, and gut. Jaw pigmentation and Post-Anal Ventral (PAV) pigment may be present. The previously described pigmentation patterns for *A. rochei* also apply to *A. thazard*, except *A. thazard* larvae possess a line of pigmentation along the tail as seen in Figure 8c. Additional dorsal midline spots appear as larvae develop.

Meristically, juvenile *Auxis* spp. are separated from other thunnine species by having less than 30 pectoral fin rays (23-25) and between 10-12 first dorsal fin rays (Table 7, Appendix Table 2). Juvenile *A. rochei* and *A. thazard* are pictured in Figure 8b and d. Adult *Auxis* spp. can be distinguished from other tuna species by the wide gap between the first and second dorsal fins, which is approximately 80% of their HL. However, the interdorsal length of juvenile *Auxis* spp. ranging from 17.8 to 108.4 mm SL had not reached the adult ratio (80% of their HL, Figure 9 and Table 5). The ratio increased, but did not level off at the adult ratio. Additionally, the interdorsal length of adult *Auxis* spp. is approximately equal to the first dorsal length. Juvenile *A. rochei* exceeded the 1:1 ratio, while juvenile *A. thazard* possessed a ratio that is slightly lower than the previously recorded adult ratio (Figure 10 and Table 5).

Adult identifications between the two *Auxis* spp. is problematic. Both *Auxis* spp. have between 38 and 47 gill rakers, which indicates that gill rakers are not useful in identifying the two species. While investigating the relationship between interdorsal length and SL, it appeared that the two species could possibly be separated (Figure 11). Results show that the interdorsal length of *A. rochei* was between 16 and 19% of the SL, while the interdorsal length of *A. thazard* was between 13 and 14% of the SL (Table 4).

In addition to interdorsal length being a key feature for identifying juvenile *Auxis* spp., the upper jaw length compared to HL was a slightly informative ratio. *Auxis* spp.

between 17.8 and 108.4 mm SL had a smaller upper jaw length to HL ratio compared to all other thunnine species and *Acanthocybium solandri* (Figure 12 and Table 5).

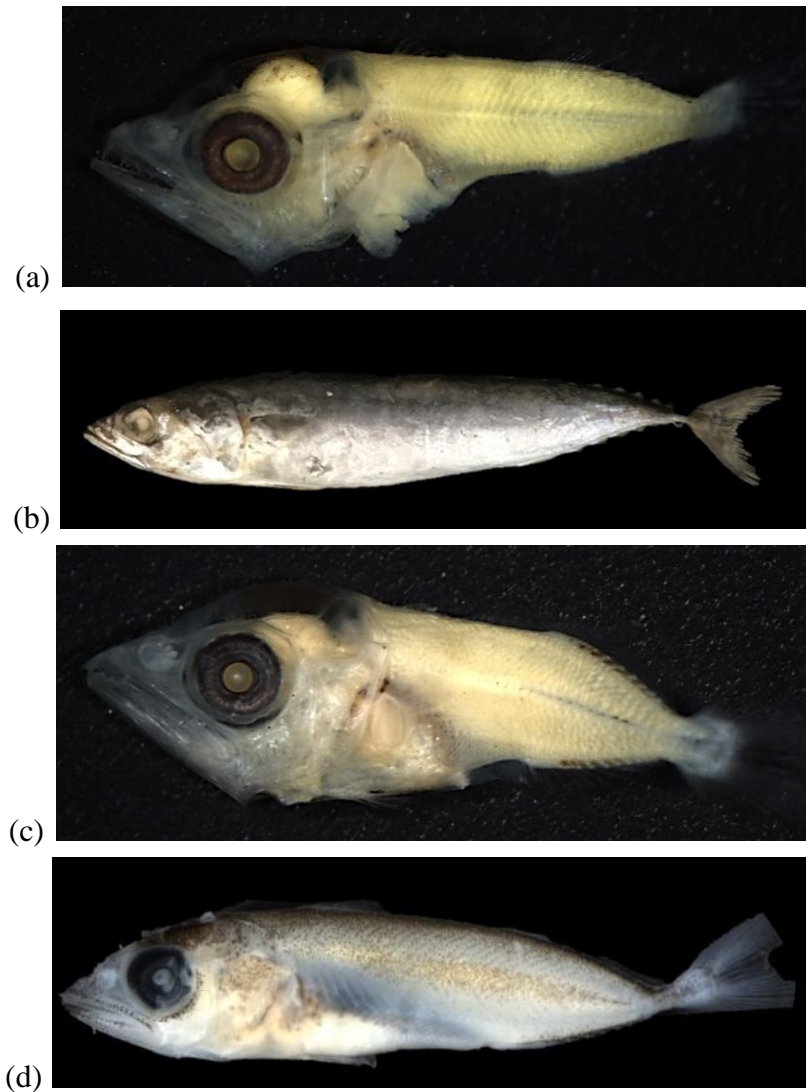


Figure 8. Images of (a) larval *Auxis rochei*, (b) juvenile *Auxis rochei*, (c) larval *Auxis thazard*, and (d) juvenile *Auxis thazard*.

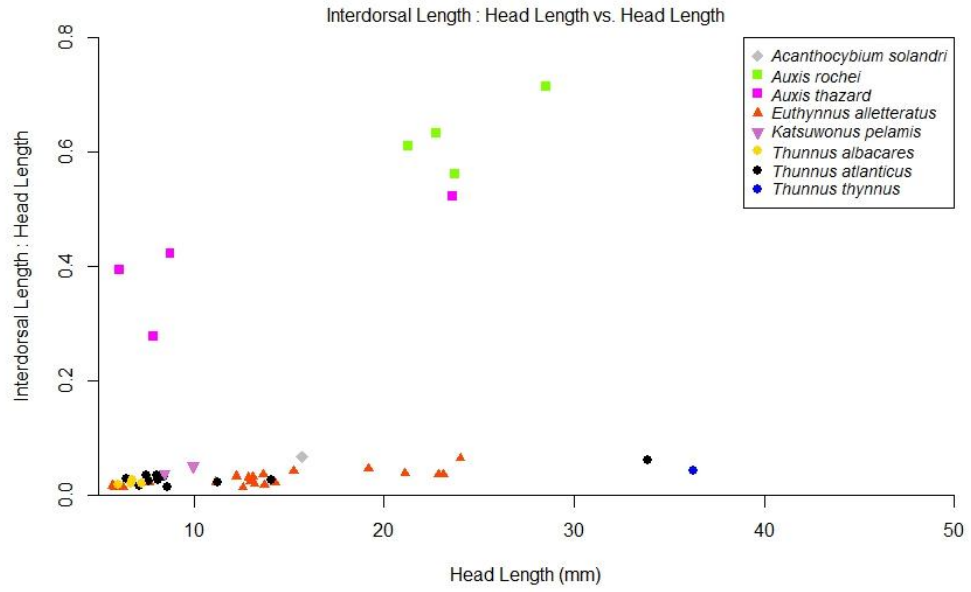


Figure 9. Ratio of interdorsal length to head length vs. head length for all genetically identified juvenile specimens.

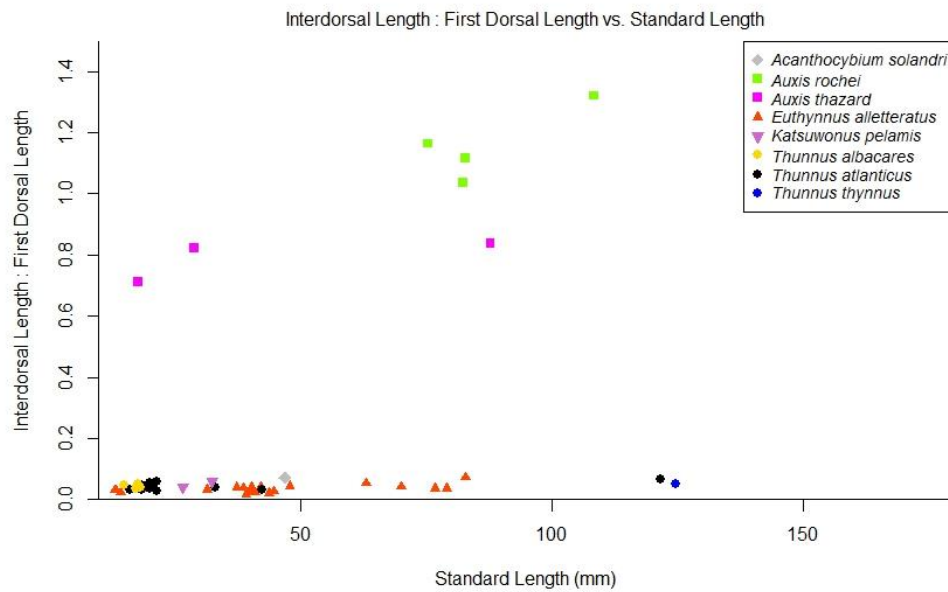


Figure 10. Ratio of interdorsal length to first dorsal length vs. standard length for all genetically identified juvenile specimens.

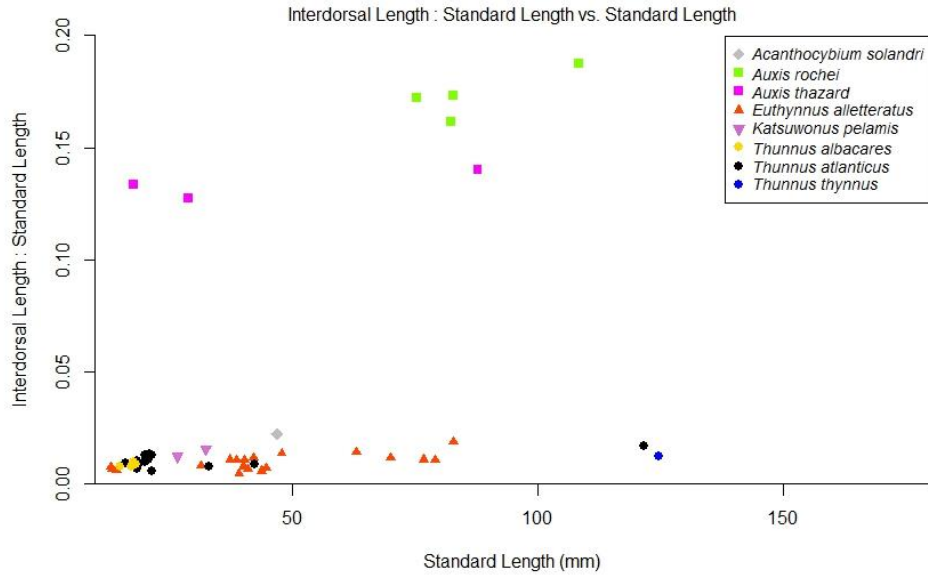


Figure 11. Ratio of interdorsal length to standard length vs. standard length for all genetically identified juvenile specimens.

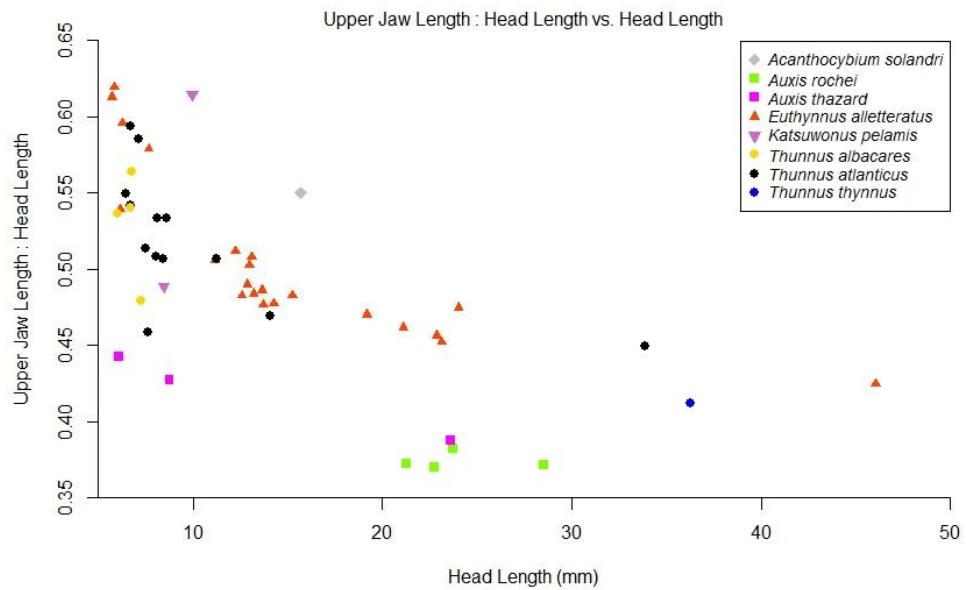


Figure 12. Ratio of upper jaw length to head length vs. head length for all genetically identified juvenile specimens.

Euthynnus alletteratus – Little Tunny

Euthynnus alletteratus (Rafinesque, 1810) larvae are distinguished from other scombrids by their unique combination of pigmentation, development patterns, and myomeres. Pigmentation on the forebrain and cleithral symphysis along with early development of the pigmented first dorsal fin (*ca.* 6.0 mm SL, Figure 13a) are critical taxonomic identifiers of *E. alletteratus*. A large amount of jaw pigment (tips of both jaws and ramus of lower jaw) is a distinct characteristic of *E. alletteratus*. Pigmentation on the jaw tip may wrap around the symphysis of the upper and lower jaws. Larval *E. alletteratus* also have pigmentation on the midbrain and a row of ventral tail midline pigment spots. *Euthynnus alletteratus* has 39 myomeres, and the PAV pigment series may be present. Larval *E. alletteratus* may have a weak, rounded supraoccipital crest, although the crest may be absent.

Juvenile *E. alletteratus* are separated from other thunnine species by having less than 30 pectoral fin rays (25-29), more than 12 first dorsal fin rays (13-17) and less than 14 second dorsal fin rays (11-13) (Table 7, Appendix Table 2). Juveniles collected in this study are pictured in Figure 13b and c. Their interdorsal length was previously recorded as less than the diameter of the eye apart; however, this feature was shared with *Thunnus* spp.

When comparing juvenile *E. alletteratus* to juvenile *Thunnus* spp., the ratios of eye diameter to snout length and eye diameter to HL were lower for *E. alletteratus* (Figure 14 and 15). However, the ratio of snout length to HL was higher in *E. alletteratus* compared to *Thunnus* spp. (Figure 16 and Table 5). Thus, these were informative ratios when determining the differences between these two taxonomic groups. The key features for morphology describing juvenile *E. alletteratus* were snout length and eye diameter.

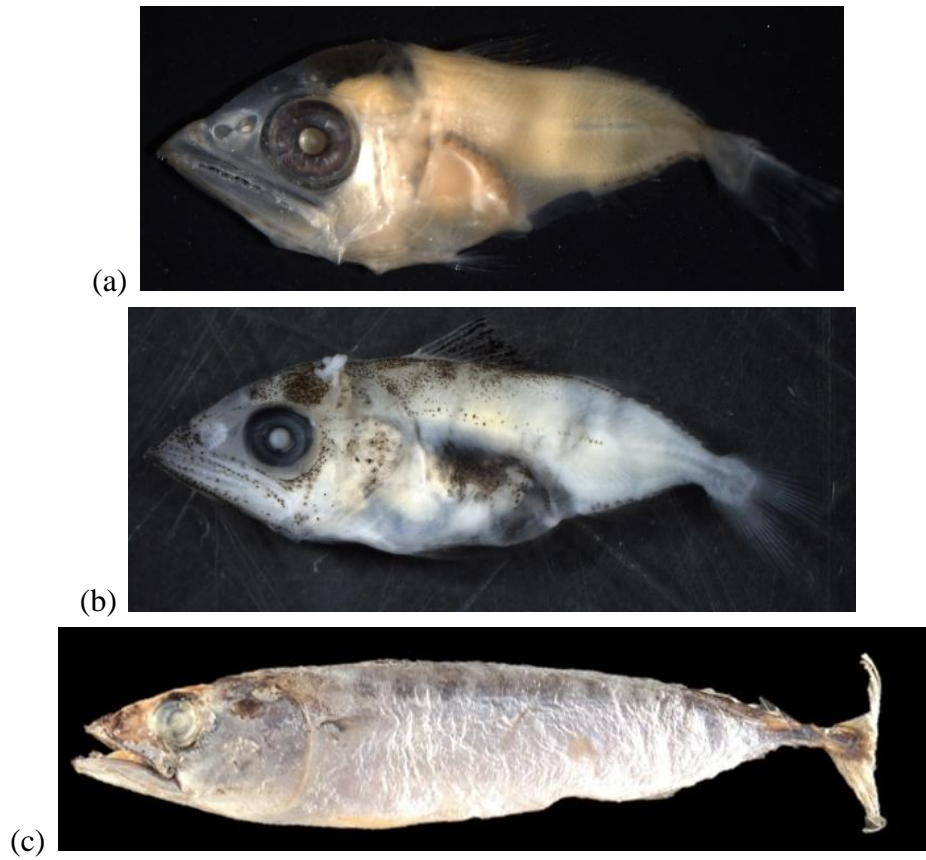


Figure 13. Images of (a) larval and (b and c) juvenile *Euthynnus alletteratus*.

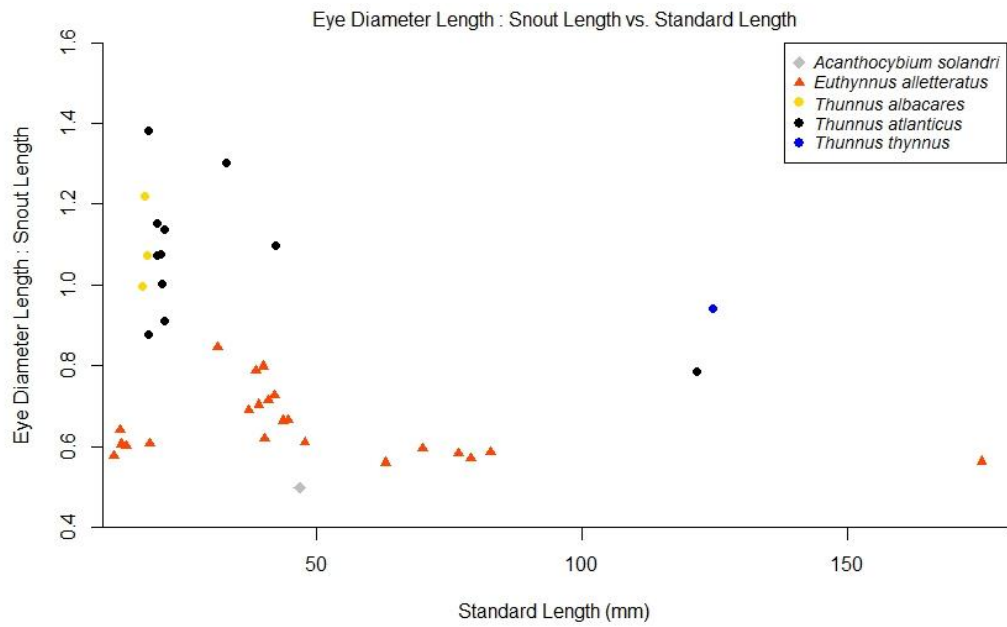


Figure 14. Ratio of eye diameter to snout length vs. standard length for genetically identified juvenile specimens, including *Acanthocybium solandri*, *Euthynnus alletteratus*, and all *Thunnus* spp.

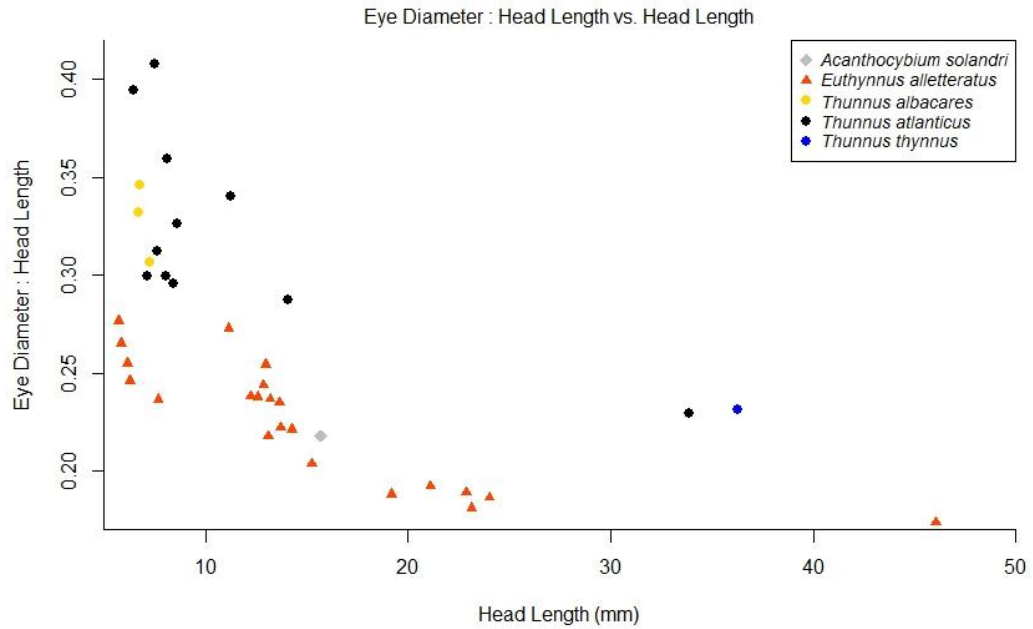


Figure 15. Ratio of eye diameter to head length vs. head length for genetically identified juvenile specimens, including *Acanthocybium solandri*, *Euthynnus alletteratus*, and all *Thunnus* spp.

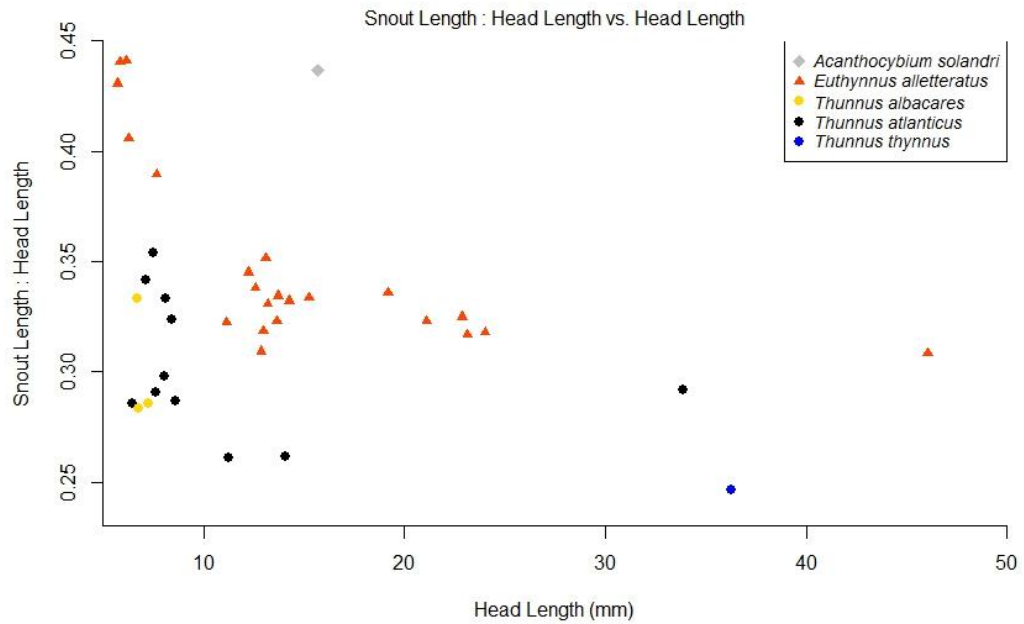


Figure 16. Ratio of snout length to head length vs. head length for genetically identified juvenile specimens, including *Acanthocybium solandri*, *Euthynnus alletteratus*, and all *Thunnus* spp.

Katsuwonus pelamis – Skipjack Tuna

Katsuwonus pelamis (Linnaeus, 1758) larvae are characterized by forebrain pigmentation, lack of pigmentation on the cleithral symphysis (separating this species from *E. alletteratus*), and two to three ventral tail midline spots as seen in Figure 17a. A ventral tail midline spot appears blotchier on *K. pelamis* compared to single dot, which is distinct of *T. atlanticus* larvae. Pigmentation is rarely found on the dorsal margin of the tail. Black pigmented spots may appear on the jawline, but they do not create a full jawline of pigmentation, such as *E. alletteratus*. Larvae also have pigmentation on the midbrain, hindbrain, and gut. The first dorsal fin appears late (*ca.* 8.0 mm SL), and *K. pelamis* has 41 myomeres.

Juvenile *K. pelamis* are separated from other thunnine species by having less than 30 pectoral fin rays (26-28), more than 12 first dorsal fin rays (14-16), and greater than or equal to 14 second dorsal fin rays (14-16, Table 7, Appendix Table 2). Fin ray counts of well-developed second dorsal fins can be used to differentiate smaller *E. alletteratus* (11-13) and *K. pelamis* (14-16) specimens. Juvenile *K. pelamis* are pictured in Figure 17b.

The morphometric analyses in this study did not differentiate this species from the other scombrids, thus the gill raker counts of the two genetically identified specimens were analyzed. Adult *K. pelamis* have between 53 and 63 gill rakers. At 26.8 mm SL, *K. pelamis* had 25 gill rakers (3+1+21). The top gill rakers were small buds and underdeveloped. The lower lobe had several notches where more gill rakers were apparently going to develop. Additionally at 32.5 mm SL, a juvenile *K. pelamis* had approximately 29 gill rakers (4+25). Again, the four gill rakers on the top were small buds and underdeveloped, and the bend did not possess a gill raker in this specimen. The lower lobe of this specimen had developed more gill rakers than the smaller specimen. It is most likely that as the bone grows, more gill rakers would grow, mainly on the longer lower lobe. Because the juvenile *K. pelamis* still did not possess the full complement of adult gill rakers at 32.5 mm SL, gill raker counts could not be used to identify this species. However, it is important to note that *K. pelamis* appears to have higher gill raker counts, even at this smaller size, compared to other thunnine species.

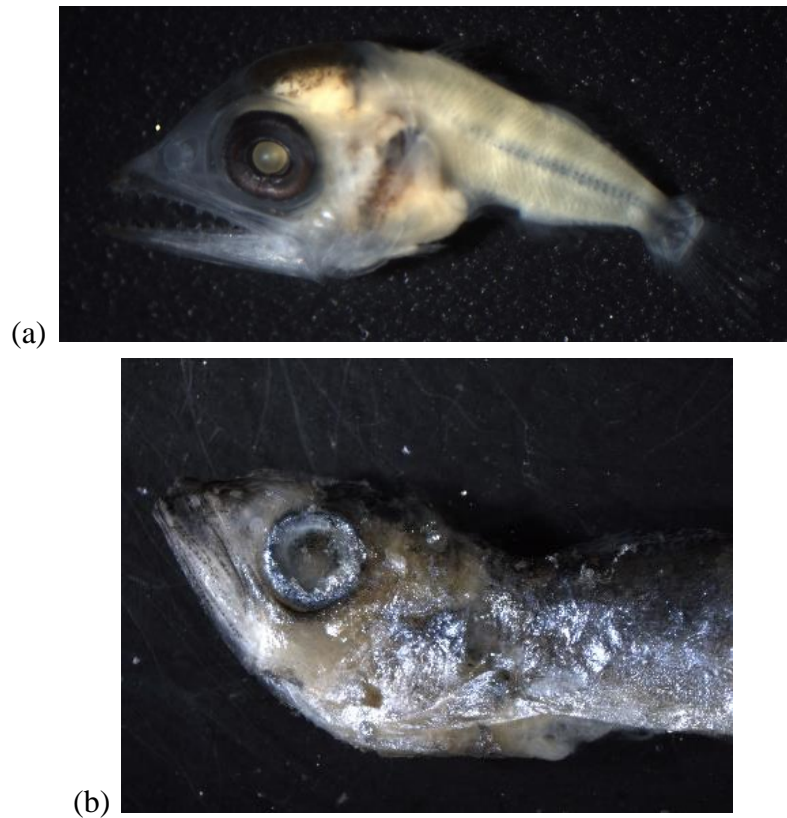


Figure 17. Images of (a) larval and (b) juvenile *Katsuwonus pelamis*.

Thunnus spp. – “True Tunas”

Thunnus larvae have large heads, triangular guts, a short body, and large jaws. They lack pigmentation on the cleithral symphysis and forebrain. There are a few or no spots on ventral tail midline. Larval species-specific pigmentation patterns are explained below. Meristically, juvenile *Thunnus* spp. are separated from other thunnine species by having greater than or equal to 30 pectoral fin rays (30-36, Table 7, Appendix Table 2). However, species cannot be distinguished based on fin ray counts. As a result, other characteristics needed to be analyzed.

When comparing juvenile *Thunnus* spp. to juvenile *E. alletteratus*, the ratios of eye diameter to snout length and eye diameter to HL were higher for *Thunnus* spp. (Figure 14 and 15). However, the ratio of snout length to HL was lower in *Thunnus* spp. compared to *E. alletteratus* (Figure 16). Thus, these were informative ratios when determining the differences between these two taxonomic groups. The key morphological features for identifying juvenile *Thunnus* spp. were snout length and eye diameter.

Figures 9-12 and 14-16 show that juvenile *Thunnus* spp. could not be separated with the available sample set. Larger *T. thynnus* and *T. atlanticus* had similar ratios throughout (Table 4 and 5). Additionally, smaller *T. albacares* and *T. atlanticus* possessed similar ratios as well, which is comparable to their larval stage, when *T. atlanticus* specimens lack ventral midline pigmentation. Larval and juvenile *T. alalunga* and *T. obesus* were excluded from the morphometric analyses, as they were not collected in this study. Genetic identifications remain necessary for juvenile *Thunnus* spp. until more distinct characteristics are identified.

Thunnus alalunga – Albacore

Thunnus alalunga (Bonnaterre, 1788) larvae possess pigmentation on their midbrain, gut, first dorsal fin (when greater than 5.0 mm SL) and tips of their jaws (when greater than 7.0 mm SL). From 5.0 to 9.0 mm SL, pigment is only seen on the upper jaw. Pigmentation is not present on the ventral tail or lower jaw tip. Specimens between 9.0 and 10.8 mm SL start developing juvenile pigment, which begins appearing on the outside of the lower jaw. Larval and juvenile *T. alalunga* were not collected in this study. Adults have a striated liver with a large center lobe and between 25 and 31 gill rakers.

Thunnus albacares – Yellowfin Tuna

Thunnus albacares (Bonnaterre, 1788) larvae have pigmentation on the midbrain, gut, tips of their jaws, and first dorsal fin (when greater than 5.0 mm SL, Figure 18a). From 4.5 to 7.0 mm SL (and as early as 3.8 mm SL), pigment is only seen on the lower jaw tip, but from 7.0 to 9.0 mm SL, pigment is present on both the upper and lower jaws. Lower jaw pigment is found inside the jaw of *T. albacares* that are 9.0 to 10.0 mm SL. For specimens less than 4.5 mm SL, *T. albacares* and *T. alalunga* are morphologically indistinguishable, unless there is lower jaw pigment present, in which the larval specimen would be *T. albacares*.

Larval *T. albacares* are differentiated from *T. atlanticus* by the absence of ventral tail midline spots. Due to the lack of pigmentation being the defining characteristic for this species, the certainty of morphological identifications is lacking. Therefore, questionable specimens in this study were labeled as *Thunnus* spp. Genetic analyses would verify

identifications, although the majority of specimens in this study were previously preserved in formalin. Moreover, the genetically identified juvenile *T. albacares* (Figure 18b) showed that they develop spots along their ventral tail midline, similar to larval *T. atlanticus*. This identifies a controversial feature for differentiating these two species and it needs to be reconsidered once the individual scombrid is considered a juvenile.

The morphometric analyses in this study did not differentiate *T. albacares* from other *Thunnus* spp. (Table 4 and 5). Thus, the gill raker counts of the largest, undamaged genetically identified specimen (17.9 mm SL) were analyzed. Adult *T. albacares* have between 26 and 34 gill rakers. The gill rakers of a juvenile *T. albacares* at 17.9 mm SL has underdeveloped gill rakers. The top and bend of the gill raker did not have gill rakers, and there were approximately four gill rakers that were visible on the bottom. Since the genetically identified juvenile *T. albacares* still did not possess the full complement of adult counts, gill rakers could not be used to identify this species. The size range at which adult gill rakers fully develop remains unknown. Additionally, the livers of adult *T. albacares* lack striations and have a larger right lobe. Due to the small size of the genetically identified specimens, the livers were not analyzed.



Figure 18. Images of (a) larval and (b) juvenile *Thunnus albacares*.

Thunnus atlanticus – Blackfin Tuna

Thunnus atlanticus (Lesson, 1831) larvae have pigmentation on the midbrain, gut, jaw tips, and first dorsal fin (when greater than 5.0 mm SL). The diagnostic characteristics of *T. atlanticus* include: the presence of small pigment spots on the ventral tail midline and the absence of black pigmentation on the forebrain, hindbrain, and cleithral symphysis (Figure 19a). The ventral tail midline spot on *T. atlanticus* appears as a more circular dot compared to a blotchy spot, which identifies *K. pelamis* larvae. A well-developed first dorsal fin also helps differentiate *T. atlanticus* and *K. pelamis*, in which the latter develops the dorsal fin later. Moreover, *T. atlanticus* has two morphs: one with ventral tail midline pigment and the other without, which in turn could easily be misidentified as *T. albacares*. Thus, the lack of ventral pigmentation led to *Thunnus* spp. as the lowest taxonomic identification of these taxonomically challenging specimens.

The morphometric analyses in this study did not differentiate *T. atlanticus* from other *Thunnus* spp. (Table 4 and 5). At smaller sizes, their ratios were similar to *T. albacares*, and at larger sizes, they mimicked *T. thynnus* ratios. Thus, the gill raker counts of the two largest genetically identified specimens were analyzed. Adult *T. atlanticus* have between 19 and 25 gill rakers. The largest *T. atlanticus* specimen (121.7 mm SL) had 21 gill rakers (5+1+15), exhibiting adult counts. The second largest specimen (42.5 mm SL) only had 16 gill rakers (6+10), which demonstrated that a juvenile at this size does not possess adult gill raker counts. As a result, gill raker counts could only identify *T. atlanticus* specimens that were greater than or equal to 121.7 mm SL. In addition, adult *T. atlanticus* livers lack striations and have a larger right lobe. The livers of both the 121.7 and 42.5 mm SL (Figure 20a and b) genetically identified specimens possessed these features. Juvenile *T. atlanticus* are pictured in Figure 19b and c.

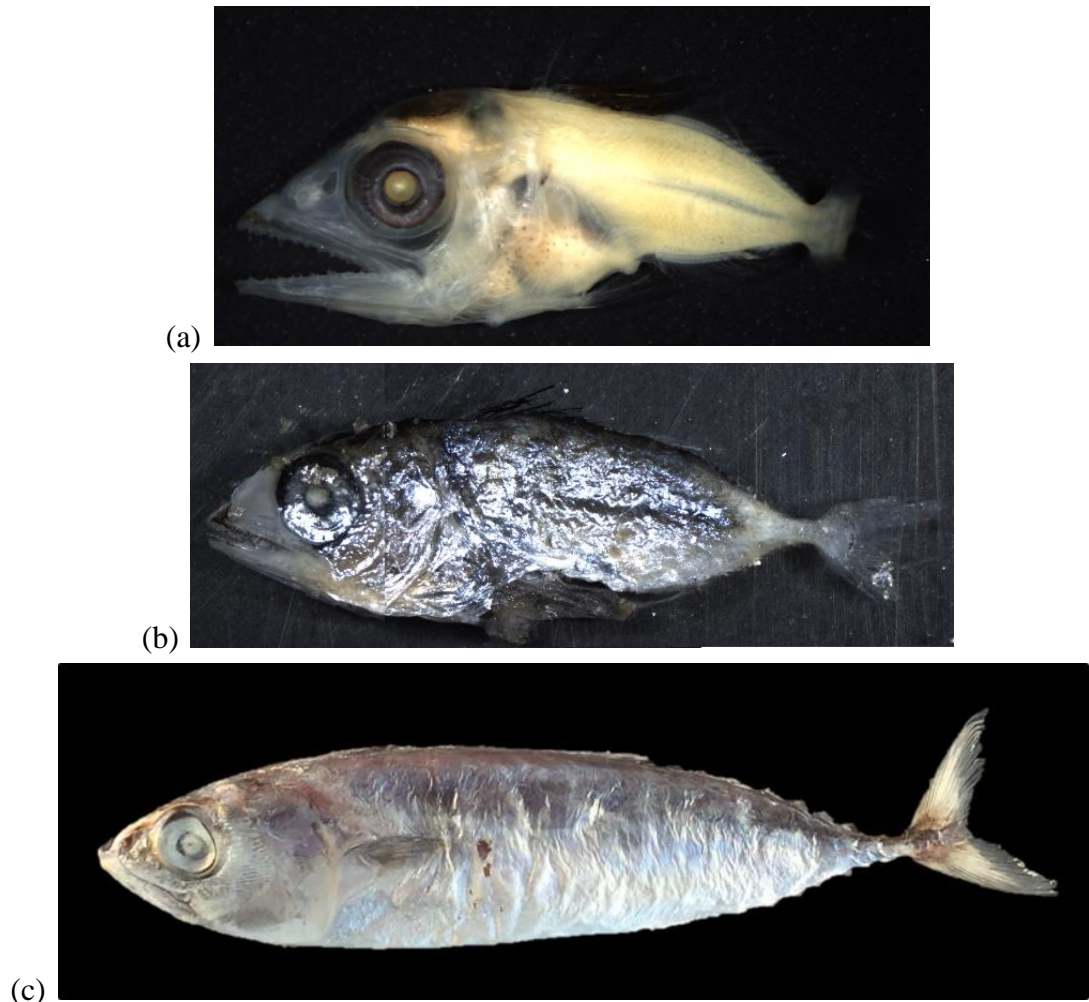


Figure 19. Images of (a) larval, and (b and c) juvenile *Thunnus atlanticus*.

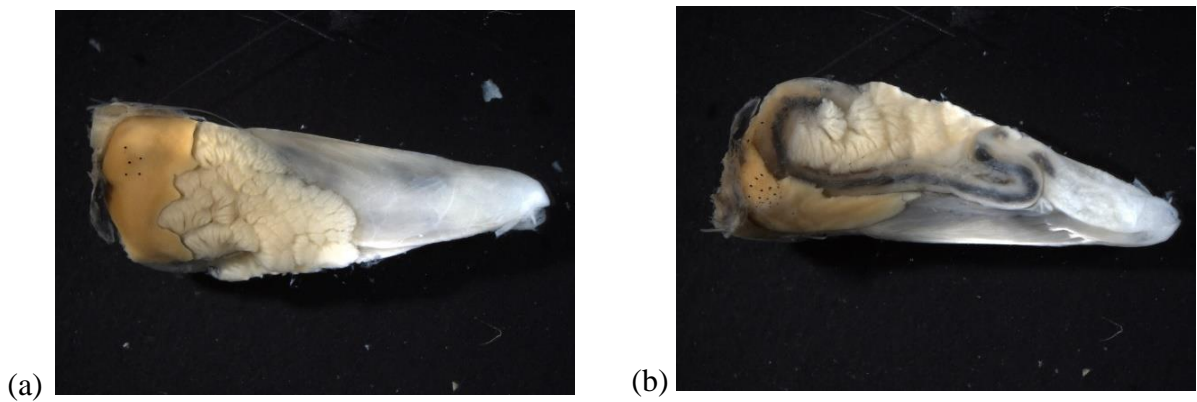


Figure 20. The (a) left and (b) right lobes of a liver from a genetically identified *Thunnus atlanticus* specimen (42.5 mm SL), preserved in 99% ethanol.

Thunnus obesus – Bigeye Tuna

Thunnus obesus (Lowe, 1839) larvae possess pigmentation on the midbrain, gut, tips of the jaws, ventral margin of the tail, and first dorsal fin (when greater than 5.0 mm SL). The ventral tail spots are large and distinct, which is characteristic of this species. The larger size of the ventral spots differentiates *T. obesus* from *T. atlanticus*. The presence or absence of the large, distinct ventral tail spots is the only method for distinguishing *T. obesus* from *T. albacares*, as clearing and staining mechanisms do not separate the two species. Adults have 23 to 31 gill rakers and livers with striations along the ventral edges of the three equal-sized lobes. Larval and juvenile *T. obesus* were not collected in this study.

Thunnus thynnus – Atlantic bluefin tuna

Thunnus thynnus (Linnaeus, 1758) larvae have pigment on the midbrain, hindbrain, gut, tips of jaws, dorsal and ventral margins of the tail, and first dorsal fin (when greater than 5.0 mm SL, Figure 21a and b). One to four pigment spots on the dorsal midline identify *T. thynnus* larvae. *Thunnus thynnus* is the only species of the genus *Thunnus* to have dorsal tail pigmentation, and it rarely possesses lateral pigmentation as well. The lack of forebrain pigmentation differentiates *T. thynnus* from *K. pelamis* when there is a single pigment spot on dorsal edge of caudal peduncle. *Thunnus thynnus* larvae also lack pigmentation on the cleithral symphysis.

The morphometric analyses in this study did not differentiate *T. thynnus* from other *Thunnus* spp. Thus, the gill raker counts of the only genetically identified specimen were analyzed. Adult *T. thynnus* have between 34 and 43 gill rakers. The *T. thynnus* specimen (124.8 mm SL, Figure 21c) had 36 gill rakers (9+1+26), exhibiting adult counts. As a result, gill raker counts could only identify *T. thynnus* specimens that were greater than or equal to 124.8 mm SL. Additionally, adult *T. thynnus* livers possess striations and all three lobes are equal in length. The liver of the frozen, genetically identified specimen (124.8 mm SL) had equal lobes, but lacked striations, indicating that preservation methods may have altered its appearance or the striations do not develop at this size.

The pectoral fin length for an adult *T. thynnus* is less than 80% of the HL (ICCAT 2016a). However, the pectoral fin length for a juvenile *T. thynnus* at 124.8 mm SL was 43% of the HL (Table 5). Presumably the pectoral fin length in juveniles will grow allometrically until reaching the adult proportion. This study shows that a 124.8 mm SL, *T. thynnus* does not yet have the adult length ratios.

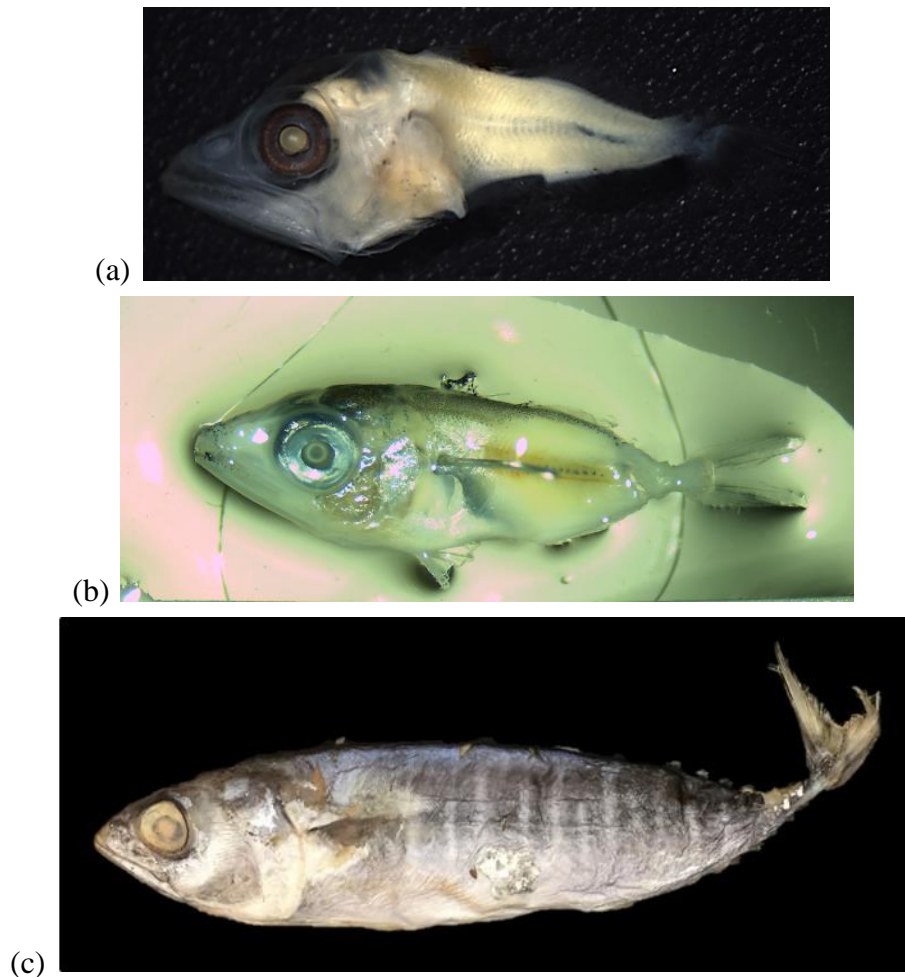


Figure 21. Images of (a and b) larval and (c) juvenile *Thunnus thynnus*.

3.1.2.2. Sardini (bonitos).

One species of the Sardini tribe occurs throughout the GoM and Atlantic Ocean, *Sarda sarda*.

Sarda sarda – Atlantic Bonito

Sarda sarda (Bloch, 1793) larvae have a weakly developed and rounded supraoccipital crest. The snout is about 1-1.5 times the eye diameter and the mouth is large.

Pigmentation is present on the tips of the jaws, but there is no pigment found inside the mouth or on the gular area (Figure 22). Additional pigmentation is found on the forebrain, midbrain, gut, cleithral symphysis and pelvic fin rays. A prominent pigment spot on the caudal peduncle above the hypural plate along with ventral tail pigment spots distinguish *Sarda* spp. larvae from other scombrids. Ventral tail pigment spots migrate dorsally above the ventral midline between the myomeres. *Sarda sarda* have 53 myomeres, which is similar to *Scomberomorus maculatus*. Juvenile *Sarda sarda* were not collected in this study. Fin ray counts (Appendix Table 2) and gill raker counts (16-22) can differentiate this species from other scombrids once the adult features fully develop.



Figure 22. Image of a larval *Sarda sarda*.

3.1.2.3. Scombrini (mackerels).

One species of the Sardini tribe spawns in the GoM, *Scomber colias*. Unlike other scombrid species in the GoM, *Scomber* is the only genus that lacks preopercular spines, a large head, and large jaws in the larval phase.

Scomber colias – Atlantic Chub Mackerel

The absence of preopercular spines and the order of fin development distinguish *Scomber colias* Gmelin, 1789 from other scombrid larvae. Additionally, the first dorsal fin of *S. colias* appears late, specifically after the second dorsal and anal fins, which is also unique to this species. Larval *S. colias* have pigmentation on their midbrain, hindbrain, over the gut and ventral margin of tail. *Scomber colias* larvae have smaller jaws and a rounder snout compared to other scombrid species. *Scomber colias* has 31 myomeres. Larval *S. colias* were not collected in this study.

Juvenile *S. colias* are separated from other scombrids by having 4-5 top finlets and 5 bottom finlets (Figure 22, Appendix Table 2) Moreover, fin ray counts and gill raker counts (25-35) can be used to identify this species once the adult features are fully developed.



Figure 23. Image of a juvenile *Scomber colias*.

3.1.2.4. Scomberomorini (Spanish mackerels).

The Scomberomorini tribe consists of two distinct genera: the monotypic *Acanthocybium solandri* and *Scomberomorus* spp. All larval *Scomberomorus* spp. possess a pointed and distinct supraoccipital crest, preopercular spines, a long snout that is about twice the diameter of their eye, a large mouth, and well-developed teeth. The first dorsal fin of *Scomberomorus* spp. develops before the second dorsal fin. This genus usually has pigment in the mouth or gular area. *Scomberomorus* spp. have more than 48 myomeres, except for *Scomberomorus cavalla* (41-43). Meristic counts used to identify *Scomberomorus* spp. are found in Appendix Table 2. The monotypic *Acanthocybium solandri* has a unique morphology, which will be explained below.

Acanthocybium solandri – Wahoo

Acanthocybium solandri (Cuvier, 1832) larvae possess a long and slender body. Larval *A. solandri* have long snouts that distinguish them from other larval scombrid species. High myomere counts (62-64) characterize this species. *Acanthocybium solandri* larvae develop the second dorsal fin before the first dorsal fin and lack a supraoccipital crest. Pigmentation is found on the jaw tips, nasal area, forebrain, midbrain, and over the gut. There is also a ventral spot on the tail in addition to a spot under their second dorsal fin (Figure 24a).

Juveniles are separated by their fin ray counts, with their high first dorsal counts (23-27) and low second dorsal counts (11-16; Figure 24b, Appendix Table 2). They also lack gill rakers. When analyzing the ratio of eye diameter to snout length, *A. solandri* has the lowest ratio compared to *E. alletteratus* and *Thunnus* spp. (Table 5 and Figure 14). The snout length is approximately two times the eye diameter (eye diameter was 50% of the snout length) for an individual at 47.0 mm SL. Similar to the larval and adult phases, the snouts of juvenile *A. solandri* cover a large proportion of the head. It has been previously reported that the snout length is 50% of the HL in adult *A. solandri*. Results from this study indicate that for an individual at 47.0 mm SL, the snout length was approximately 44% of the HL. Therefore, the adult size range is still not obtained by an individual at 47.0 mm SL. Thus, the ratio of eye diameter to snout length and the ratio of snout length to HL were informative ratios used to identify this species. The key features for morphologically identifying juvenile *A. solandri* were snout length and eye diameter.

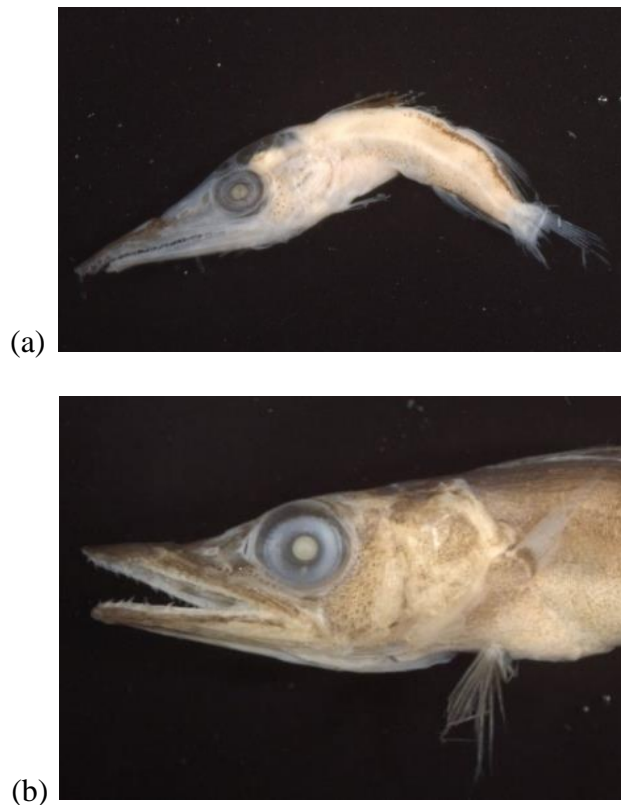


Figure 24. Images of (a) larval and (b) juvenile *Acanthocybium solandri*.

Scomberomorus brasiliensis – Serra

Scomberomorus brasiliensis Collette, Russo & Zavala-Camin, 1978 larvae remain undescribed. In past studies, *S. brasiliensis* has been erroneously identified as *Scomberomorus maculatus*. All *Scomberomorus* spp. in this study were identified to species, prolonging the taxonomic uncertainty of *S. brasiliensis*.

Scomberomorus cavalla – King mackerel

The previous morphological description of *Scomberomorus* spp. applies to *Scomberomorus cavalla* (Cuvier, 1829). Larval *S. cavalla* have pigmentation on their forebrain, midbrain, over their gut, cleithral symphysis, and ventral margin of their tail (Figure 25). Its long preopercular spine, distinct patch of pigmentation on each side of the tongue, and low myomeres counts (41-43) characterize *S. cavalla* from other *Scomberomorus* spp. The PAV pigment series and pigment spots on the inside of the lower jaw rami are present. Juvenile *S. cavalla* were not collected in this study. Adults possess 9 – 10 gill rakers.



Figure 25. Image of a larval *Scomberomorus cavalla*.

Scomberomorus maculatus – Spanish Mackerel

Scomberomorus maculatus (Mitchill, 1815) larvae possess pigmentation on the forebrain, midbrain, over gut, cleithral symphysis, ventral margin of the tail, and gular area. *Scomberomorus maculatus* larvae are distinguished from other *Scomberomorus* spp. by a distinct patch of pigment by the gular area. *Scomberomorus maculatus* have 53 myomeres. Adults possess 10-16 gill rakers. Larval and juvenile *S. maculatus* were not collected in this study.

Scomberomorus regalis – Cero

Scomberomorus regalis (Bloch, 1793) larvae have pigmentation on the forebrain, midbrain, over gut, cleithral symphysis, ventral margin of tail, and gular area. Gular pigmentation is used to distinguish *S. regalis* from other *Scomberomorus* spp. The supraoccipital crest, myomeres, and pigmentation separate *S. regalis* larvae from other scombrid species. *Scomberomorus regalis* has 38 myomeres, similar to *S. brasiliensis*. Adults have between 12 and 18 gill rakers. Larval and juvenile *S. regalis* were not collected in this study.

3.2. Larval and juvenile scombrids faunal composition and ecology.

3.2.1. Assemblage structure.

3.2.1.1. Comparison of fauna collected by different gear types and at different times of collection.

Table 8 lists the ranked abundances and frequency of occurrence of all scombrids collected during the three cruise series. The highest number of species collected ($n = 11$) occurred during the MOCNESS 2011 sampling, while the lowest number ($n = 6$) was collected during the MOCNESS 2015 – 2017 sampling (Table 8 and Figure 26). During the three cruise series, the five most frequently caught taxa included: *E. alletteratus*, *T. atlanticus*, *Auxis thazard*, *Thunnus* spp., and *K. pelamis*. However, differences in abundances and catch frequencies were observed.

Higher abundance estimates were associated with the MOCNESS sampling, typically 10-fold higher than those of high-speed rope trawl sampling. In 2011, the MOCNESS collected 10.85 individuals (ind., hereafter) 10^{-6} m^{-3} , while in 2015-2017 a total of 7.67 ind. 10^{-6} m^{-3} were collected. The high-speed rope trawl collected 1.15 ind. 10^{-6} m^{-3} . However, taxa were collected more frequently with the high-speed rope trawl. The frequency of occurrence for the family Scombridae was highest with the high-speed rope trawl (50%) compared to the MOCNESS in 2011 (15 %) and 2015-2017 (5%).

Differences were also seen in the size ranges collected by each gear type. Figure 27 shows the lengths of scombrids collected by each sampling method. The MOCNESS primarily collected larval scombrids, with a few juveniles. The high-speed rope trawl

collected only juveniles, and these were typically larger than the juveniles collected by the MOCNESS. The null hypothesis of a non-parametric Kruskal-Wallis test was rejected, which indicated that there was a significant difference between the SLs of three cruise series ($p \ll 0.0001$). A non-parametric, multiple-comparison, post-hoc test utilizing the *pgirmess* package in R indicated that there were significant differences among the three cruise series.

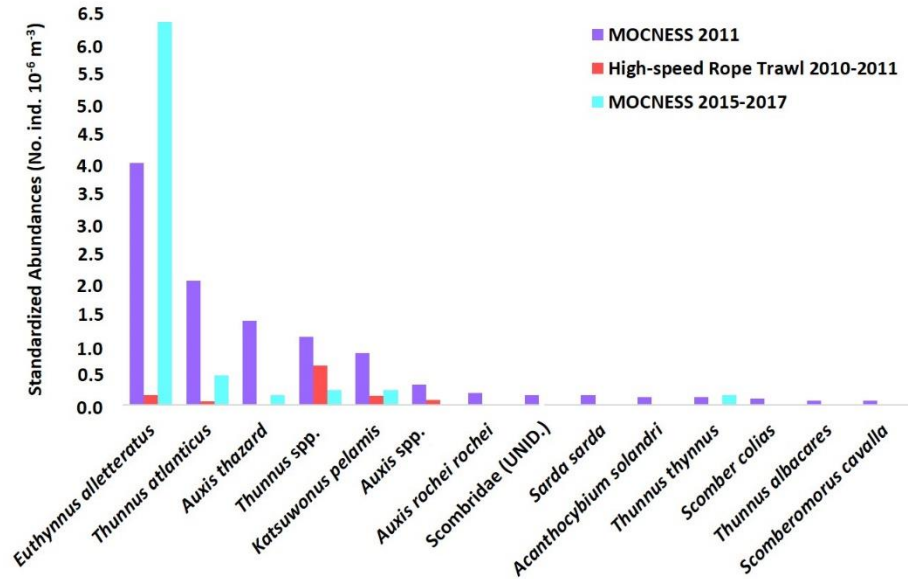


Figure 26. Standardized abundances from the three cruise series.

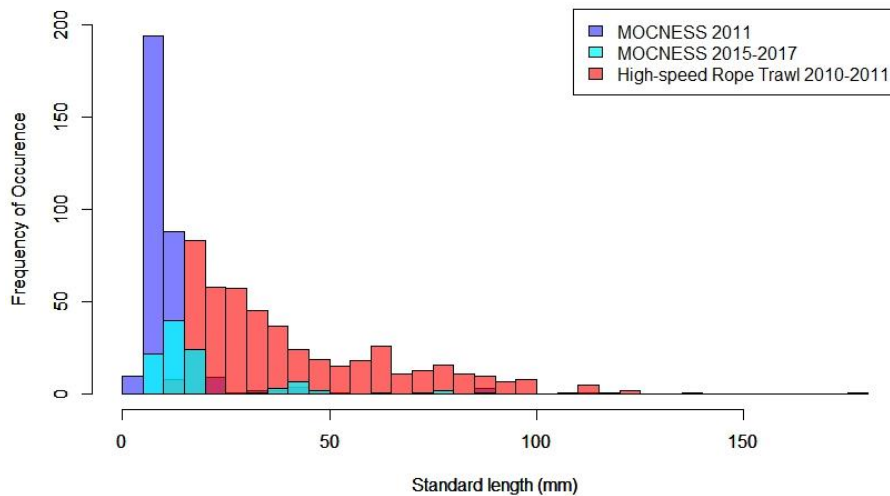


Figure 27. Size-frequency plot of larval and juvenile scombrids, color-coded by cruise series.

Table 8. Standardized abundance (No. ind. 10^{-6} m^{-3}), rank, and frequency of occurrence (F_o) of each species collected during the three cruise series. F_o is listed as percent of trawls in which taxon was collected. Dashes indicate no collections

Species	MOCNESSS 2011			High-speed rope trawl 2010-2011			MOCNESS 2015 - 2017		
	Abundance	Rank	F_o	Abundance	Rank	F_o	Abundance	Rank	F_o
<i>Euthynnus alletteratus</i>	4.026	1	5.2	0.160	2	20.0	6.366	1	2.6
<i>Thunnus atlanticus</i>	2.063	2	4.7	0.059	5	7.8	0.490	2	0.8
<i>Auxis thazard</i>	1.397	3	1.9	0.007	9	1.7	0.163	6	0.5
<i>Thunnus</i> spp.	1.131	4	2.7	0.650	1	28.7	0.245	4	0.3
<i>Katsuwonus pelamis</i>	0.865	5	2.4	0.154	3	7.0	0.245	4	0.8
<i>Auxis</i> spp.	0.333	6	0.7	0.078	4	7.0	-	-	-
<i>Auxis rochei</i>	0.200	7	0.6	0.013	8	1.7	-	-	-
<i>Sarda sarda</i>	0.166	9	0.5	-	-	-	-	-	-
Scombridae (UNID.)	0.166	9	0.6	0.003	11	0.9	-	-	-
<i>Acanthocybium solandri</i>	0.133	11	0.5	0.013	8	3.5	-	-	-
<i>Thunnus thynnus</i>	0.133	11	0.5	0.003	11	0.9	0.163	6	0.5
<i>Scomber colias</i>	0.100	12	0.3	-	-	-	-	-	-
<i>Scomberomorus cavalla</i>	0.067	14	0.2	-	-	-	-	-	-
<i>Thunnus albacares</i>	0.067	14	0.2	0.013	8	0.9	-	-	-

3.2.1.1.1. MOCNESS 2011.

A total of 344 individuals were collected in the GoM from January to September in 2011 (Table 9). The scombrid assemblage comprised seven genera and 11 species. A total of 84.6% of individuals were identified to species, 13.7% to genus only, and 1.7% to family only. A total of 79.9% were classified as larvae and 20.1% as juveniles.

Specimens ranged in size from 3.0 to 111.4 mm SL. The smallest identifiable larval scombrid was *K. pelamis* (3.2 mm SL) and the largest was *Auxis* sp. (111.4 mm SL). From 890 quantitative tows, *E. alletteratus* was the most-abundant species caught in these surveys (4.03 ind. 10^{-6} m⁻³), making up roughly 38% of the total abundance of scombrids. *Thunnus atlanticus* was the second-most abundant species collected (2.06 ind. 10^{-6} m⁻³), comprising 19% of the scombrid abundance. *Thunnus atlanticus*, along with the other *Thunnus* spp., comprised 32% of the total scombrid abundance. *Thunnus thynnus* was collected in low abundance (0.13 ind. 10^{-6} m⁻³).

Table 9. Counts and size range of scombrid specimens caught during the MOCNESS 2011 survey. Dashes indicate no collections

Species	Larvae	Juvenile	Total	Size range (mm SL)
<i>Euthynnus alletteratus</i>	91	34	125	4.9 - 44.5
<i>Thunnus atlanticus</i>	65	1	66	4.0 - 16.0
<i>Auxis thazard</i>	34	13	47	5.7 - 21.0
<i>Thunnus</i> spp.	34	1	35	4.3 - 47.0
<i>Katsuwonus pelamis</i>	25	3	28	3.2 - 16.0
<i>Auxis</i> spp. juv.	-	11	11	15.2 - 111.4
<i>Auxis rochei</i>	5	1	6	5.4 - 86.7
Scombridae UNID.	5	1	6	3.0 - 9.0
<i>Sarda sarda</i>	5	-	5	5.0 - 9.0
<i>Acanthocybium solandri</i>	4	-	4	7.5 - 13.0
<i>Thunnus thynnus</i>	4	-	4	5.3 - 7.0
<i>Scomber colias</i>	-	3	3	11.4 - 51.9
<i>Scomberomorus cavalla</i>	1	1	2	6.3 - 16.2
<i>Thunnus albacares</i>	2	-	2	5.0 - 8.5
Total	275	69	344	3 - 111.4

3.2.1.1.2. MOCNESS 2015-2017.

A total of 108 individuals were collected in the GoM during both the spring (April-May) and late summer (August) of 2015, 2016, and 2017 (Table 10). The scombrid assemblage comprised four genera and six species. A total of 97.2% of individuals were identified to species and 2.8% to genus. A total of 42.6% of individuals were larvae and 57.4% were juveniles (namely individuals that recently transformed into juveniles).

Specimens ranged in size from 6.8 - 87.8 mm SL, with a larger *E. alletteratus* specimen (175.2 mm SL) collected with a dip net. The smallest scombrid was *T. atlanticus*, while the largest was *Auxis thazard*. From 390 quantitative tows, *E. alletteratus* was the most-abundant species caught in these surveys (6.37 ind. 10^{-6} m⁻³), making up 83% of the total abundance of scombrids. One tow collected 51 specimens, suggesting patchiness and/or schooling behavior. *Thunnus atlanticus* was the second-most abundant species collected (0.49 ind. 10^{-6} m⁻³). This species, along with the other *Thunnus* spp., combined made up 12% of the total scombrid abundance. *Thunnus thynnus* was collected in low abundance (0.16 ind. 10^{-6} m⁻³).

Table 10. Counts and size range of scombrid specimens caught during the MOCNESS 2015-2017 survey. Dashes indicate no collections

Species	Larvae	Juvenile	Total	Size range (mm SL)
<i>Euthynnus alletteratus</i>	32	58	90	7.3 - 79.1 (175.2 dip-netted)
<i>Thunnus atlanticus</i>	6	1	7	6.8 - 42.5
<i>Katsuwonus pelamis</i>	3	-	3	8.8 - 12.1
<i>Thunnus</i> spp.	2	1	3	9.8 - 14.6
<i>Auxis thazard</i>	-	2	2	17.8 - 87.8
<i>Thunnus thynnus</i>	2	-	2	10.5 - 12.5
Total	46	62	108	6.8 - 87.8

3.2.1.1.3. High-speed rope trawl 2010-2011.

A total of 492 individuals were collected in the GoM from December 2010 to September 2011 (Table 11). The scombrid assemblage comprised six genera and nine species. A total of 43.9% of individuals were identified to species, 55.9% to genus only, and 0.2% to family only.

All individuals were juveniles, ranging in size from 10.2 - 136.7 mm SL. Both the smallest and largest scombrids were *T. atlanticus*. *Scomber colias* was the numerically dominant species caught throughout these surveys, but all specimens were collected in tows designated as non-quantitative (i.e. gear malfunction, no volume filtered calculation, and/or irregular towing pattern). Patchiness and/or schooling behavior was indicated for *S. colias*, as 83% of specimens were collected during one tow. Thus, from 115 quantitative tows, the taxonomically problematic genus *Thunnus* was collected in the highest abundance. The remaining *Thunnus* spp. (23 individuals) were identified to species using genetic barcoding and existing pigmentation. *Euthynnus alletteratus* ranked second in abundance (0.16 ind. 10^{-6} m^{-3}) and *K. pelamis* ranked third (0.15 ind. 10^{-6} m^{-3}).

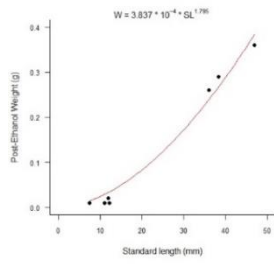
Table 11. Counts and size range of scombrid specimens caught during the high-speed rope trawl 2010-2011 survey. Dashes indicate no collections

Species	Larvae	Juvenile	Size range (mm SL)
<i>Thunnus</i> spp.	-	205	12.7 - 118.9
<i>Scomber colias</i>	-	106	27.3 - 97.5
<i>Euthynnus alletteratus</i>	-	61	13.3 - 112.5
<i>Katsuwonus pelamis</i>	-	49	17.2 - 91.1
<i>Auxis</i> spp.	-	36	18.7 - 111.8
<i>Thunnus atlanticus</i>	-	18	10.2 - 136.7
<i>Acanthocybium solandri</i>	-	4	36.0 - 63.0
<i>Auxis rochei</i>	-	4	75.4 - 108.4
<i>Thunnus albacares</i>	-	4	15.0 - 18.3
<i>Auxis thazard</i>	-	3	13.6 - 28.9
Scombridae UNID.	-	1	damaged
<i>Thunnus thynnus</i>	-	1	124.8
Total	-	492	10.2 - 136.7

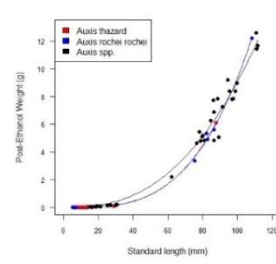
3.3. Length-weight regressions of larval and juvenile scombrids in the northern Gulf of Mexico.

Species and taxa length-weight regressions exhibited a curvilinear relationship. Thus, non-linear regressions were analyzed (e.g., power, exponential, and logarithmic models), and the best model was chosen using the AIC values. The power model was the best model for all species and taxa. This model is represented by the equation: $W = aSL^b$, where W is weight (g), SL is standard length (mm), a is the scaling factor that moves values of SL^b up or down as a increases or decreases, and b is the exponent or power that determines the function's rate of growth or decline.

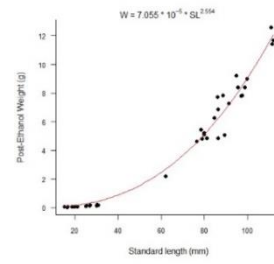
Power models were created for species and taxa with a sample size greater than 10 individuals and data that encapsulated a wide range of lengths and weights (Figure 28). The majority of species had a slope close to three, which is common for all fish species. However, *Acanthocybium solandri* had a value of 1.795, due to the small range in lengths (7.5 – 47.0 mm SL). Species with a low sample size and size ranges, and thus omitted in this section, included: *Sarda sarda*, *T. thynnus*, *T. albacares*, and *Scomberomorus cavalla*.



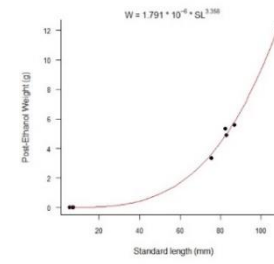
Acanthocybium solandri



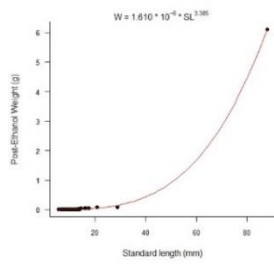
All *Auxis* spp.



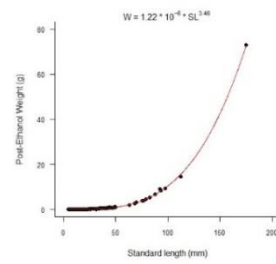
Unidentified *Auxis* spp.



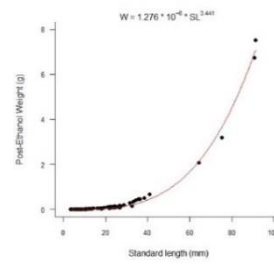
Auxis rochei



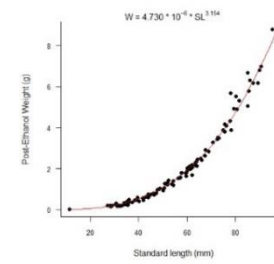
Auxis thazard



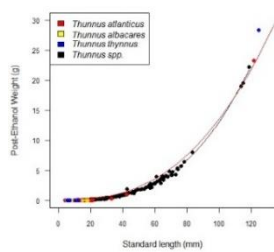
Euthynnus alletteratus



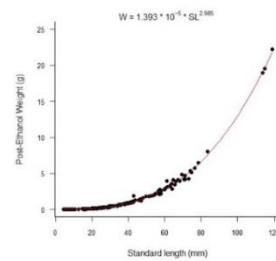
Katsuwonus pelamis



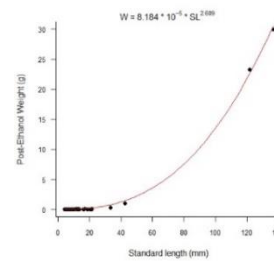
Scomber colias



All *Thunnus* spp.



Unidentified *Thunnus* spp.



Thunnus atlanticus

Figure 28. Length-weight regressions of all species/taxa collected during the three cruise series.

3.4. Variation in the morphometrics of juvenile Euthynnus alletteratus and Thunnus atlanticus.

The differences in morphometric ratios were analyzed for the two genetically identified juvenile species with the largest sample size, *Euthynnus alletteratus* and *Thunnus atlanticus*. Power regressions were plotted in Figures 29-32. SL was plotted against the ratio of HL to SL (Figure 29). The species curves overlapped and maintained a similar declining pattern, indicating smaller individuals have larger heads compared to their body length. HL was plotted against the ratio of snout length to HL (Figure 30). Both species possessed declining power curves, but *E. alletteratus* maintained a larger ratio than *T. atlanticus* at all sizes, indicating that juvenile *E. alletteratus* have larger snouts than *T. atlanticus*. HL was also plotted against the ratio of upper jaw length to HL (Figure 31). The power curves of *E. alletteratus* and *T. atlanticus* overlapped, and followed the same declining pattern, with smaller specimens having larger jaws compared to their HL. HL was plotted against the ratio of eye diameter to HL (Figure 32). Both species possessed decreasing power curves, indicating that smaller specimens have larger eyes compared to their head. *Thunnus atlanticus* maintained a higher ratio at all sizes, indicating that juvenile *T. atlanticus* have larger eyes than *E. alletteratus*.

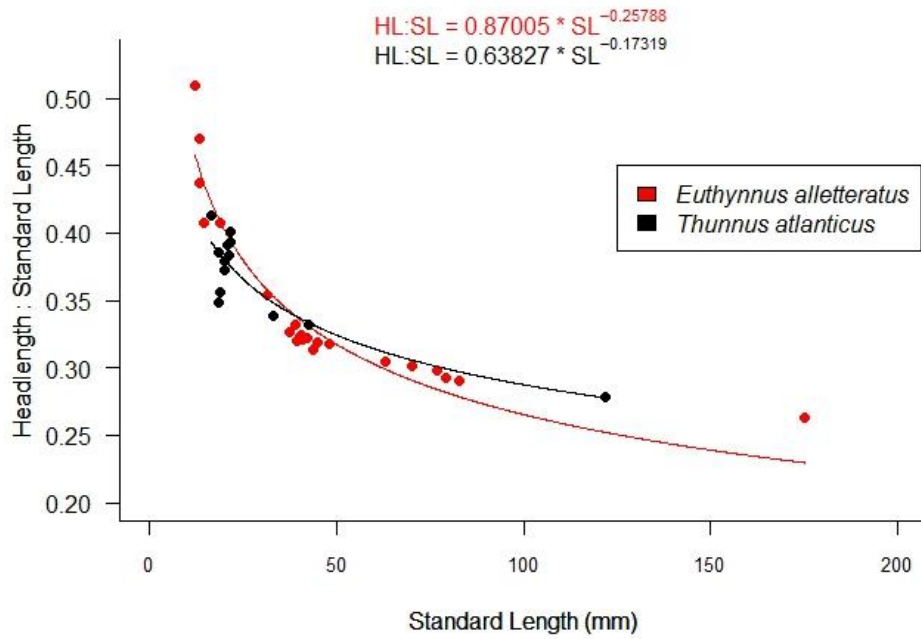


Figure 29. Ratio of head length (HL) to standard length (SL) vs. standard length for genetically identified juvenile *Euthynnus alletteratus* and *Thunnus atlanticus* specimens.

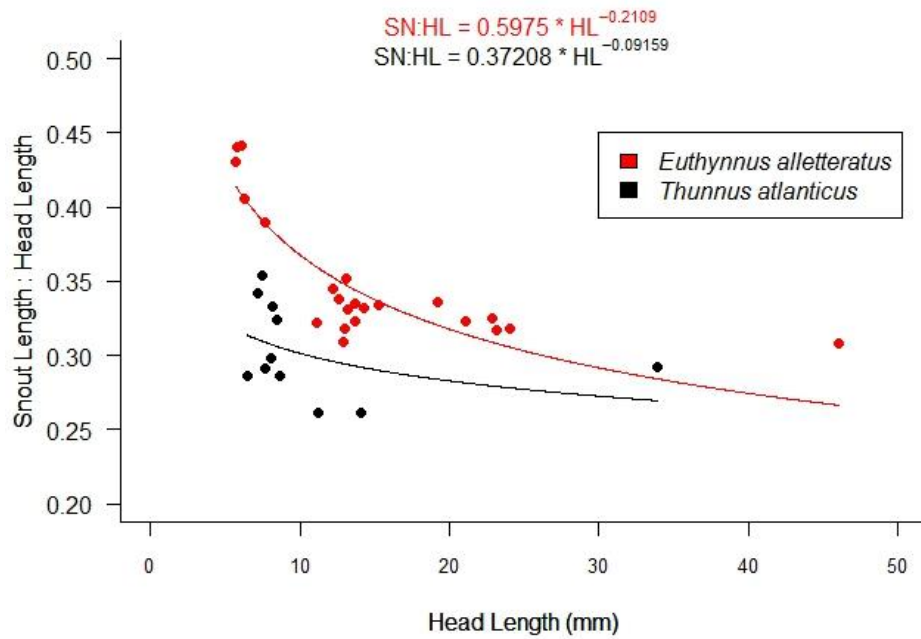


Figure 30. Ratio of snout length (SN) to head length (HL) vs. head length for genetically identified juvenile *Euthynnus alletteratus* and *Thunnus atlanticus* specimens.

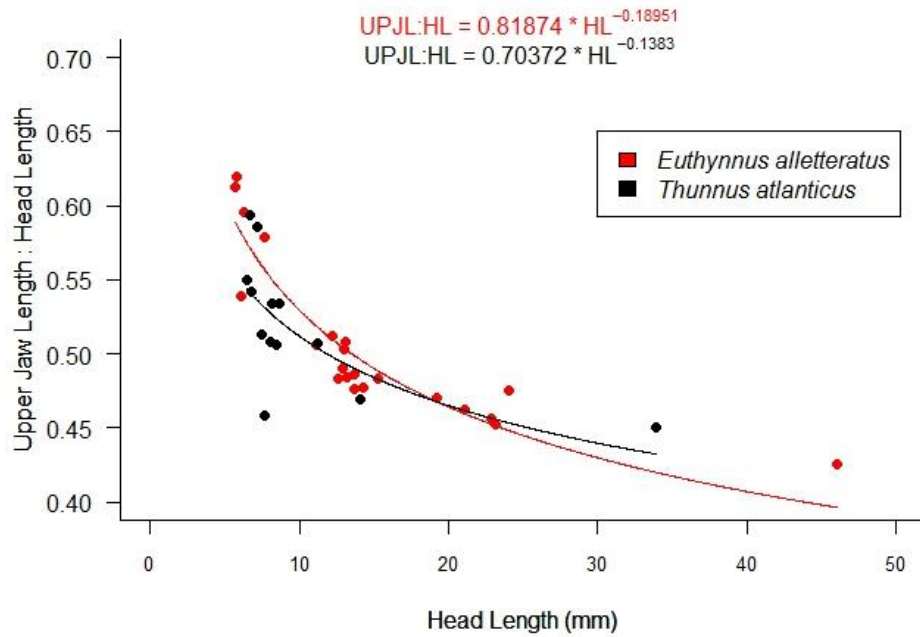


Figure 31. Ratio of upper jaw length (UPJL) to head length (HL) vs. head length for genetically identified juvenile *Euthynnus alletteratus* and *Thunnus atlanticus* specimens.

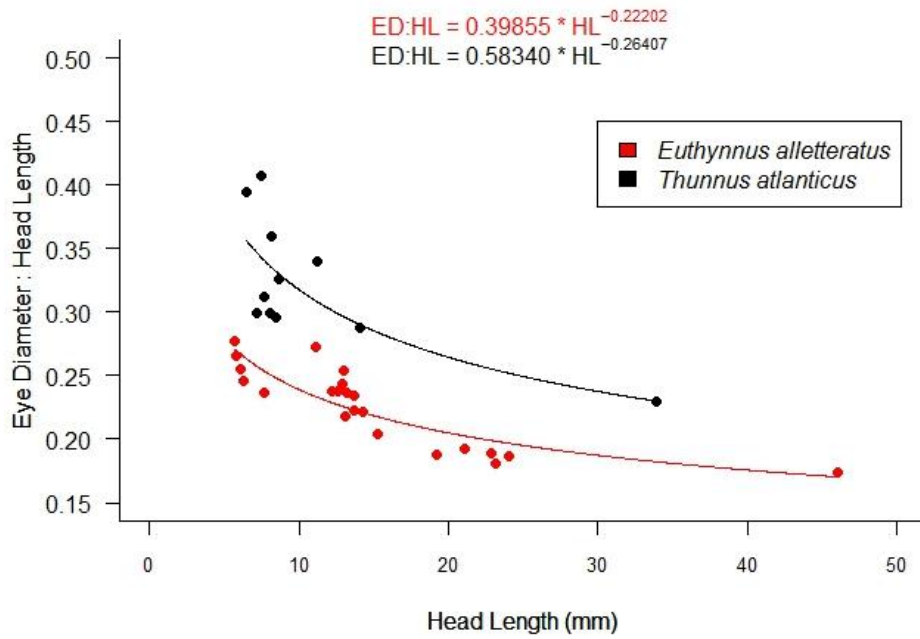


Figure 32. Ratio of eye diameter (ED) to head length (HL) vs. head length for genetically identified juvenile *Euthynnus alletteratus* and *Thunnus atlanticus* specimens.

3.5. Spatiotemporal distributions of larval and juvenile scombrid fishes in the northern Gulf of Mexico.

3.5.1. Vertical distributions and diel catch rates.

Vertical distributions and diel catch rates were identified using MOCNESS data from the 2011 and 2015-2017 cruise series. The sampling effort is presented in Table 12.

Table 12. Sampling effort (number of tows) based on day (D) vs. night (N) sampling, depth (m), and cruise series.

Depth	MOCNESS 2011		MOCNESS 2015-2017	
	D	N	D	N
0 - 200	100	107	33	41
200 - 600	104	103	35	41
600 - 1000	92	91	33	39
1000 - 1200	80	82	34	42
1200 - 1500	64	67	36	39

3.5.1.1. MOCNESS 2011.

The majority of Scombridae collected occurred in the epipelagic zone during both day and night samples, confirming their epipelagic tendencies for early life stages (Richards 2005, Figure 33). Higher abundances were recorded at night (69.84 ind. 10^{-6} m^{-3}) than during the day (23.06 ind. 10^{-6} m^{-3}). A few larval scombrids were collected in deeper waters, reaching 1500 m depth. However, these deeper catches were observed in small numbers (e.g., four *T. thynnus* larvae were collected below the epipelagic zone).

The dominant species, *E. alletteratus*, occurred in highest abundances in the epipelagic zone. More *E. alletteratus* were collected at night (25.02 ind. 10^{-6} m^{-3}) than during the day (11.93 ind. 10^{-6} m^{-3}). *Thunnus atlanticus* larvae were also most-abundant in the epipelagic zone, with higher abundances at night (12.70 ind. 10^{-6} m^{-3}).

Auxis thazard and *K. pelamis* abundances were highest in the epipelagic zone, with higher abundances at night (13.45 ind. 10^{-6} m^{-3} and 5.23 ind. 10^{-6} m^{-3} , respectively). The remaining species (e.g., *Acanthocybium solandri*, *Auxis rochei*, *Sarda sarda*, *Scomber colias*, *Scomberomorus cavalla*, *T. albacares* and *T. thynnus*) were collected at low abundances and had patchy distributions throughout the water column.

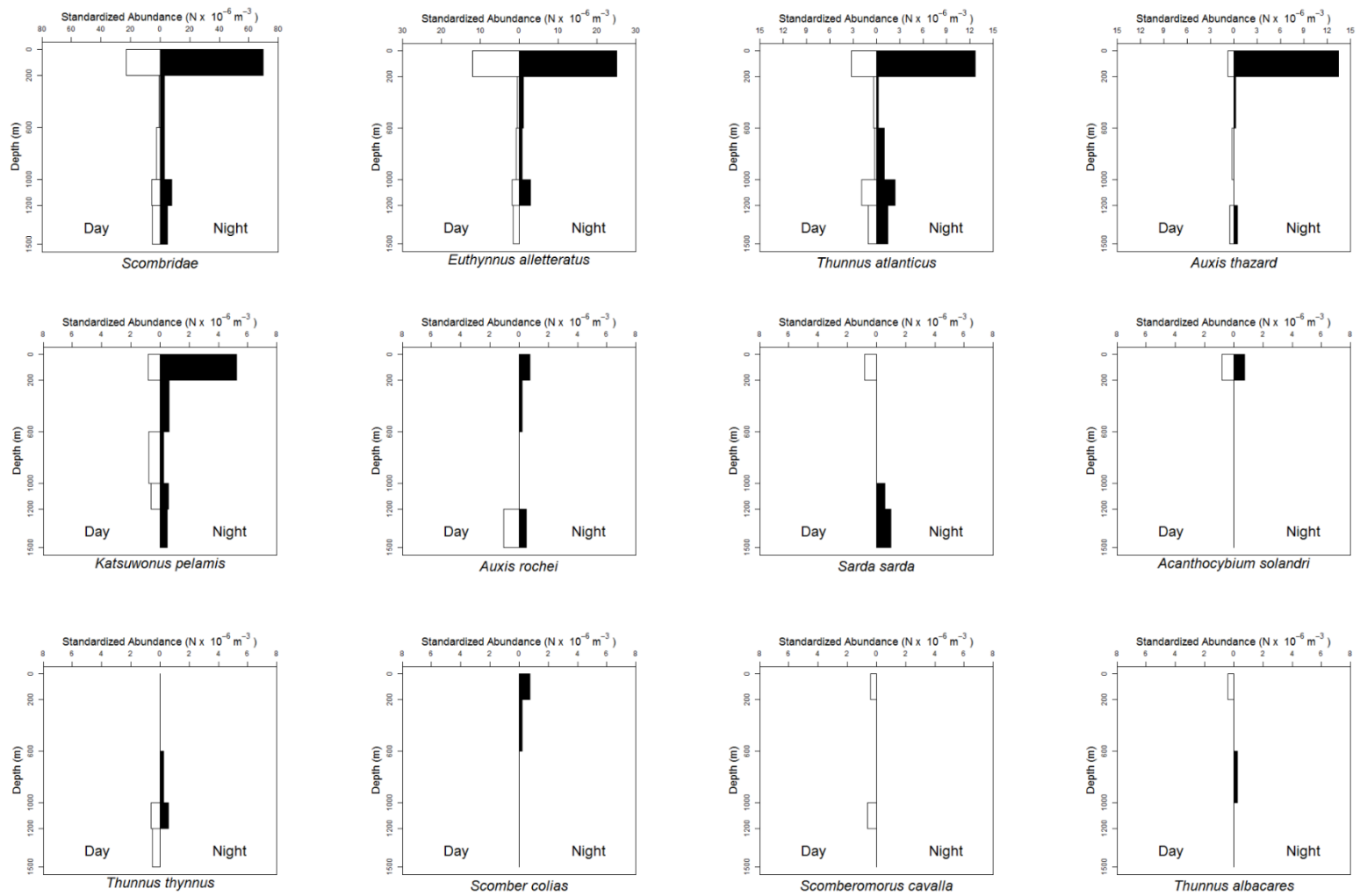


Figure 33. Vertical distribution of larval and juvenile scombrids collected during the MOCNESS 2011 survey.

3.5.1.2. MOCNESS 2015-2017.

Results from the MOCNESS 2015-2017 survey were similar to those of MOCNESS 2011 survey, in which larval and juvenile scombrids were predominately collected in the upper 200 m of the water column. From 2015 – 2017, all scombrids were collected in the epipelagic zone (Figure 34). At night, 79.41 ind. 10^{-6} m^{-3} were caught, while only 1.42 ind. 10^{-6} m^{-3} were caught during the day. This further confirms the epipelagic distribution of early life stages and higher catch rates at night.

The dominant species, *E. alletteratus*, occurred in highest abundances in the epipelagic zone at night (65.75 ind. 10^{-6} m^{-3}), and was the only species collected during the daytime (1.42 ind. 10^{-6} m^{-3}). *Thunnus atlanticus* (5.12 ind. 10^{-6} m^{-3}), *K. pelamis* (2.56 ind. 10^{-6} m^{-3}), *Auxis thazard* (1.70 ind. 10^{-6} m^{-3}), and *T. thynnus* (1.70 ind. 10^{-6} m^{-3}) were caught at lower abundances, also occurring only in the epipelagic zone at night.

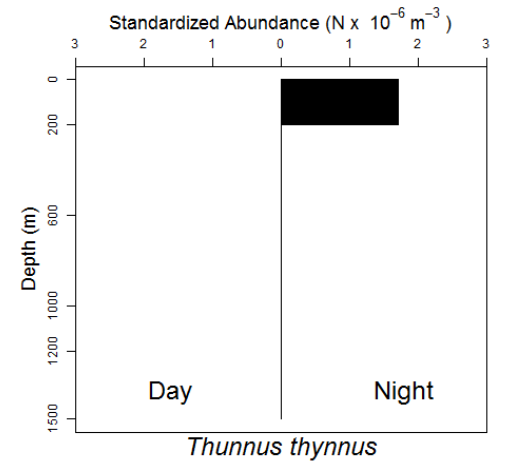
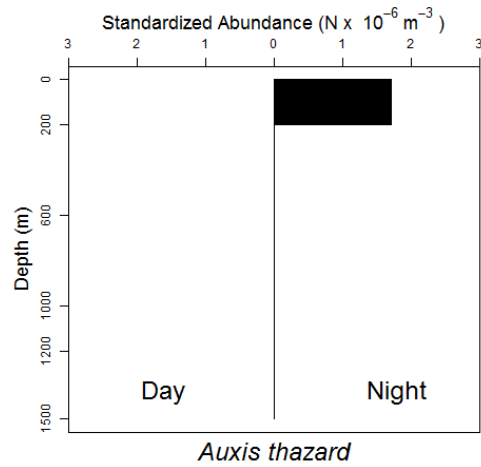
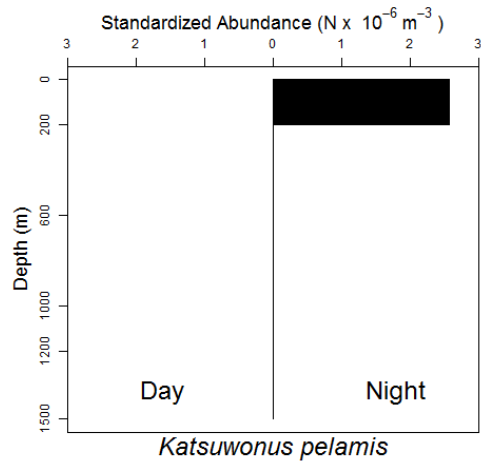
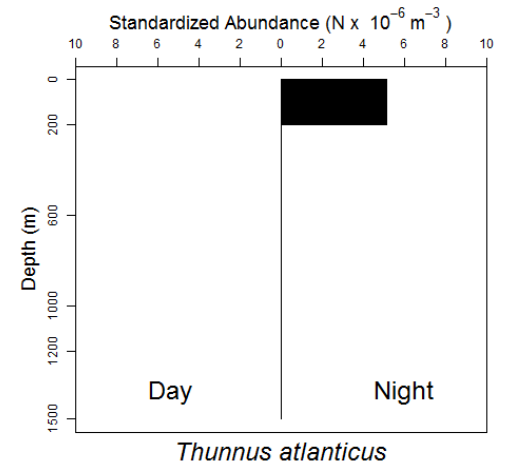
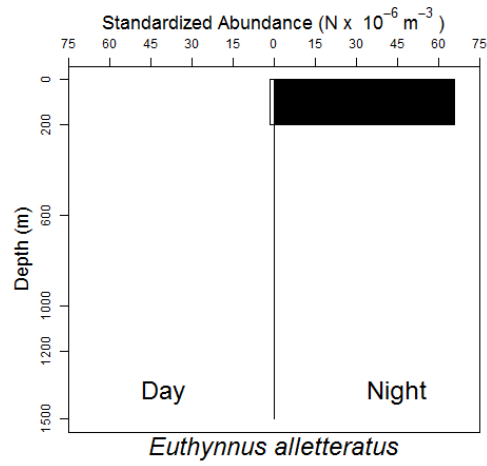
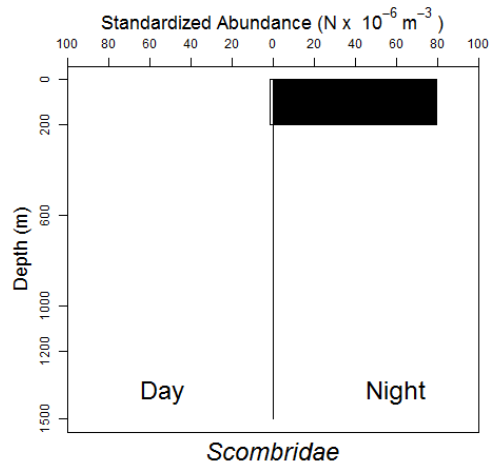


Figure 34. Vertical distribution of scombrids collected during the MOCNESS 2015 – 2017 survey.

3.5.1.3. Epipelagic abundances and frequency of occurrence – all MOCNESS data.

MOCNESS discrete-depth sampling results clearly demonstrated that scombrid early life stages are primarily distributed within the epipelagic zone. Thus, further analysis of the abundances and frequency of occurrence of all species and taxa collected were restricted to samples collected in the top 200 m of the water column (Table 13). In 2011, the scombrid abundance estimates were 23.09 ind. 10^{-6} m^{-3} during the day and 69.84 ind. 10^{-6} m^{-3} at night. From 2015-2017, scombrid abundance estimates were 1.41 ind. 10^{-6} m^{-3} during the day and 79.41 ind. 10^{-6} m^{-3} at night. *Euthynnus alletteratus* exhibited the highest abundance in the epipelagic zone during both day and night over both cruise series.

For both cruise series, the majority of species and taxa were collected at higher abundances and higher frequencies at night than during the day. In 2011, there was 27.0% frequency of occurrence during the day and 43.9% at night. From 2015 – 2017, there was 3.0% frequency of occurrence during the day and 48.8% at night.

In 2011, *E. alletteratus* also had a higher frequency, occurring in 11.0% of the day trawls and 15.0% of the night trawls. From 2015-2017, *E. alletteratus* occurred in 3.0% of day trawls and 22.0% of night trawls. *Thunnus atlanticus* exhibited a frequency of occurring in 7.0% (2011) of the day trawls and 7.3 - 14.2% (2015-2017 and 2011, respectively) of the night trawls. *Auxis thazard* frequency of occurring increased between day and night samples, with 2% of the day trawls (2011) and 4.9 - 10.3% (2015-2017 and 2011, respectively) of the night trawls. *Katsuwonus pelamis* exhibited a frequency of occurring in 2% of day trawls (2011) and 7.3 - 8% (2015-2017 and 2011, respectively) of night trawls.

A few rare-event species and taxa were not collected more often at night in the 2011 series. For example, *Acanthocybium solandri* was caught at relatively similar abundances and frequencies at night (0.75 ind. 10^{-6} m^{-3} and 1.9%, respectively) compared to the daytime (0.80 ind. 10^{-6} m^{-3} and 2.0%, respectively). Similarly, *Sarda sarda* and *Scomberomorus cavalla* were only collected during the daytime in 2011.

For the MOCNESS 2011 cruise series, the results of a Mann-Whitney Wilcoxon test for the family Scombridae ($p = 0.0032$) rejected the null hypothesis of no significant

difference in abundances by diel cycle, as higher abundances were caught at night than during the day. However, there were no significant differences in the abundance of fish caught based on diel cycle for *E. alletteratus* ($p = 0.343$) and *T. atlanticus* ($p = 0.088$). *Auxis thazard* ($p= 0.013$) and *K. pelamis* ($p= 0.0396$) were caught at significantly higher abundances at night than during the day. Statistical significance was not tested on the MOCNESS 2015-2017 samples due to only one specimen (*E. alletteratus*) being collected during the daytime, showing higher catch rates at night. Thus, all abundances and frequencies were higher at night than during the day from 2015 – 2017.

Table 13. Standardized abundance (No. ind. 10^{-6} m^{-3}) and frequency of occurrence (F_o) of scombrid larvae and juveniles collected in the epipelagic zone of the GoM using a MOCNESS trawl. F_o is listed as percent of trawls in which a taxon was collected. Samples were separated based on day (D) and night (N) sampling. Dashes indicate no collections

Species	MOCNESS 2011				MOCNESS 2015 – 2017			
	Abundance		F_o		Abundance		F_o	
	D	N	D	N	D	N	D	N
<i>Euthynnus alletteratus</i>	11.93	25.02	11.0	15.0	1.42	65.75	3.0	22.0
<i>Thunnus atlanticus</i>	3.18	12.70	7.0	14.0	-	5.12	-	7.3
<i>Auxis thazard</i>	0.80	13.45	2.0	10.3	-	1.71	-	4.9
<i>Katsuwonus pelamis</i>	0.80	5.23	2.0	8.4	-	2.56	-	7.3
<i>Auxis rochei</i>	-	0.75	-	0.9	-	-	-	-
<i>Sarda sarda</i>	0.80	-	2.0	-	-	-	-	-
<i>Acanthocybium solandri</i>	0.80	0.75	2.0	1.9	-	-	-	-
<i>Thunnus thynnus</i>	-	-	-	-	-	1.71	-	4.9
<i>Scomber colias</i>	-	0.75	-	2.8	-	-	-	-
<i>Scomberomorus cavalla</i>	0.40	-	1.0	-	-	-	-	-
<i>Thunnus albacares</i>	0.40	-	1.0	-	-	-	-	-
<i>Thunnus</i> spp.	3.98	6.35	7.0	9.3	-	2.56	-	2.4
<i>Auxis</i> spp.	-	3.74	-	5.6	-	-	-	-
UNID. Scombridae	-	1.10	-	1.9	-	-	-	-
Family Scombridae	23.09	69.84	27.0	43.9	1.42	79.41	3.0	48.8

3.5.1.4. Diel differences in the high-speed rope trawl 2010-2011 survey shallow tows.

Since the high-speed rope trawl does not have the capacity to open or close during a tow, it only allows for oblique tows from the surface to some depth. Since scombrids were most likely caught near the surface, vertical distributions and day vs. night abundances were analyzed only for the “shallow” (0 – 700 m depth) tows (Figure 35). *Euthynnus alletteratus*, *Thunnus* spp. juveniles, and *T. atlanticus* were collected during the day and at night. *Acanthocybium solandri* and *Auxis thazard* were only collected during the day, while *Auxis* spp. juveniles, *Auxis rochei*, *K. pelamis*, and *T. thynnus* were only collected at night.

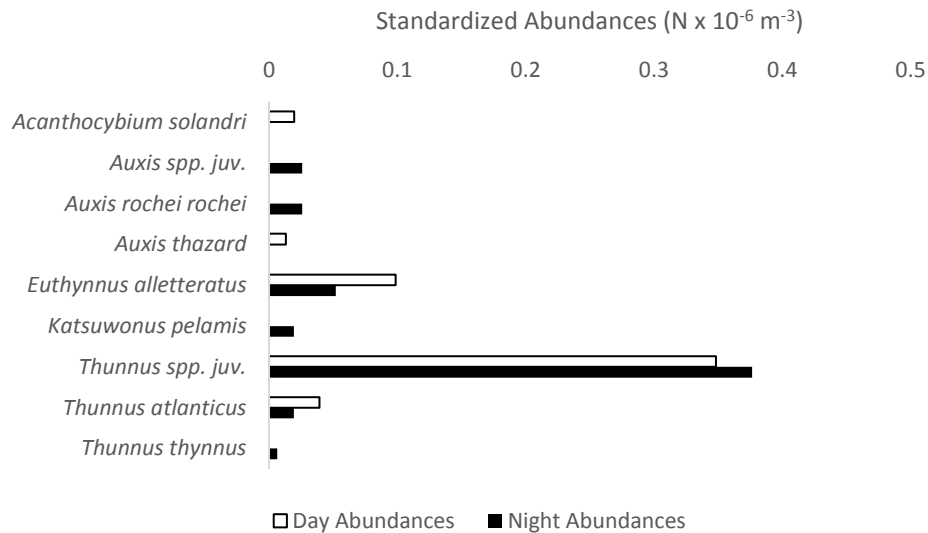


Figure 35. Standardized abundances collected in quantitative shallow tows separated by day vs. nighttime sampling.

3.5.2. *Horizontal distributions of larval and juvenile scombrids in the northern Gulf of Mexico.*

3.5.2.1. MOCNESS 2011.

3.5.2.1.1. Mapping the spatial distributions of the three most-abundant scombrids.

Spatial distribution plots were created for the three most-abundant species (e.g., *Euthynnus alletteratus*, *Thunnus atlanticus*, and *Auxis thazard*) collected in 2011. The abundances of each species were analyzed across the sampling grid by month and diel cycle (day vs. night). Each species abundance was compared to three environmental features by month (chlorophyll *a*, SSHA, and minimum salinity, Appendix Figures 1-3).

Euthynnus alletteratus was collected over three months during the day (March, August, and September, Figure 36) and six months at night (March-August, Figure 50). Seasonal abundances were evident, with an increase in August in both day and night sampling. *Euthynnus alletteratus* was rarely collected west of -90° , except for one catch in July at night. Specimens were predominantly collected in the center of the sampling grid. High abundances appeared to be related to higher chlorophyll *a* concentrations, specifically in August when a large plume was funneled into the GoM from the Mississippi River. *Euthynnus alletteratus* was also collected along the cusps of these plume waters in April and May, however, a few specimens were sampled in low chlorophyll *a* concentrated waters. Moreover, *E. alletteratus* were collected in Common Water and along frontal boundaries, indicated by SSHA. High abundances in August were associated with low salinity levels, but some individuals were collected in areas of higher salinity as well, indicating a wide range of salinity preferences. Thus, pristine conditions appeared in August for *E. alletteratus*, although individuals persisted outside of these suitable areas.

Thunnus atlanticus was collected over five months during the day (May-September, Figure 38) and four months at night (May-August, Figure 39). Individuals were collected across the entire sampling grid throughout the year. However, seasonality was evident, with more individuals collected in August and more specifically, at night. *Thunnus atlanticus* appeared to be found in high salinity and low chlorophyll *a* concentrated waters. This species also was collected in Common Water and along frontal boundaries.

Auxis thazard individuals were collected during the day in July and August (Figure 40) and at night from February-May and July-September (Figure 41). Highest abundances appeared at night in April along the shelf break and slope. *Auxis thazard* was mainly caught along the southern-most section of the sampling grid, but abundances were also found along the shelf break and slope. *Auxis thazard* appeared to prefer intermediate and low chlorophyll *a* concentrations, as this species was prevalent along the edges of the Mississippi River Plume. This species concentrated in areas of low SSHA, along with some possible frontal boundaries. *Auxis thazard* was collected in high salinity waters.

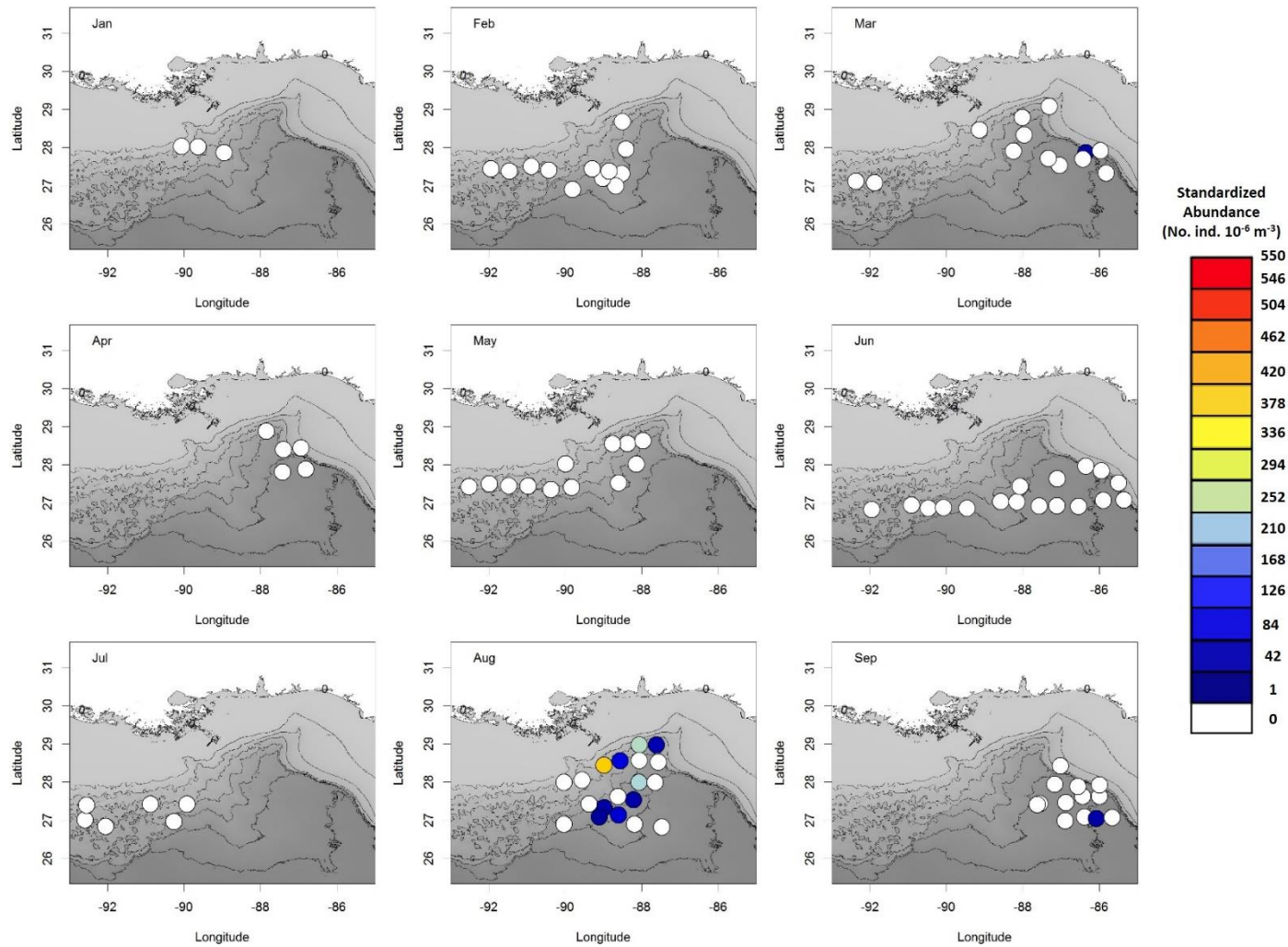


Figure 36. A heat map of *Euthynnus alletteratus* standardized abundances in the epipelagic zone collected during the day time in 2011 using the MOCNESS. White indicates that no individuals were collected. Abundances range from blue (1 ind. 10^{-6} m^{-3}) to red (550 ind. 10^{-6} m^{-3}).

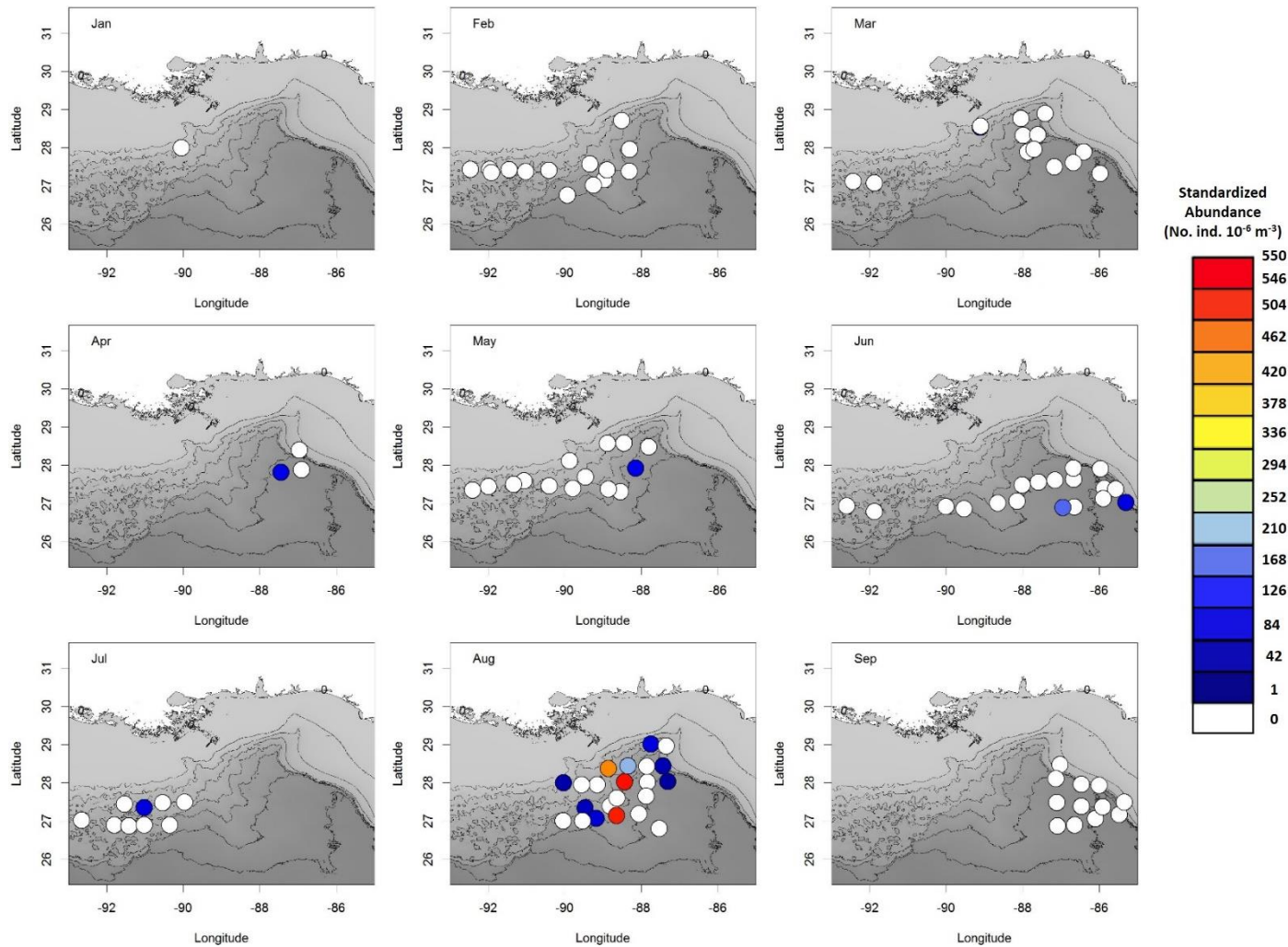


Figure 37. A heat map of *Euthymus alletteratus* standardized abundances in the epipelagic zone collected at night in 2011 using the MOCNESS. White indicates that no individuals were collected. Abundances range from blue (1 ind. 10^{-6} m^{-3}) to red (550 ind. 10^{-6} m^{-3}).

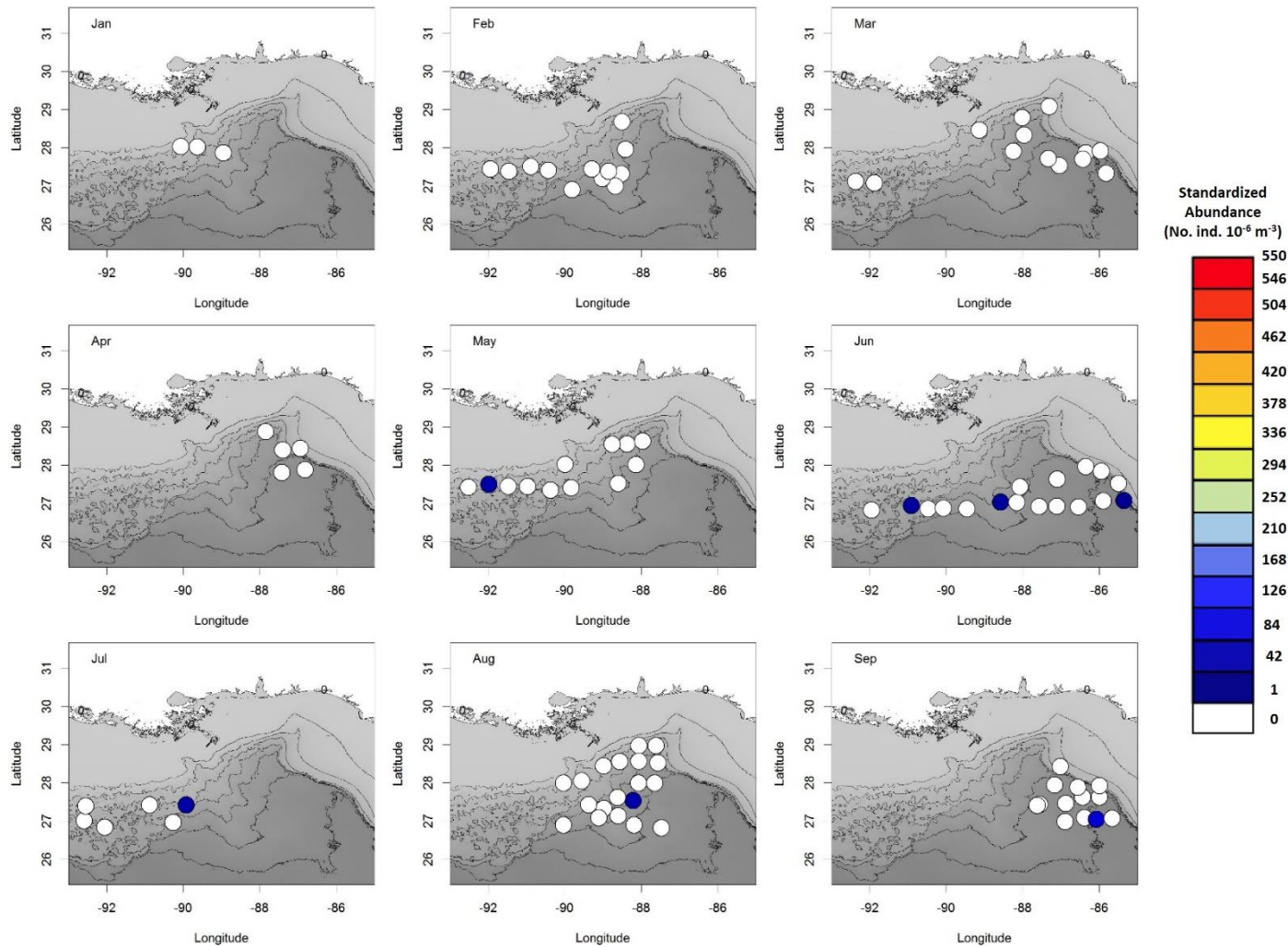


Figure 38. A heat map of *Thunnus atlanticus* standardized abundances in the epipelagic zone collected during the day time in 2011 using the MOCNESS. White indicates that no individuals were collected. Abundances range from blue (1 ind. 10^{-6} m^{-3}) to red (550 ind. 10^{-6} m^{-3}).

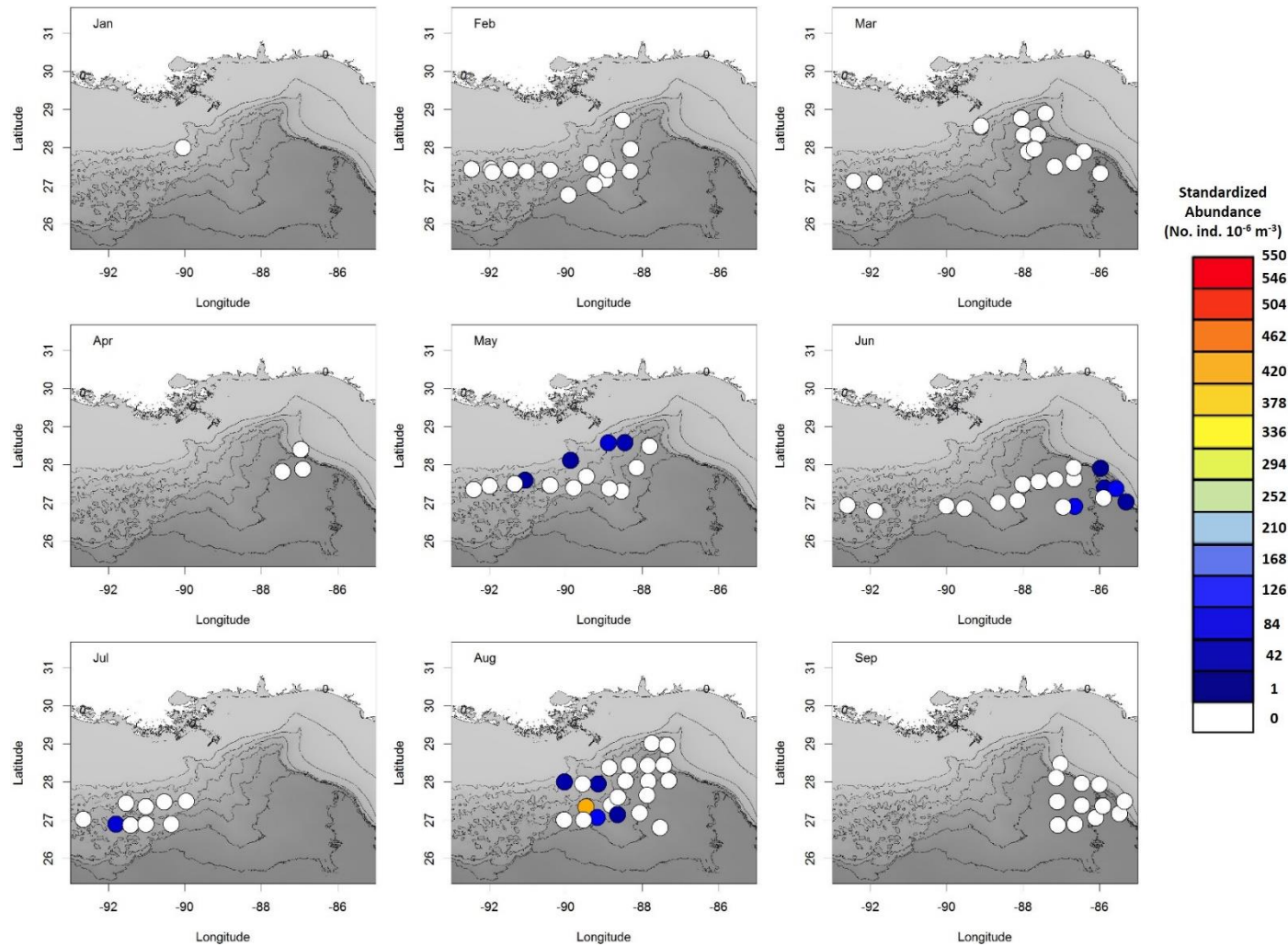


Figure 39. A heat map of *Thunnus atlanticus* standardized abundances in the epipelagic zone collected at night in 2011 using the MOCNESS. White indicates that no individuals were collected. Abundances range from blue (1 ind. 10^6 m^{-3}) to red (550 ind. 10^6 m^{-3}).

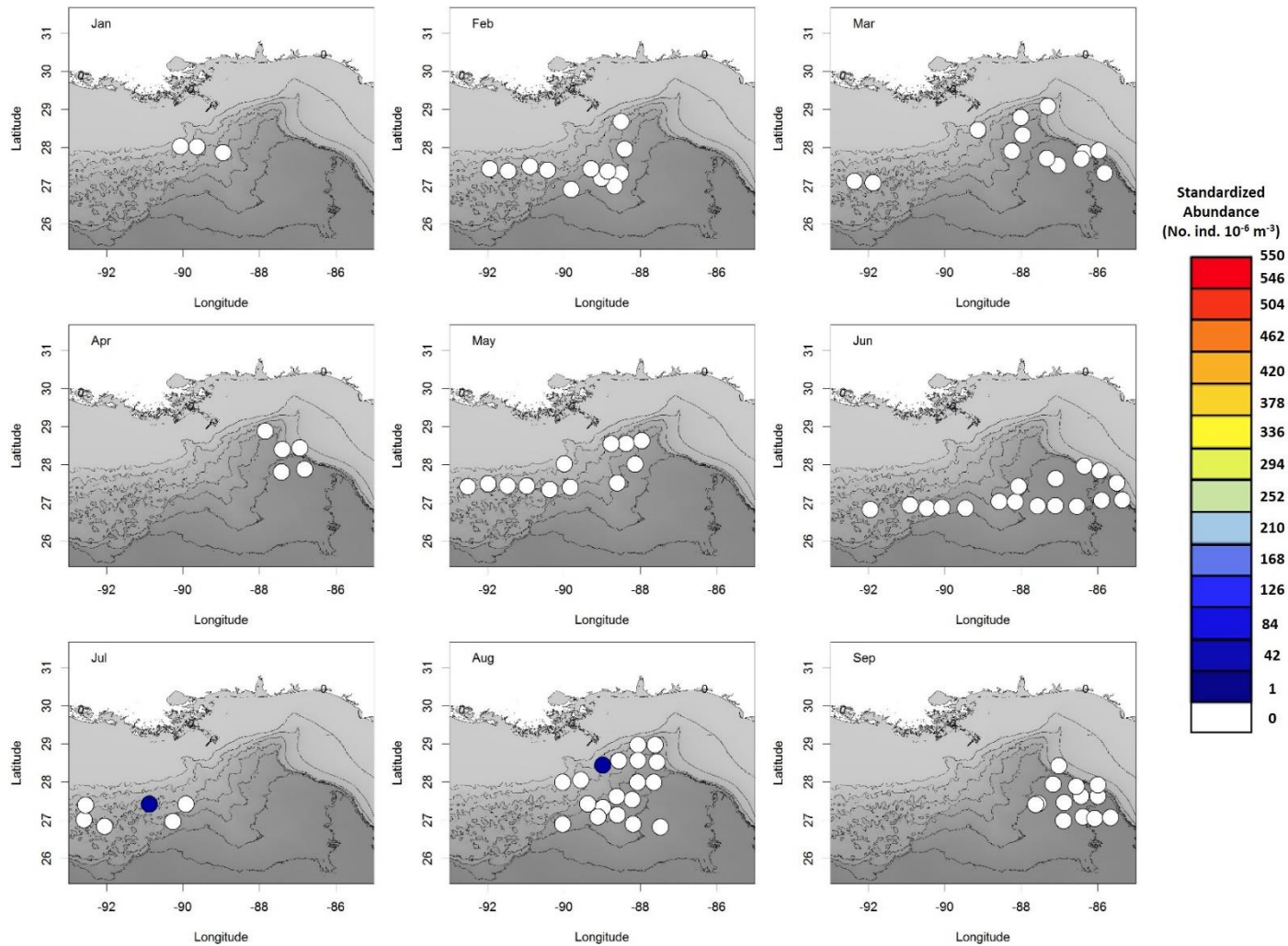


Figure 40. A heat map of *Auxis thazard* standardized abundances in the epipelagic zone collected during the day time in 2011 using the MOCNESS. White indicates that no individuals were collected. Abundances range from blue (1 ind. 10^{-6} m^{-3}) to red (550 ind. 10^{-6} m^{-3}).

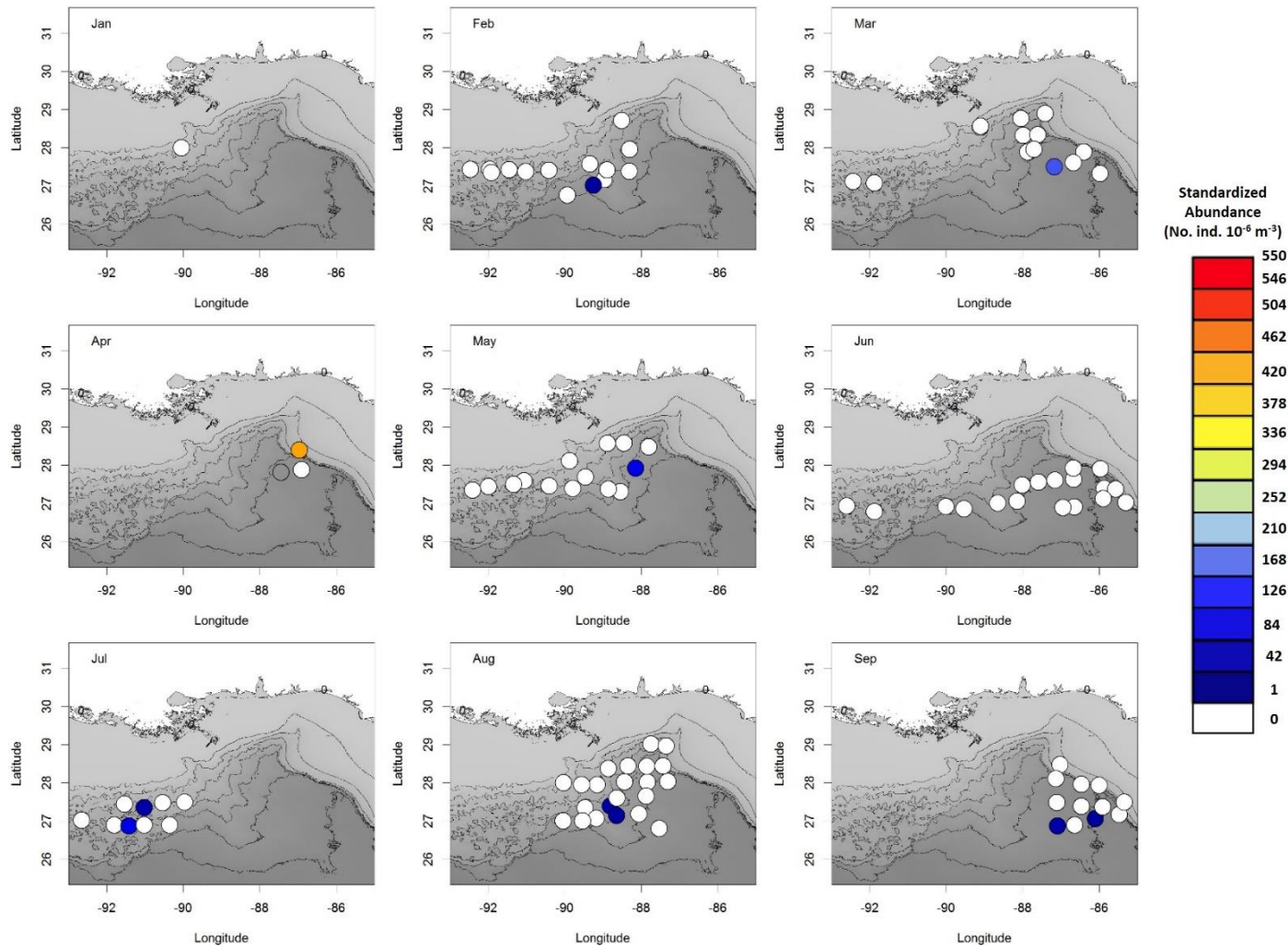


Figure 41. A heat map of *Auxis thazard* standardized abundances in the epipelagic zone collected at night in 2011 using the MOCNESS. White indicates that no individuals were collected. Abundances range from blue (1 ind. 10^6 m^{-3}) to red (550 ind. 10^6 m^{-3}).

3.5.2.1.2. Generalized additive models of the three most-abundant scombrids.

Data were obtained from 326 specimens collected from 890 quantitative samples in the GoM from January 28 - September 30, 2011. Due to the high amount of zeros in the dataset, GAMs were used to analyze the abundance and distribution of entire family Scombridae and the three most-abundant species collected in this study, *Euthynnus alletteratus*, *Thunnus atlanticus*, and *Auxis thazard*. The Poisson residuals suggested over-dispersion, and the zero-inflated models were not required in this study based on the residuals. Therefore, the negative binomial distribution models were used to assess the importance of the explanatory variables with respect to scombrid abundances (Table 14, Figures 42-45). GAMs only investigated patterns within the upper 200 m of the water column.

Table 14. AIC values and degrees of freedom (df) of each GAM tested for the family Scombridae, and the species *Euthynnus alletteratus*, *Thunnus atlanticus*, and *Auxis thazard*. The best models with the lowest AIC score are bolded

GAM	AIC	df	Notes
Scombridae			
Poisson	569.9	17	Highest AIC/high df
Negative binomial	441.2	15	Lowest AIC value
Zero-inflated Poisson	456.3	25	High AIC/df
Zero-inflated negative binomial	470.9	9	More complex model than negative binomial
<i>Euthynnus alletteratus</i>			
Poisson	200.3	22	Lowest AIC, but high df/over dispersion
Negative binomial	205.1	12	Simplest model
Zero-inflated Poisson	-	-	Model did not compile
Zero-inflated negative binomial	235.1	7	Highest AIC value
<i>Thunnus atlanticus</i>			
Poisson	153.3	17	High df/over dispersion
Negative binomial	152.6	7	Lowest AIC value
Zero-inflated Poisson	154.9	7	Negative binomial is better
Zero-inflated negative binomial	-	-	Model did not compile
<i>Auxis thazard</i>			
Poisson	195.0	5	High df/over dispersion
Negative binomial	115.3	6	Lowest AIC value
Zero-inflated Poisson	134.8	6	Higher AIC
Zero-inflated negative binomial	-	-	Model did not compile

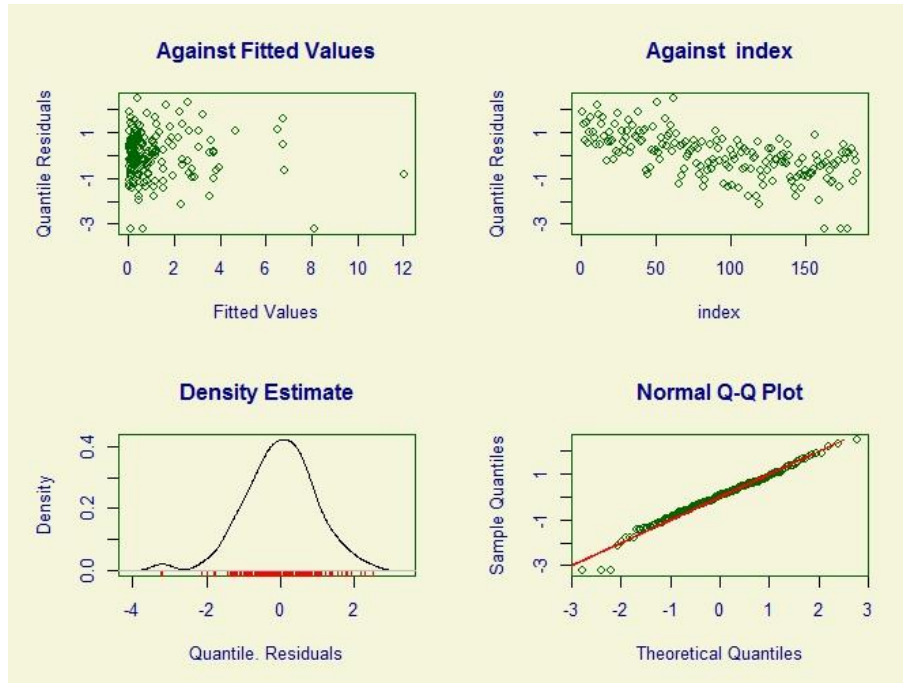


Figure 42. Scombridae negative binomial residuals.

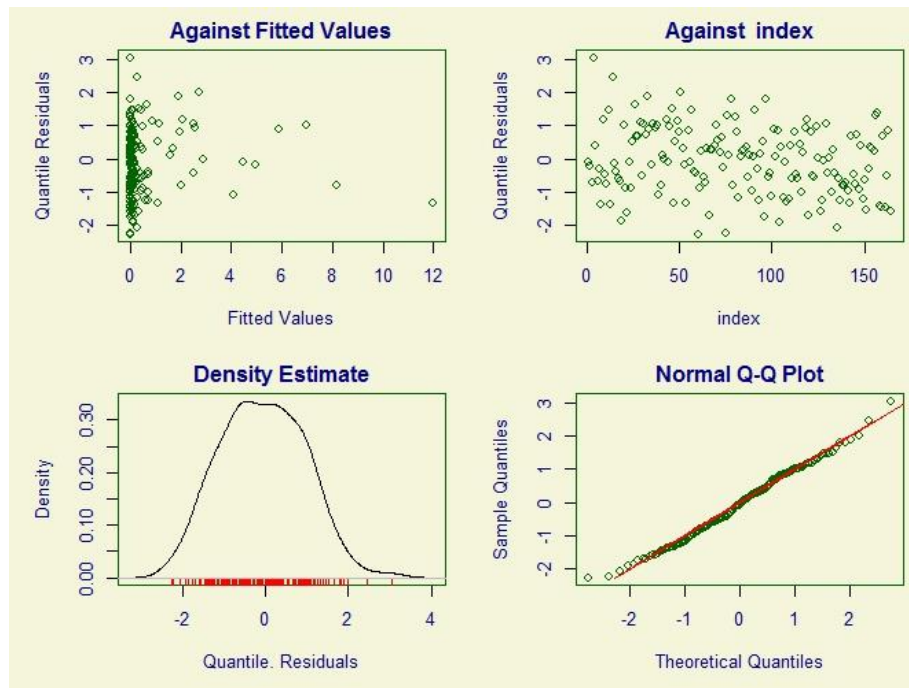


Figure 43. Euthymus alletteratus negative binomial residuals.

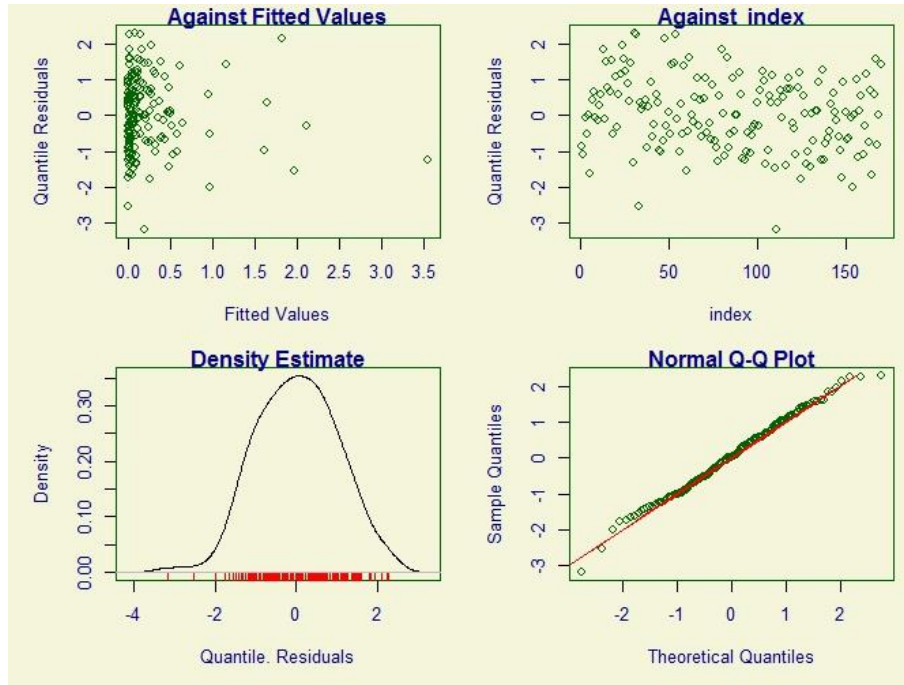


Figure 44. *Thunnus atlanticus* negative binomial residuals.

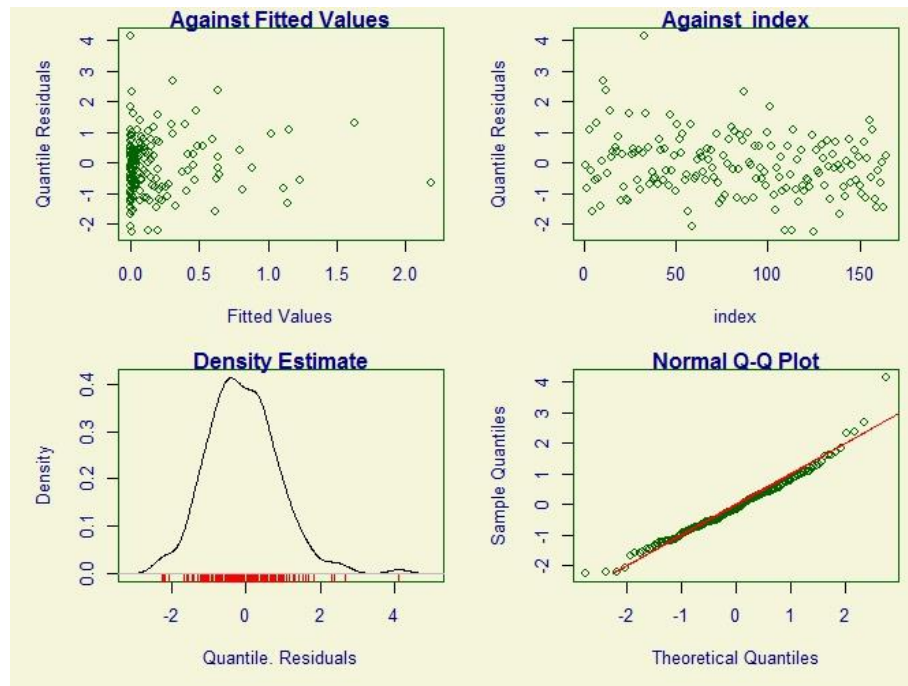


Figure 45. *Auxis thazard* negative binomial residuals.

Table 15. AIC values of GAMs with dropping one explanatory variable for (a) Scombridae, (b) *Euthynnus alletteratus*, (c) *Thunnus atlanticus*, and (d) *Auxis thazard*. The full models' AIC values are highlighted in gray and are referred to as "none." Important explanatory variables are bolded

Explanatory variable dropped	AIC value	dAIC	Explanatory variable dropped	AIC value	dAIC
Julian date	471.9	+30.7	Julian Date	226.5	+21.4
Water mass	451.7	+10.5	Minimum salinity	212.9	+7.8
Diel cycle	449.6	+8.4	Distance to 200-m isobath	212.7	+7.6
Distance to 200-m isobath	448.2	+7.0	Diel cycle	205.7	+0.6
<i>None</i>	441.2	-	<i>None</i>	205.1	-
Minimum salinity	439.0	-2.2			
a. Scombridae			b. <i>Euthynnus alletteratus</i>		
Explanatory variable dropped	AIC value	dAIC	Explanatory variable dropped	AIC value	dAIC
Julian date	169.3	+16.7	Diel cycle	119.4	+4.1
Minimum salinity	163.9	+11.3	Distance to 200-m isobath	115.4	+0.1
Diel cycle	154.8	+2.2	<i>None</i>	115.3	-
<i>None</i>	152.6	-	Julian date	113.6	-1.7
Water mass (LCOW/CW)	150.4	-2.2	Minimum salinity	113.2	-2.1
Distance to 200-m isobath	148.3	-4.3			
c. <i>Thunnus atlanticus</i>			d. <i>Auxis thazard</i>		

The highest catches of the family Scombridae were associated with Julian date (dAIC: +30.7), water mass (dAIC: +10.5, Common Water), diel cycle (dAIC: +8.4, nighttime sampling), and distance to the nearest 200-m isobath (dAIC: +7.0), as seen in Table 15a. The most prominent findings were that scombrids preferred Common Water (Figure 46a) and were caught at higher abundances at night (Figure 46b). The abundances of the entire family Scombridae in relation to Julian date and distance to the nearest 200-m isobath were driven by *E. alletteratus*, *T. atlanticus*, and *Auxis thazard*. Thus, species-specific environmental preferences in the GoM were investigated for these three species.

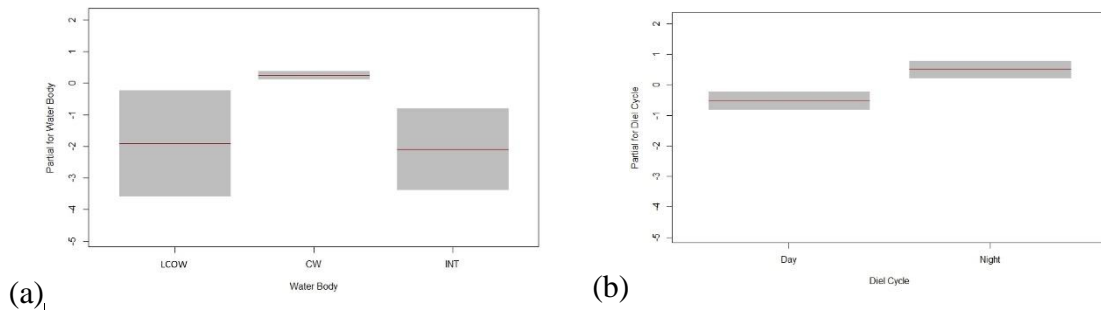


Figure 46. Term plots for Scombridae abundances in relation to (a) water body with LCOW as Loop Current Origin Water, CW as Common Water, and INT as Intermediate/Mixed Water, and (b) diel cycle.

Euthynnus alletteratus, the most-abundant species in the study, was only collected in Common Water; therefore, *E. alletteratus* GAMs only included samples caught in Common Water. Results of the full and reduced models are seen in Table 15b. *Euthynnus alletteratus* abundances were highly seasonal (Julian date, dAIC: +21.4, Figure 47a and b) with a peak occurring later in the sampling period around August. Minimum salinity was also an important determinant (dAIC: +7.8, Figure 47c and d), with more *E. alletteratus* caught in lower salinity waters. *Euthynnus alletteratus* abundances were also associated with distance to the nearest 200-m isobath (dAIC: +7.6, Figure 47e and f), with more individuals collected near the shelf break and continental slope regions.

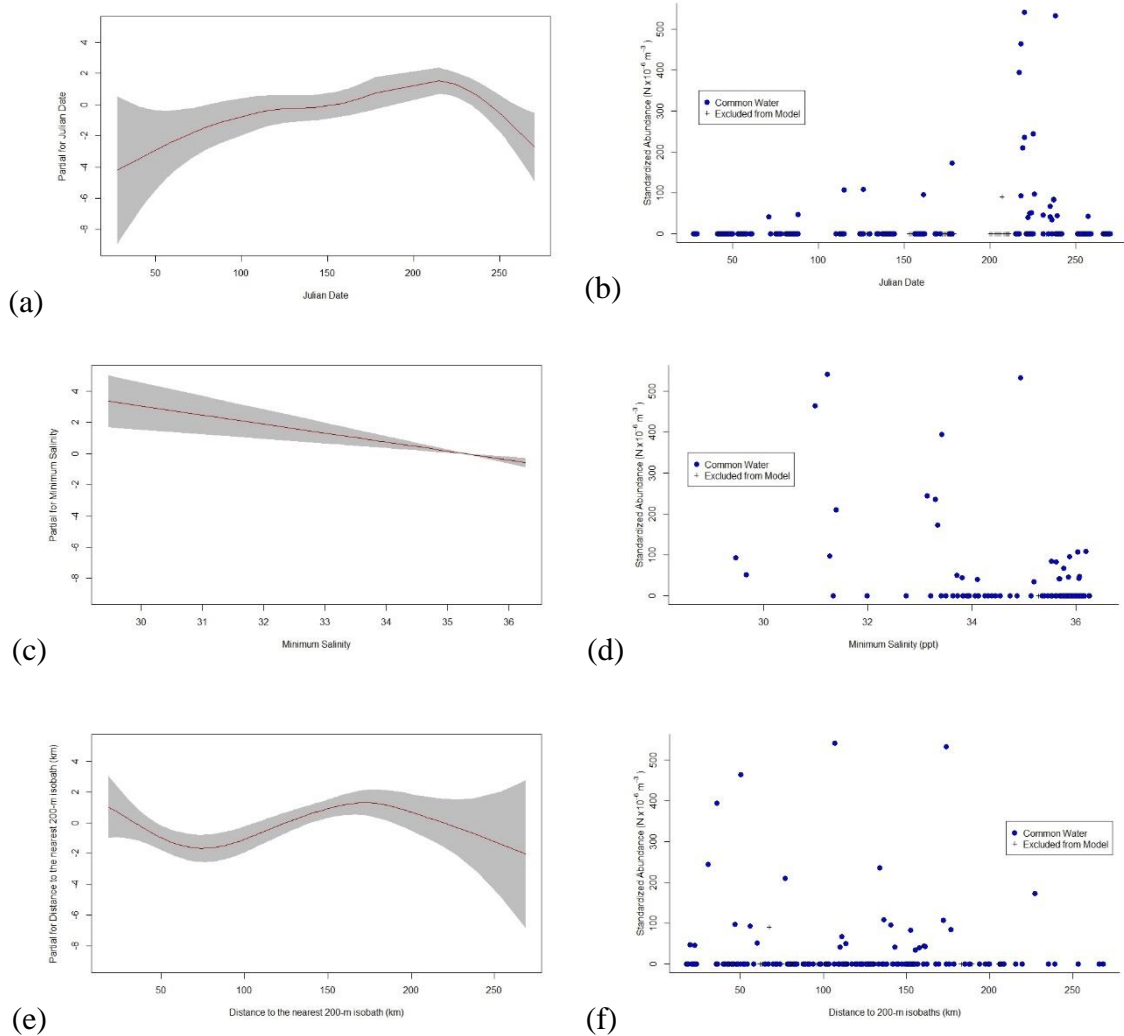


Figure 47. Term plots and standardized abundances for *Euthynnus alletteratus* in relation to (a and b) Julian date, (c and d) minimum salinity, and (e and f) distance to the nearest 200-m isobath.

Thunnus atlanticus was the second-most abundant species caught during this study. Only one *T. atlanticus* specimen was collected in Intermediate/Mixed Water; thus, the GAMs only included samples from Loop Current Origin Water and Common Water. Results of the full and reduced models are seen in Table 15c. *Thunnus atlanticus* abundances were strongly seasonal (Julian date, dAIC: +16.7, Figure 48a and b), with higher abundances beginning in June and continuing through September. Higher *T. atlanticus* abundances strongly related to high salinity levels (dAIC: +11.3, Figure 48c and d) and marginally to diel cycle (dAIC: +2.2, Figure 48e and f), more specifically nighttime sampling. Lastly, *Auxis thazard* was the third-most abundant species caught in this study. In Common Water, *A. thazard* was caught at higher abundances at night than during the day (dAIC: +4.1, Table 15d, Figure 49a and b). The remaining variables were not important indicators of scombrid distributions in the GoM, and the model could not be applied to the other scombrid species due to insufficient sample size.

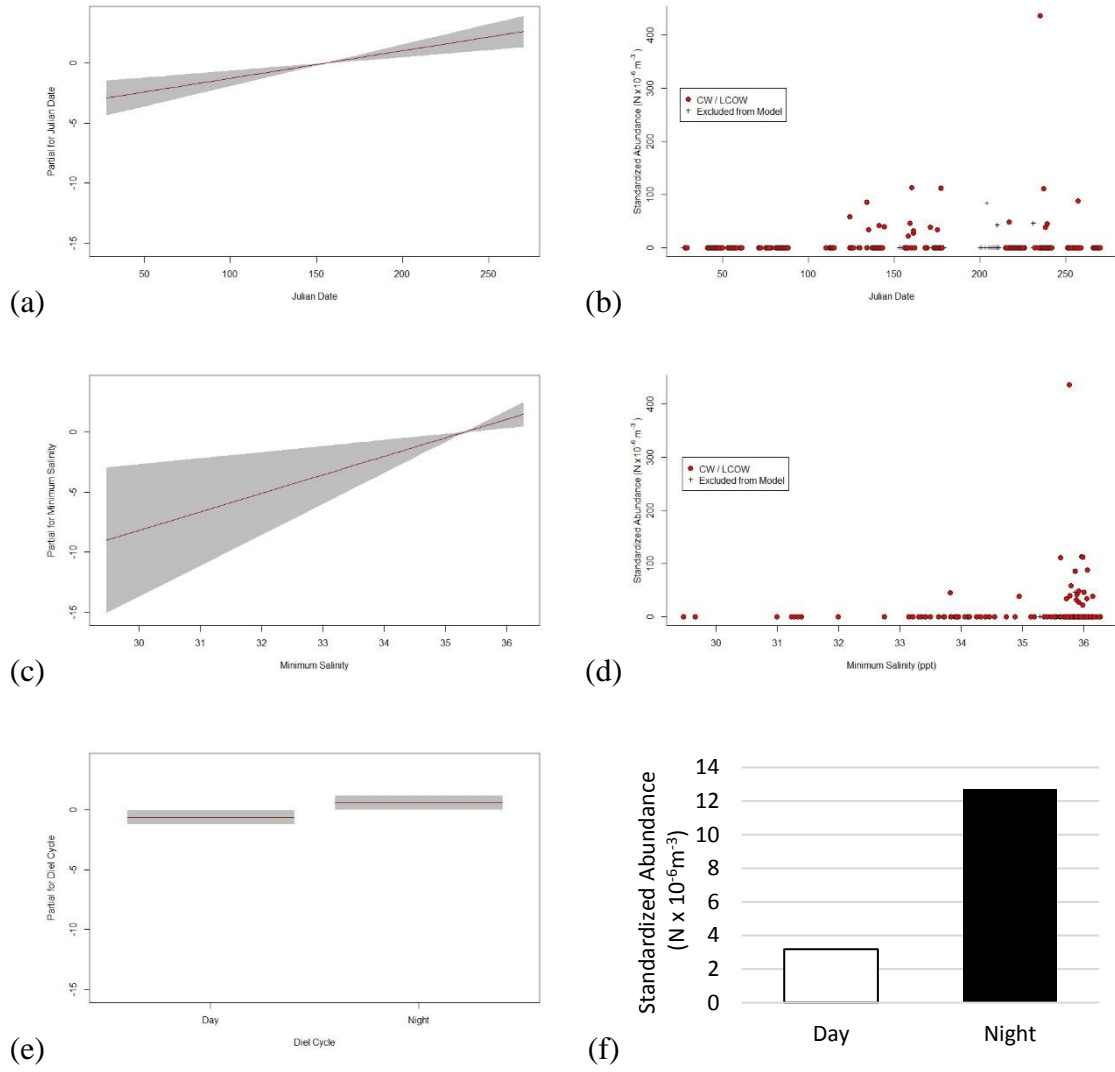


Figure 48. Term plots and standardized abundances of *Thunnus atlanticus* in relation to (a and b) Julian date, (c and d) minimum salinity, and (e and f) diel cycle.

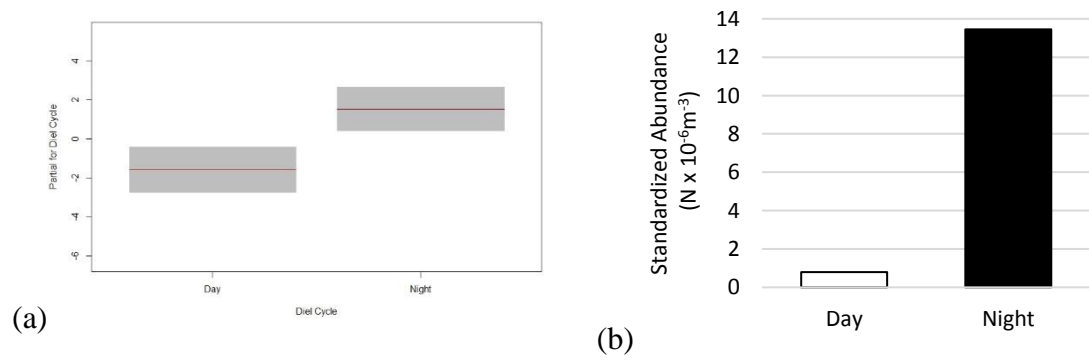


Figure 49. (a) Term plot and (b) standardized abundances of *Auxis thazard* in relation to diel cycle, showing a dominance in nighttime samples.

3.5.2.1.3. Presence-absence models of the three most-abundant scombrids.

Presence-absence models with a binomial distribution were used to investigate the probability that a given scombrid (e.g., family Scombridae, *E. alletteratus*, *T. atlanticus*, and *A. thazard*) would be caught in the epipelagic zone based on each explanatory variable. As a whole, the family Scombridae catches were most correlated to Julian date (dAIC: +13.1, Table 16a, Figure 50a) and marginally to water mass (dAIC: +2.1, Table 16a, Figure 50b). Similar to the GAMs results, more scombrids were collected later in the year and in Common Water.

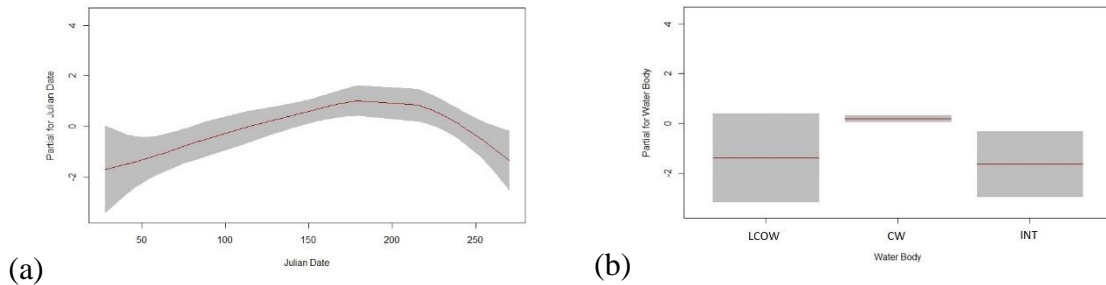


Figure 50. Term plots of Scombridae in relation to (a) Julian date and (b) water mass.

Table 16. AIC values of the presence-absence models with dropping one explanatory variable for (a) Scombridae, (b) *Euthynnus alletteratus*, (c) *Thunnus atlanticus*, and (d) *Auxis thazard*. The full model's AIC values are highlighted in gray and are referred to as “none.” Important explanatory variables are bolded

Explanatory variable dropped	AIC value	dAIC
Julian date	235.7	+13.1
Water mass	224.7	+2.1
Diel cycle	224.4	+1.8
Distance to 200-m isobath	223.4	+0.8
<i>None</i>	222.6	-
Minimum salinity	222.0	-0.6

a. Scombridae

Explanatory variable dropped	AIC value	dAIC
Julian date	122.6	+20.8
Minimum salinity	105.6	+3.8
Diel cycle	102.3	+0.5
<i>None</i>	101.8	-
Distance to 200-m isobath	101.3	-0.5
Water mass (LCOW/CW)	100.6	-1.2

c. *Thunnus atlanticus*

Explanatory variable dropped	AIC value	dAIC
Julian Date	111.2	+11.0
Minimum salinity	106.4	+6.2
Distance to 200-m isobath	103.6	+3.4
<i>None</i>	100.2	-
Diel cycle	98.0	-2.2

b. *Euthynnus alletteratus*

Explanatory variable dropped	AIC value	dAIC
Diel cycle	119.4	+4.1
Distance to 200-m isobath	115.4	+0.1
<i>None</i>	115.3	-
Julian date	113.6	-1.7
Minimum salinity	113.2	-2.1

d. *Auxis thazard*

Euthynnus alletteratus and *T. atlanticus* abundances were associated with seasonality (dAIC: +11.0, Table 16b, Figure 51a; and dAIC: +20.8, Table 16c, Figure 51d, respectively) and salinity levels. Both species were caught later in the year, but the probability of being caught varied with salinity levels. *Euthynnus alletteratus* was most likely caught in lower salinities (dAIC: +6.2, Table 16b, Figure 51b), while *T. atlanticus* was marginally associated with higher salinities (dAIC: +3.8, Table 16c, Figure 51e). *Euthynnus alletteratus* was marginally associated with distance to the nearest 200-m isobath (dAIC: +3.4, Table 16b, Figure 51c), where it was more likely to be collected closer to the shelf break. The probability of catching *A. thazard* was higher at night (dAIC: +4.1, Table 16d, Figure 51f).

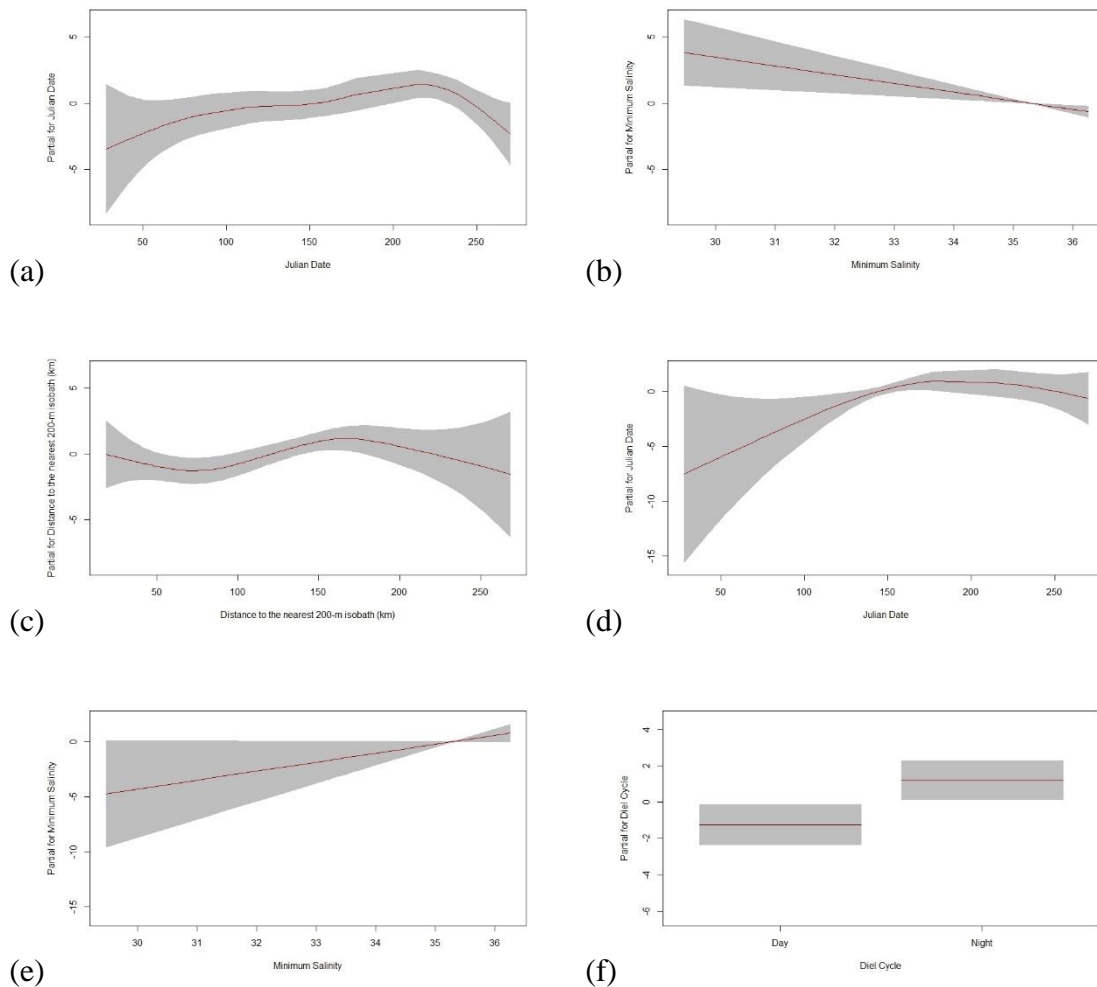


Figure 51. Term plots of: *Euthynnus alletteratus* in relation to (a) Julian date, (b) minimum salinity, and (c) distance to 200-m isobath; *Thunnus atlanticus* in relation to (d) Julian date and (e) minimum salinity; and *Auxis thazard* in relation to (f) diel cycle.

3.5.2.2. MOCNESS 2015-2017.

The spatiotemporal distributions of the most-abundant species, *E. alletteratus*, was investigated. GAMs were unable to be conducted on the *E. alletteratus* count data due to the detection of patchiness (i.e. about 47% of the specimens were collected in one tow). Presence-absence models did not work as well due to a small sample size and variance across tows. Thus, the environmental conditions previously investigated in the MOCNESS 2011 survey (i.e. epipelagic minimum salinity, Julian date, distance to the nearest 200-m isobath, water body, and diel cycle) in relation to larval *E. alletteratus* catches are described below.

Euthynnus alletteratus was only caught in August, with higher abundances collected in 2016 compared to 2015 due to patchiness. Larvae were only collected in the epipelagic zone in Common Water, and all specimens were caught at night except for one. Individuals were collected in waters with minimum salinities ranging from 32.39 to 35.72. *Euthynnus alletteratus* larvae were caught from 69.5 to 243.8 km from the nearest 200-m isobath.

3.5.2.3. High-speed rope trawl 2010-2011.

Spatial distribution maps were created for the three most-abundant species and/or taxa (e.g., *Thunnus* spp., *E. alletteratus*, and *K. pelamis*) collected from December 2010 to September 2011, with only quantitative tows and months plotted. The standardized abundances of each species were analyzed across the sampling grid by both month and diel cycle (day vs. night). Each species abundances were compared with three environmental features (chlorophyll *a*, SSHA, and minimum salinity; Appendix Figures 1-3). None of the three taxa were collected in December 2010 and April 2011.

Thunnus spp. were the most-abundant taxa in this study and were collected across the entire sampling grid during both the day and night, specifically in the northern and eastern stations (Figure 52 and 53). *Thunnus* spp. were collected over three months during the day and night (June, July, and September). Seasonal abundances were evident, as individuals were not collected in December and April. High abundances related to Common Water with low chlorophyll *a* concentrations. Individuals were collected between the 1200- and 2700-m isobaths.

Euthynnus alletteratus, the second-most abundant species, was collected over three months (June, July and September) during the day and at night (Figure 54 and 55). *Euthynnus alletteratus* was collected in the northern portion of the grid in June, the eastern stations in July, and both the eastern and northern sections in September. *Euthynnus alletteratus* appeared to reside in water bodies with maximum depths between 1200 and 2700 m and additionally near the De Soto Canyon and DWHOS site. High abundances were associated with Common Waters with moderate chlorophyll *a* concentrations.

Katsuwonus pelamis was the third-most abundant species collected with the high-speed rope trawl. This species was only caught in June, July and September at night, with highest abundances in July (Figure 56 and 57). *Katsuwonus pelamis* was found in offshore waters between the 2200- and 2700-m isobaths, and this species was typically collected in Common Waters with moderate chlorophyll *a* concentrations and moderate salinity levels.

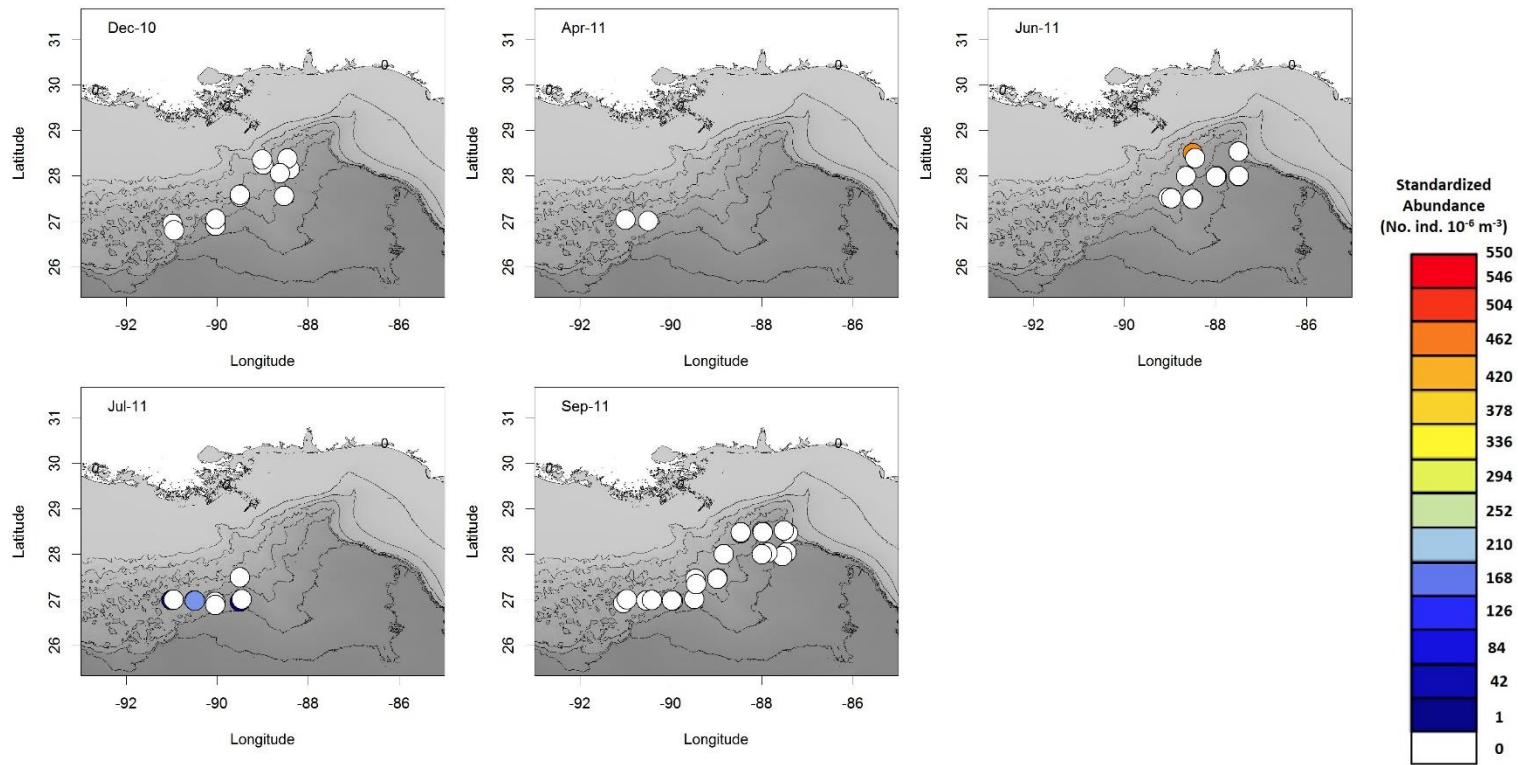


Figure 52. A heat map of *Thunnus* spp. standardized abundances in the epipelagic zone collected during the day using the high-speed rope trawl from 2010-2011. White indicates that no individuals were collected. Abundances range from blue (1 ind. 10^{-6} m^{-3}) to red (550 ind. 10^{-6} m^{-3}).

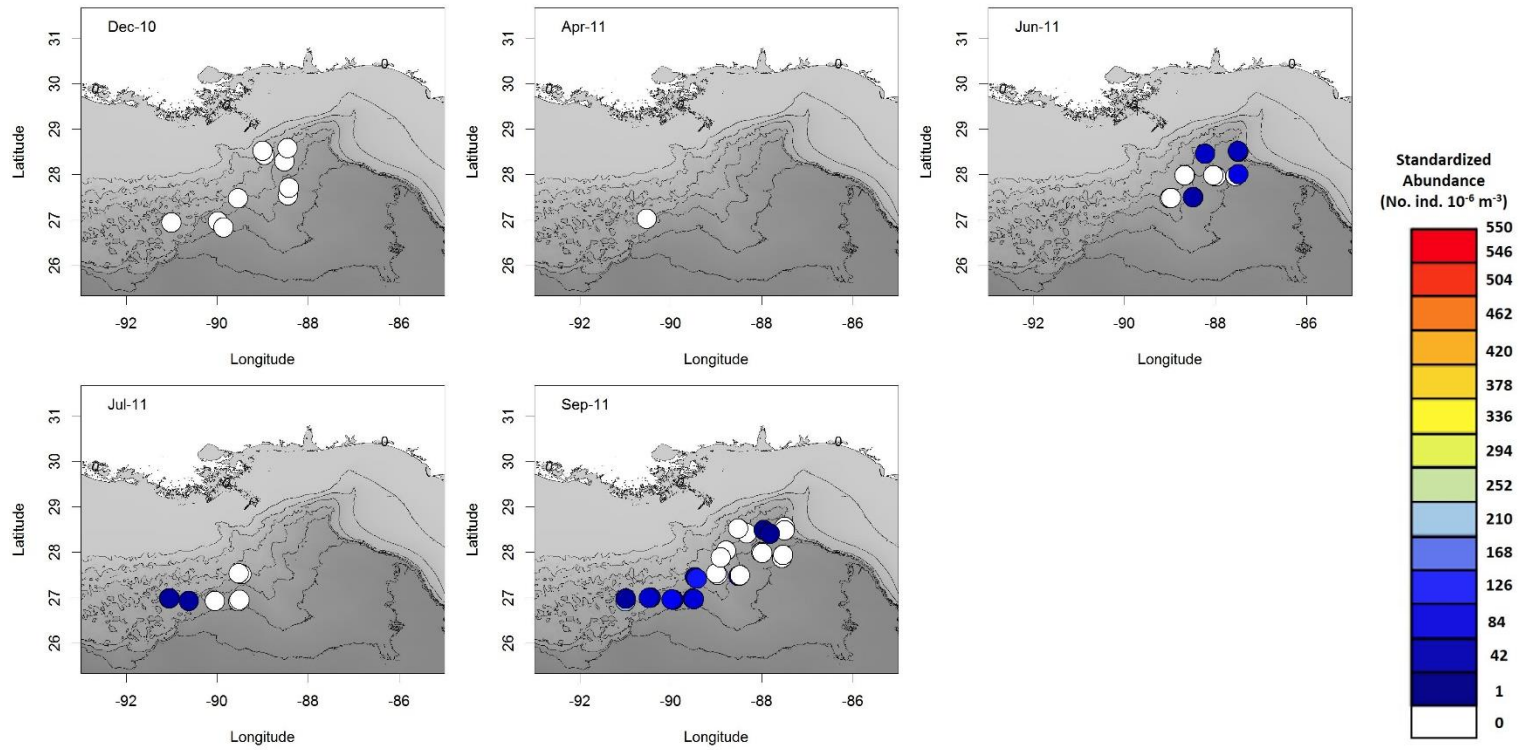


Figure 53. A heat map of *Thunnus* spp. standardized abundances in the epipelagic zone collected at night using the high-speed rope trawl from 2010-2011. White indicates that no individuals were collected. Abundances range from blue (1 ind. $10^{-6} m^{-3}$) to r to red (550 ind. $10^{-6} m^{-3}$).

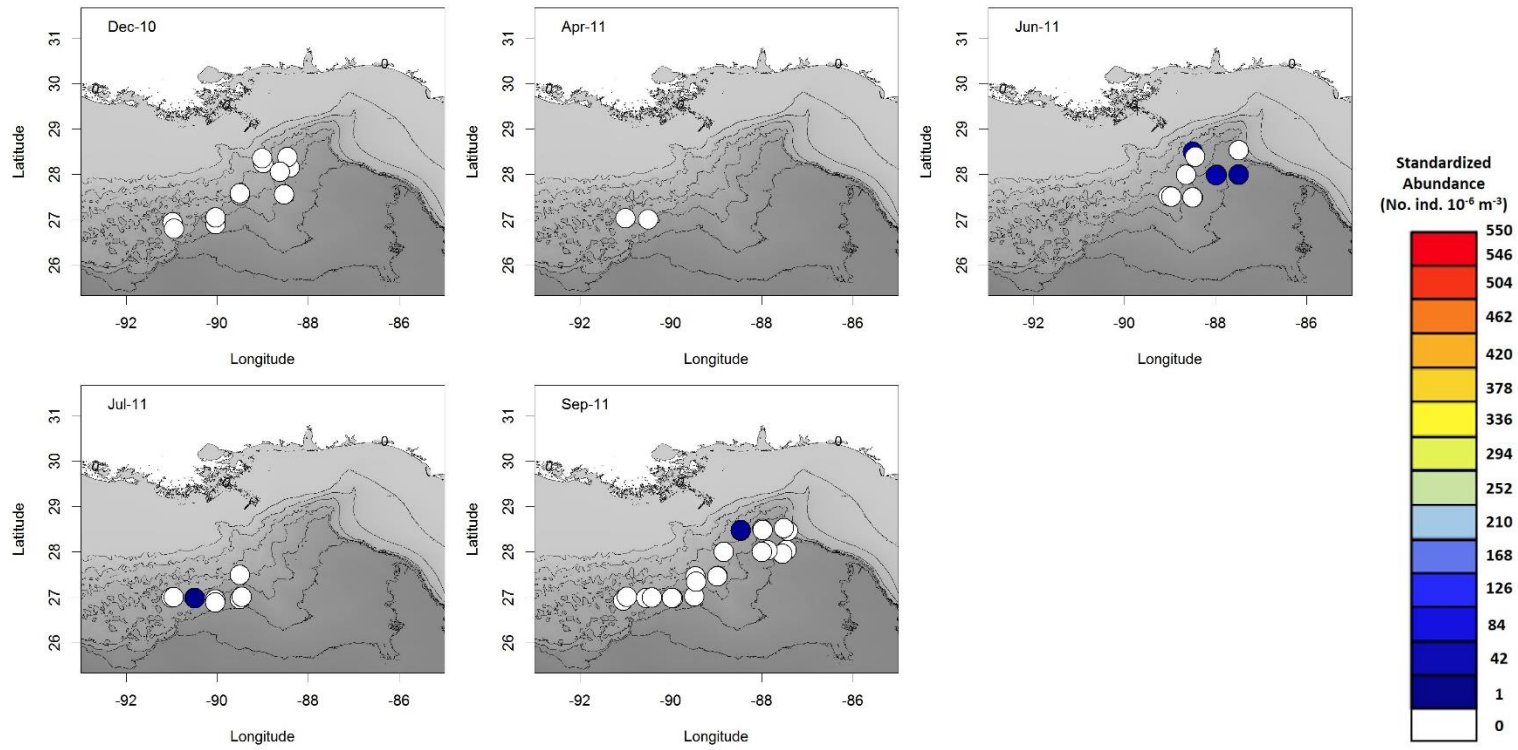


Figure 54. A heat map of *Euthynnus alletteratus* standardized abundances in the epipelagic zone collected during the day using the high-speed rope trawl from 2010-2011. White indicates that no individuals were collected. Abundances range from blue (1 ind. 10^{-6} m^{-3}) to red (550 ind. 10^{-6} m^{-3}).

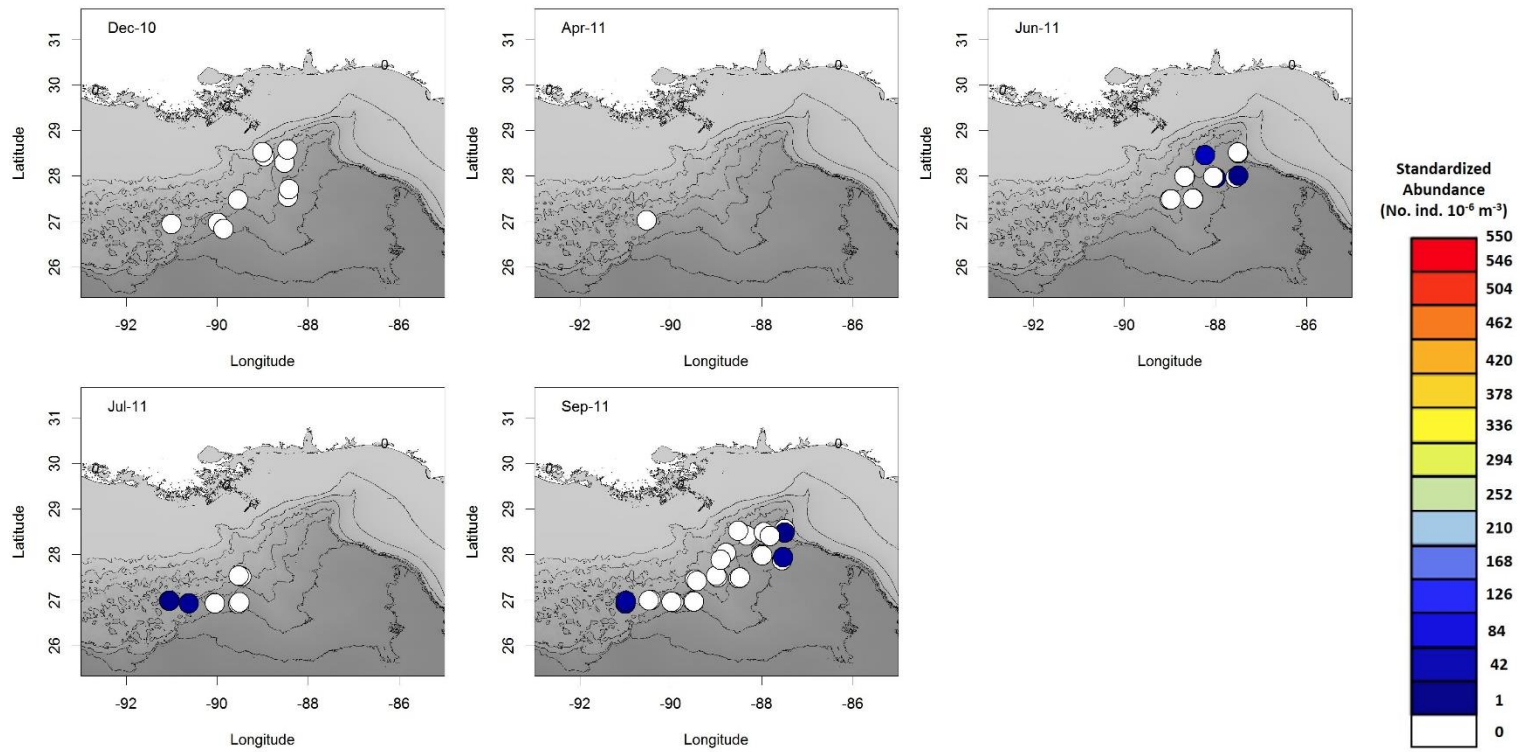


Figure 55. A heat map of *Euthynnus alletteratus* standardized abundances in the epipelagic zone collected at night using the high-speed rope trawl from 2010-2011. White indicates that no individuals were collected. Abundances range from blue (1 ind. 10^{-6} m^{-3}) to red (550 ind. 10^{-6} m^{-3}).

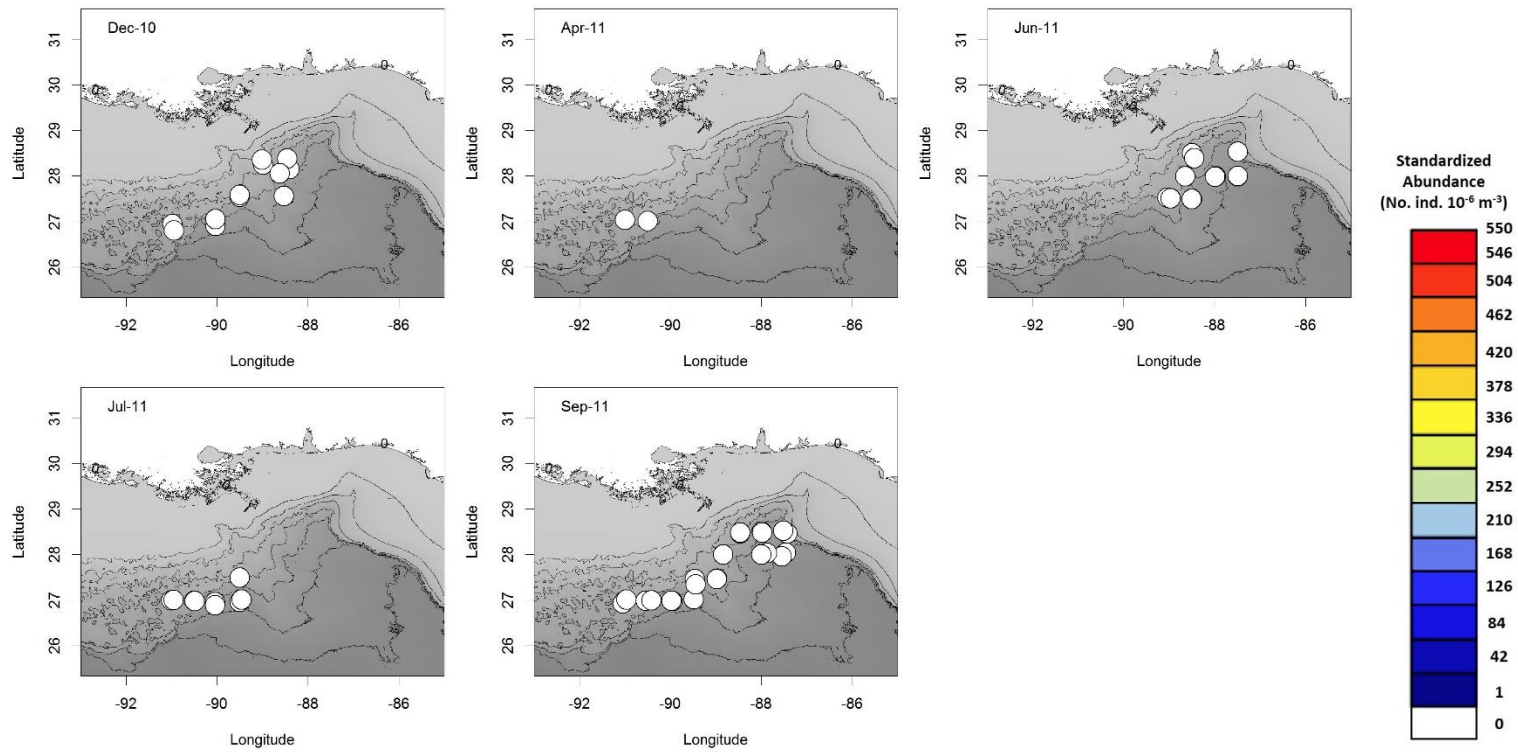


Figure 56. A heat map of *Katsuwonus pelamis* standardized abundances in the epipelagic zone collected during the day using the high-speed rope trawl from 2010-2011. White indicates that no individuals were collected. Abundances range from blue (1 ind. 10^{-6} m^{-3}) to red (550 ind. 10^{-6} m^{-3}).

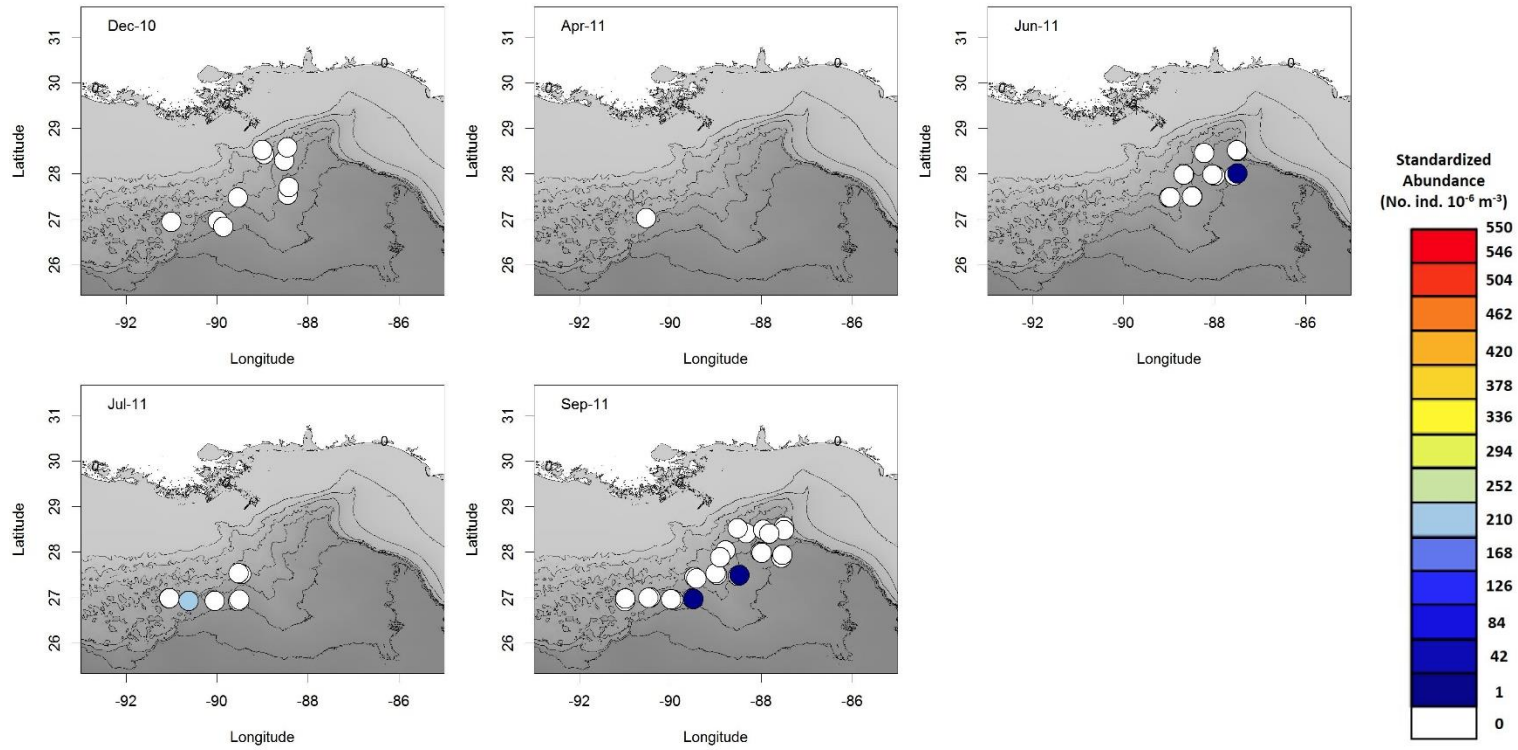


Figure 57. A heat map of *Katsuwonus pelamis* standardized abundances in the epipelagic zone collected at night using the high-speed rope trawl from 2010-2011. White indicates that no individuals were collected. Abundances range from blue (1 ind. 10^{-6} m^{-3}) to red (550 ind. 10^{-6} m^{-3}).

3.5.3. Seasonal distributions.

3.5.3.1. MOCNESS 2011.

Euthynnus alletteratus was collected from March to September, with highest abundances in August (Figure 58a). *Thunnus atlanticus* was collected in March and also from May to September at higher abundances (Figure 58b). Higher abundances of *T. atlanticus* were collected in June and August. *Auxis thazard* was collected from February to September (Figure 58c), with highest abundances in April. None of the three species were collected in January (Figure 58).

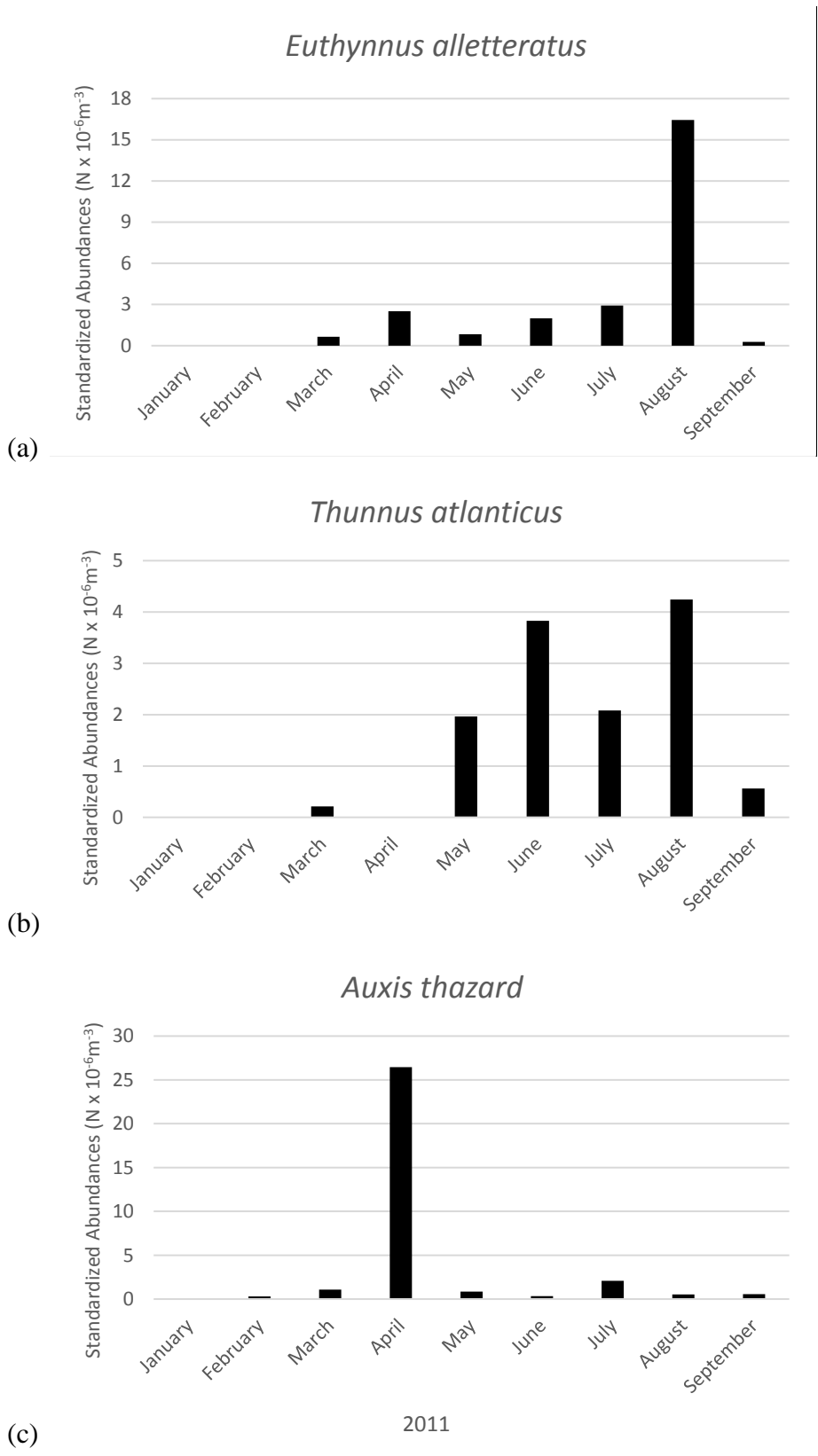


Figure 58. Seasonal occurrence of the top three most-abundant scombrid species, (a) *Euthynnus alletteratus*, (b) *Thunnus atlanticus*, and (c) *Auxis thazard*, collected during the MOCNESS 2011 survey.

3.5.3.2. MOCNESS 2015 – 2017.

Euthynnus alletteratus was caught in August 2015 and 2016, with higher abundances in 2016 due to patchiness (i.e. about 47% of the specimens from this cruise were collected in one tow, Figure 59a). *Thunnus atlanticus*, *Thunnus* spp., and *Auxis thazard* were only collected in August 2016, while *T. thynnus* was only collected in May 2016 (Figure 59b). *Katsuwonus pelamis* was collected in May and August 2016 and in May 2017 (Figure 59b).

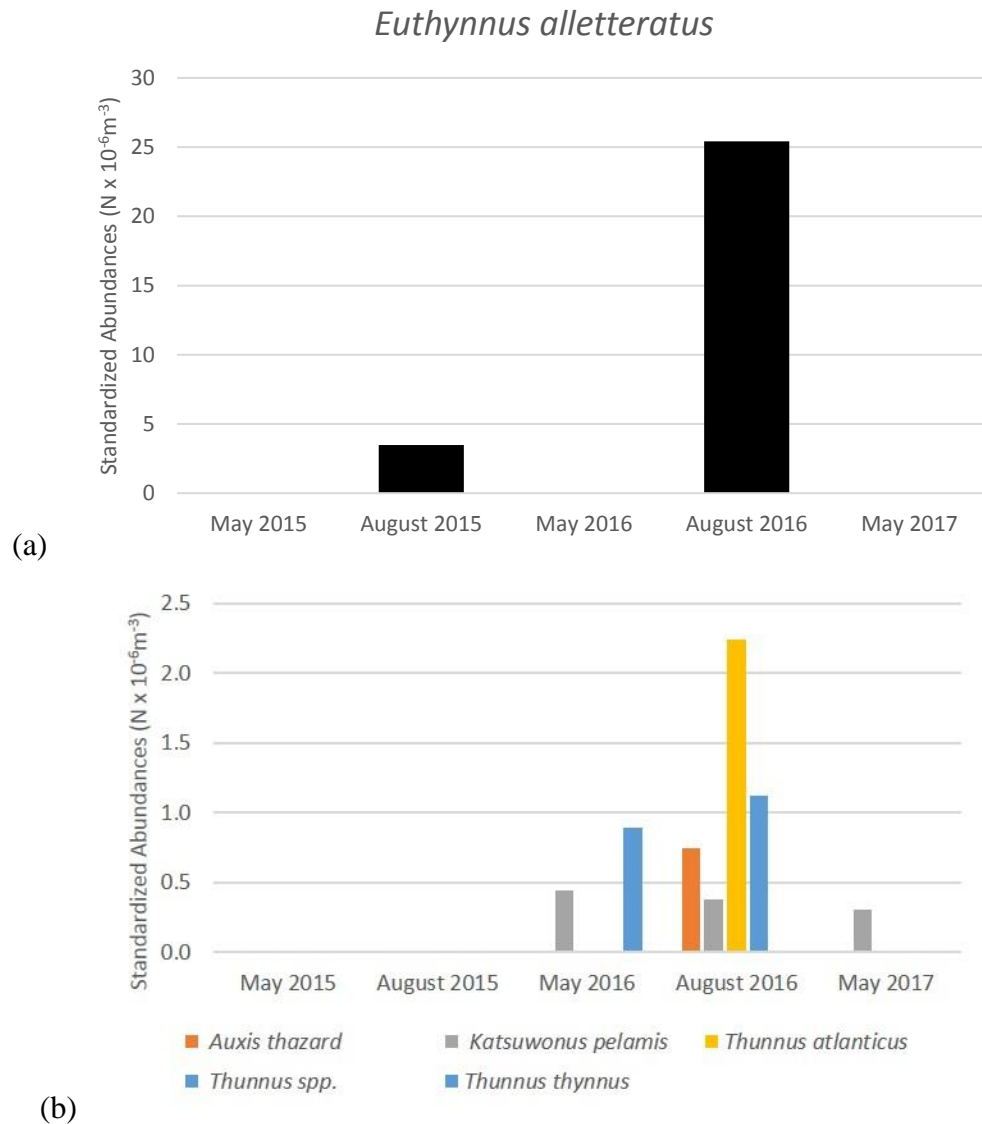


Figure 59. Seasonal occurrence of (a) *Euthynnus alletteratus* and (b) all other scombrids collected during the MOCNESS 2015 - 2017 survey.

3.5.3.3. High-speed rope trawl 2010 – 2011.

Months that contained quantitative tows were only included in the seasonal analyses for the high-speed rope trawl 2010-2011 survey. *Thunnus* spp. was the most-abundant taxon group, high taxonomic uncertainty at the species-level precluding further faunal resolution. *Thunnus* spp. were collected in June, July and September with highest abundances in June (Figure 60a). *Euthynnus alletteratus* was the second-most abundant species, which was also caught in June, July and September with highest abundances in June (Figure 60b). *Katsuwonus pelamis* was caught in June, July and September. Highest abundances peaked in July, with relatively low abundances in June and September (Figure 60c). These three species were not collected in December 2010 and April 2011.

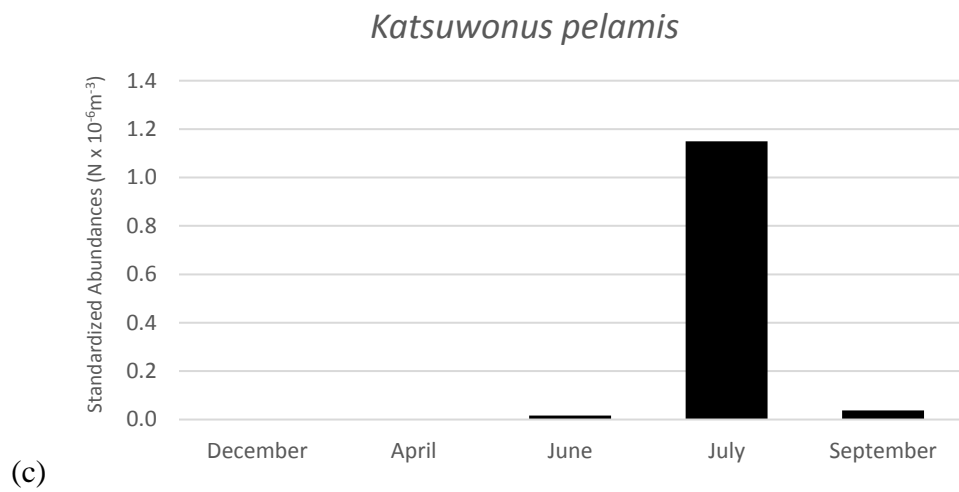
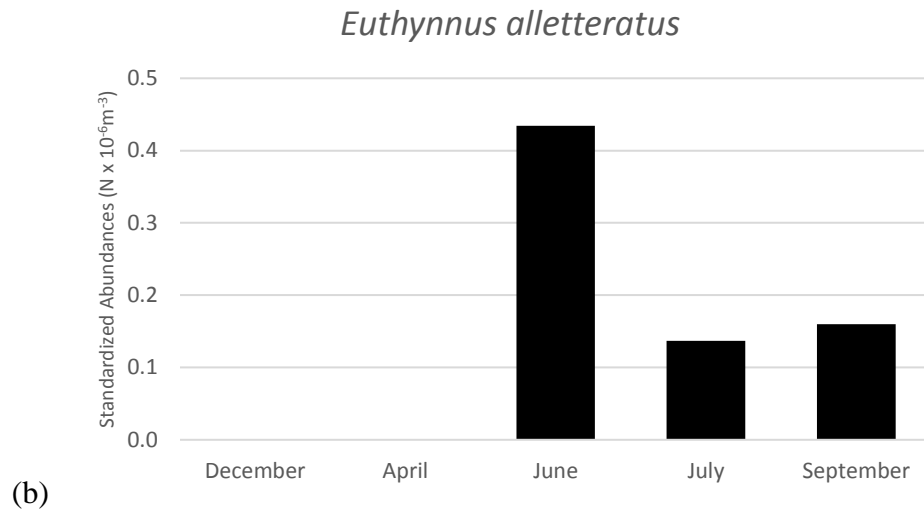
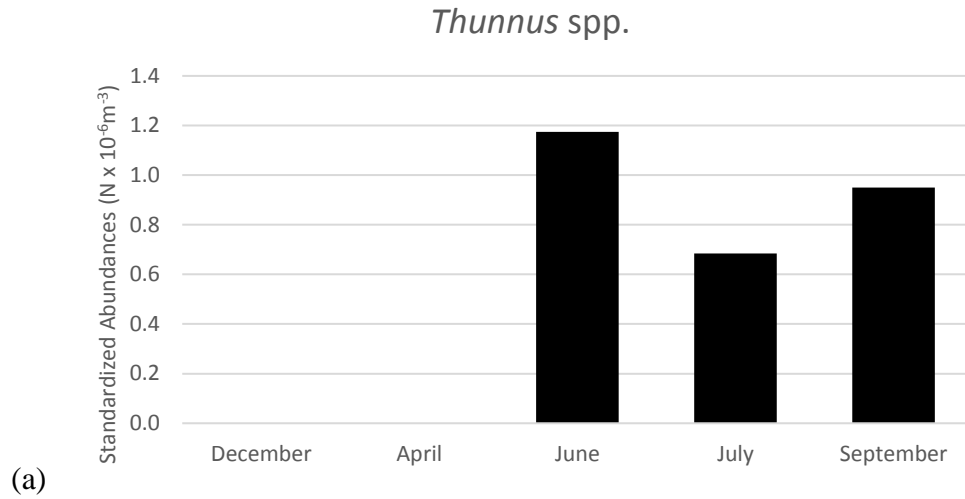


Figure 60. Seasonal occurrence of the top three most-abundant scombrid taxon (a) *Thunnus* spp., (b) *Euthynnus alletteratus*, and (c) *Katsuwonus pelamis* collected during the high-speed rope trawl 2010-2011 survey. Only months with quantitative samples were included.

4. DISCUSSION

While adult scombrids are well-described, this thesis developed and updated taxonomic descriptions for the GoM scombrid early life stages (larvae and more specifically, juveniles). Gear selectively was observed, with the MOCNESS collecting predominately larvae and the high-speed rope trawl catching only juveniles. The dominant species and taxa in the GoM during all cruise series included: *Euthynnus alletteratus*, *Thunnus atlanticus*, *Auxis thazard*, *Katsuwonus pelamis*, *Thunnus* spp., and *Auxis* spp. The morphometric ratios of the two most-abundant species (*E. alletteratus* and *T. atlanticus*) were compared and analyzed based on their ecology. Specific-specific environmental preferences were identified for the dominant scombrids collected in this study.

4.1. Larval and juvenile scombrid taxonomy.

Species discrimination is needed for scombrid early life stages, as this is a key element of conservation and fisheries management (Ibañez et al. 2007). The identification of species has heavily relied on morphological and meristic characteristics (Cadrin 2000), though genetic and environmental variability on growth and development processes can often create shape variation among populations. Previously, biometric descriptions have been reported for scombrid species such as *T. thynnus* and *E. alletteratus* from the eastern and/or western Mediterranean, Pacific Ocean, and the eastern Atlantic Ocean (Frade 1931, Miyashita et al. 2001, Hajjej et al. 2011, Tičina et al. 2011, Hajjej et al. 2013, Addis et al. 2014, Karakulak et al. 2016). However, juveniles from these previous studies ranged from 12.2 – 130.0 cm FL. Scombrids from previous studies were larger and from different regions than the size range of specimens used in this thesis from the GoM. Thus, understanding the different methodologies used to identify scombrids can aid in the management of fish stocks and sustainable fishing and identify differences among regions.

4.1.1. Genetic analyses.

Puncher et al. (2015) found that genetic barcoding studies have previously revealed misidentifications of larval and juvenile tunas solely using morphology-based taxonomy, due to the lack of defined characters. As juvenile scombrids remain taxonomically challenging, it was necessary to obtain several genetically identified specimens in order to initiate the morphological analyses of this taxonomically challenging life stage. The change

in pigmentation patterns and the lack of adult features complicates the juvenile identification process. Incorrect identifications are probable until further genetic and morphometric analyses are conducted in combination and distinct characteristics by life stage and size class are identified. Thus, genetic barcoding remains obligatory for juvenile scombrids in order to ensure proper identifications.

4.1.2. *Morphological analyses.*

This thesis improved the knowledge of larval diagnostic features in regard to their pigmentation patterns for all scombrid species, except for *T. alalunga*, *T. obesus*, *Scomber colias*, *Scomberomorus brasiliensis*, *Scomberomorus maculatus*, and *Scomberomorus regalis*, which were not identified in this study. After the analysis of the different larval morphologies, there still remains some taxonomic issues and data gaps. The quick reference chart for identifying thunnine larvae can successfully guide the identification of these difficult larval stages if all pigmentation is present. However, *Thunnus* remains the most difficult genus to identify, as previously noted by Richards (2005). For example, the lack of pigmentation along the ventral tail region makes distinguishing the difference between *T. albacares* and *T. atlanticus* difficult. Thus, genetic analyses are necessary for correct identifications when pigmentation does not exist along the ventral midline of a *Thunnus* larva. Richards (2005) also noted that *T. atlanticus* has two larval morphs, one of which can often be misidentified as *T. albacares*, strengthening the need for using genetic barcoding. As larval specimens reach about 10.0 to 13.0 mm SL, their larval pigmentation patterns change and these descriptions cannot be used for identification purposes. For example, *Auxis* spp. develop additional dorsal midline spots as the individual grows, hindering the ability to distinguish between the two *Auxis* species. Incorrect morphological identifications will occur if these new pigmentation patterns are not recognized for these newly-transformed juvenile specimens.

Juvenile descriptions were provided for all species, except *T. alalunga*, *T. obesus*, *Sarda sarda*, *Scomberomorus brasiliensis*, *Scomberomorus cavalla*, *Scomberomorus maculatus*, and *Scomberomorus regalis*, which were not collected in this study. Similar to the larval stages, thunnine juveniles are the most difficult tribe to identify. This thesis

provided novel descriptions for these smaller juvenile specimens that were previously unidentifiable.

The diagnostic key for identifying genera/species in the Tribe Thunnini using fin ray counts is a quick and reliable method when fins are not damaged. Larval and juvenile *E. alletteratus*, *K. pelamis*, and *Acanthocybium solandri* can be identified to species using a combination of fin ray counts. There are finite characters to investigate and this study identified each of those characters that were informative and non-informative for the genetically identified species (Appendix Table 3). The juvenile descriptions in this study provide a more robust method for identifying juvenile tunas.

Meristic counts of the pectoral and first dorsal fins are useful in identifying the genus *Auxis* when a specimen is not damaged, and when gill raker counts cannot differentiate these species as adults. The morphometric ratios of this genus can also be used to distinguish these two species from the other thunnine species. *Auxis* spp. can be differentiated by having high ratios of interdorsal length to HL and low ratios of upper jaw length to HL. The ratios of the interdorsal length to HL and of the interdorsal length to first dorsal fin length are slightly informative as they do not agree with adult characteristics (interdorsal length is 80% of HL, Hammond and Cupka 1975), yet they still distinguish these two *Auxis* spp. from all other scombrids (higher ratios). Upper jaw length compared to HL was a slightly informative ratio, as *Auxis* spp. had smaller ratios compared to all other thunnine species and *Acanthocybium solandri*. This feature may be valuable for rough sorting specimens, and the usefulness of the ratio could be confirmed with a larger sample size.

Furthermore, the two species of the genus *Auxis* could possibly be separated by using interdorsal length to SL and/or interdorsal length to first dorsal length. *Auxis rochei* maintains a higher interdorsal length to SL ratio compared to *A. thazard*. Interdorsal length to the first dorsal fin length is typically 1:1 in adult *Auxis* spp. (Hammond and Cupka 1975), but *A. rochei* exceeded this ratio, while *A. thazard* possessed a slightly lower ratio. These differences could be verified with a larger sample size and wider size-range per species.

Euthynnus alletteratus can be distinguished from all other scombrids using fin ray counts (pectoral and both dorsal fins) when fins are intact. Using morphometric ratios, *E. alletteratus* have lower snout length to eye diameter and higher snout length to HL ratios compared to *Thunnus* spp. (*T. albacares*, *T. atlanticus*, and *T. thynnus*). It was previously reported that juvenile *E. alletteratus* from 14.0 to 174.0 mm SL develop the adult appearance as their body becomes a more fusiform and elongated (Hammond and Cupka 1975). This elongated body shape was observed in this study; however, fin ray counts and morphological ratios were more important for identifying *E. alletteratus*.

Katsuwonus pelamis can also be distinguished from all other scombrids using fin ray counts (pectoral and both dorsal fins) when fins are intact. *Katsuwonus pelamis* was insufficiently sampled in terms of the genetically identified specimens. Its ratios overlapped with various thunnine species. Gill raker counts were not useful as well, although this species maintained higher counts compared to other thunnine species. Gill raker counts are discussed in detail below. Further analyses need to be conducted on this species, as two individuals was not a sufficient sample size for identifying morphological differences among other thunnine species.

Additionally, *Thunnus* spp. could not be separated with a small sample size, as smaller *T. albacares* and *T. atlanticus* had similar ratios and larger *T. atlanticus* and *T. thynnus* had similar ratios. Moreover, the ratios of eye diameter to snout length and eye diameter to HL are informative for differentiating between *E. alletteratus* and an all-encompassing *Thunnus* spp. More specifically, *T. albacares* needs to be collected at a larger sample size and size range. All *T. albacares* specimens were between 12.0 - 32.5 mm SL, which did not allow for comparisons of slightly larger juveniles, like *T. atlanticus* and *T. thynnus*, which contained an individual that was approximately 120 mm SL. Moreover, *T. alalunga* and *T. obesus* were not identified in this study; in turn, the morphological comparisons of these two *Thunnus* species were impossible. Thus, further analyses of the entire *Thunnus* genus needs to be conducted in order to identify accurate morphological differences among species.

Understanding the size at which livers become reliable features for species identifications is also important in ensuring correct species identifications of juvenile

Thunnus spp. It is believed that *T. alalunga*, *T. obesus*, and *T. thynnus* develop striations (ICCAT 2016a) as the scombrid grows (B. Collette pers. comm.); thus, finding the size at which the striations develop is critical in differentiating *Thunnus* spp. The only genetically identified specimen that was expected to possess striations was *T. thynnus*. However, the specimen (124.8 mm SL) did not possess striations, as it is possible that the preservation method (frozen) may have altered its appearance or that the striations did not develop by this size. The liver of a 121.7 mm SL *T. atlanticus* fit the adult description (lack of striations and larger right lobe). Further analyses are needed in determining size (and age) at which striations appear in order to utilize livers as diagnostic characteristics for the genus *Thunnus*.

Juvenile *Scomber colias* were identifiable by having 4 to 5 top finlets and 5 bottom finlets in addition to an anal spine (Richards 2005). All three meristic features were critical in juvenile identifications. This species develops an elongate body shape as it develops into a juvenile, which also aided in the identification process.

Acanthocybium solandri can be identified by fin ray counts (high first dorsal fin counts and low second dorsal fin counts) the lack of gill rakers. Moreover, *A. solandri* had the lowest eye diameter (~50%) to snout length ratio compared to *E. alletteratus* and *Thunnus* spp., as *A. solandri* have long snouts. The snout length of adult *A. solandri* is approximately 50% of its HL (Hammond & Cupka 1975). The ratio of snout length to HL may also be a slightly informative ratio for *A. solandri*, as a juvenile maintained a higher ratio than all other scombrids (44% of HL of a 47.0 mm SL individual). Although adult ratios were not observed, using the snout length is a more robust method of identifying this species.

All of the morphometric ratios identified in this study are valuable for rough sorting specimens. These ratios need to be verified with a larger sample size of genetically identified juveniles over a wider size range of specimens. Genetic identifications remain necessary for juvenile scombrids until additional distinct characteristics are identified.

In addition to the morphometric ratios, investigating the development of adult gill raker counts is critical for identifying young scombrid species. Gill raker counts are not

useful to distinguish *Auxis* spp., as adult counts overlap (ICCAT 2016a). However, it is imperative to know when (e.g., specific size in mm SL) a juvenile possesses a full complement of gill rakers. This will help further identify the difference between poorly described juvenile scombrids (i.e. *Thunnus* spp.). This study found that a *T. atlanticus* possessed adult counts (19-25, ICCAT 2016a) at 121.7 mm SL, but did not at 42.5 mm SL. A juvenile *T. thynnus* also had adult gill raker counts (34-43, ICCAT 2016a) at 124.8 mm SL. However, there were large data gaps due the limited size range of genetically identified specimens. All other genetically identified juvenile specimens within the *Thunnus* genus did not contain adult counts. *Katsuwonus pelamis* (32.5 mm SL) did not possess adult counts, but did contain higher counts compared to all other thunnine species at that size. Having higher gill raker counts in juvenile size classes within the Tribe Thunnini mimics the adult characteristics, as adult *K. pelamis* have 53-63 gill rakers (ICCAT 2016a). Moreover, *Acanthocybium solandri* lacks gill rakers (ICCAT 2016a), which is taxonomically useful.

Overall, this thesis extended existing morphological descriptions of scombrid larvae and provided baseline descriptions of the juvenile stage as well. Larger sample sizes of juvenile specimens for genetic analyses are needed to identify the differences between species of this problematic life stage. Genetic sequencing is essential until further descriptions are developed. Samples would also ideally include all 16 species found within the GoM for proper taxonomic analyses. The combination of all features (e.g., fin ray counts, morphometric ratios, gill raker counts, liver morphology, etc.) will provide valuable knowledge for differentiating these species. An individual feature cannot stand alone for the identification process of juvenile scombrids.

4.2. Larval and juvenile scombrids faunal composition and ecology.

4.2.1. Assemblage structure.

The MOCNESS 2011 survey collected the highest number of species ($n = 11$) compared to both the MOCNESS 2015-2017 survey ($n = 6$) and the high-speed rope trawl 2010-2011 survey ($n = 8$). Similar to the ranks, this high species occurrence can relate to the continuous surveying method, the longevity of the cruise series (January to September 2011), and the specific seasons that were sampled during the MOCNESS 2011 survey.

Quantitative data from the high-speed rope trawl survey were only derived from December 2010 and April, June, July, and September 2011, while the MOCNESS 2015-2017 only sampled from April to May and in August each year.

Both MOCNESS surveys collected higher abundances of scombrids per species than the high-speed rope trawl survey. Moreover, larval and juvenile scombrids reside in the upper surface waters of the epipelagic zone, which was targeted by the MOCNESS discrete-depth sampling. However, the high-speed rope trawl conducted oblique tows to a maximum of 1500 m during each deployment; thus, this large net surveyed deeper depths at which these life stages do not often reside. The high-speed rope trawl also filtered a much larger volume than a MOCNESS net (2662579.74 m³ and 33053.00 m³, respectively on average) due to the differences in mouth size (165-m² and 10-m², respectively). On average, the high-speed rope trawl filtered approximately 80 times more water than the MOCNESS per net tow. In turn, the abundances of the high-speed rope trawl appeared lower, as the deeper strata were preferentially surveyed (at larger volumes per unit effort); tuna early life stages are not typical of these deep waters. Additionally, scombrids were collected at higher frequencies with the high-speed rope trawl (~50% F₀) compared to both MOCNESS surveys (15% and 5% F₀). This result may relate to the large mouth of the high-speed rope trawl, as it would ostensibly reduce avoidance by these highly mobile fishes.

In this study, the MOCNESS predominately caught smaller scombrid specimens compared to the high-speed rope trawl, which caught juvenile scombrids more effectively. It is an advantage to use a multiple gear types in order to survey a wider size range of midwater fishes (Kashkin & Parin 1983, Millar 1992, Willis et al. 2000). In fact, gear selectivity is inherent in previous scombrid surveys. For example, bongo tows and neuston nets are often used to survey larvae, while mark-recapture, electronic tagging methods, and catch per unit effort from pelagic longlines are used to survey adults. A specific and/or typical gear type does not exist for these small juvenile sizes that the high-speed rope trawl collected, though pair-trawling (midwater net towed between two vessels) has promise.

Gear selectivity relates directly to mesh size. As previously stated, the MOCNESS (3-mm mesh) primarily caught larvae and a few small juveniles, while the high-speed rope

trawl (graded mesh, 3.2 m to 19 mm) collected only juvenile scombrids. MacLennan (1992) found that smaller mesh sizes reduce the chance of smaller fishes escaping, and Kashkin and Parin (1983) found that larger nets effectively collect larger fishes. Thus, juvenile scombrids would have been underrepresented in this study if the high-speed rope trawl was not used. Conversely, larval scombrids would not have been collected if only the high-speed rope trawl was used. It is evident that different gear types collected different life stages and size classes of scombrids and that ideally both methods should be utilized in order to gain a more complete analysis of their ecology.

Additionally, both gear types in this study used larger mesh sizes compared to other studies that capture small larvae. Typical mesh sizes for larval surveys (e.g., bongo and neuston nets) range from 335 to 1200 μm (Richards et al. 1984, Lindo-Atichati et al. 2012, Habtes et al. 2014, Cornic et al. 2018). While avoidance is a function of mouth size, extrusion is a function of mesh size. Thus, this study did not collect as many planktonic larvae compared to other ichthyoplankton surveys, as smaller individuals were able to extrude through the larger mesh sizes utilized in our surveys. As a result, smaller larvae were underrepresented in this thesis.

Among the three cruise series, the same six species and/or taxa were collected, indicating that *E. alletteratus*, *T. atlanticus*, *Auxis thazard*, *K. pelamis*, *Thunnus* spp., and *Auxis* spp. were the dominant taxa in the GoM. Various larval surveys have also found these species and taxa at higher abundances (Lindo-Atichati et al. 2012, Habtes et al. 2014, Cornic et al. 2018). Due to the taxonomic issues with the juvenile life stage, individuals within the genera *Thunnus* and *Auxis* could not be differentiated. Differences among the ranks per cruise series was most likely caused by seasonal patterns in abundances driven by species-specific spawning preferences and the size class (larva vs. juvenile) that was being collected.

Euthynnus alletteratus was the most-abundant taxon (identified to species-level) in all of the surveys. *Euthynnus alletteratus* is a neritic, epipelagic species that is a year-round resident in the GoM. The coastal *E. alletteratus* spawns from April to November, outside the continental shelf region in temperatures greater than 25 °C. It is a multiple spawner with asynchronous oocyte development that carries out several spawning events per

reproductive season (Chur 1973, Rudomiotkina 1986, ICCAT 2016a). The spawning preferences of this species coincide with the location and time period of all cruise series, explaining its high abundance. Moreover, *E. alletteratus* is a schooling species (Chur 1973). This was observed in the MOCNESS 2015-2017 survey, as 47% of the entire scombrid catch was collected in one tow. Patchiness and schooling behaviors are typical of scombrids, as it was also observed with catches of *Scomber colias*, where 83% of specimens (88 ind.) were collected in one tow during the high-speed rope trawl 2010-2011 survey.

Thunnus atlanticus is an epipelagic, oceanic resident of the GoM that spawns offshore from June to September (Collette 2010). Similar to *E. alletteratus*, its ecology and spawning patterns relate to the time period and location of the surveys, leading to its dominance. It is also often found in large schools, typically with *K. pelamis* (Collette 2010). *Katsuwonus pelamis* is an epipelagic, oceanic species (Collette & Nauen 1983) that similarly exhibits strong schooling behaviors, often near drifting objects (Bard et al. 1991). Schooling often occurs based on size class and may occur with other species of the same size. Smaller fishes are known to school while feeding (Bayliff 1988, Hilborn 1991). *Katsuwonus pelamis* specimens were found in samples with numerous other species, which could possibly relate to its innate need to school in similar size class groups. Spawning occurs several times per seasons in surface temperatures greater than 24 °C (Cayré & Farrugio 1986, Vilela & Castello 1993). Spawning season becomes shorter further from the equator, but females spawn almost daily in tropical waters (Collette 2010).

Auxis thazard is a strongly schooling, epipelagic scombrid that is considered both a neritic species as well as an oceanic occurring species in warmer waters (Collette 1995). Spawning is recorded at SSTs between 21.6 and 30.5 °C, typically from February to November in the North Atlantic, with mass spawning between 25 and 26 °C (Rudomiotkina 1984, ICCAT 2016a). Larval *A. thazard* have the widest temperature tolerance among all tuna (ICCAT 2016a), and this species has a long spawning season, both of which can contribute to its high abundance. Adults are coastal or near-coastal, while juveniles have been reported to be more widely spread throughout the world's oceans (Collette 1995). A

widespread, coastal habitat relates to the area surveyed across the northern GoM in this study.

Other species (*Auxis rochei*, *Sarda sarda*, *Acanthocybium solandri*, *T. thynnus*, *Scomber colias*, and *T. albacares*) were collected in these surveys at lower abundances. Some species, such as the non-resident *T. thynnus*, were rare in these collections most likely due to their restricted and shorter spawning seasons in the GoM compared to other resident spawners (ICCAT 2016a). Moreover, higher taxonomic resolution of larval and juvenile *Thunnus* spp. and juvenile *Auxis* spp. would result in increased detection of individual species in these genera (e.g., *T. albacares* and *T. thynnus*), in addition to possibly identifying new species that were not recorded in this study (e.g., *T. obesus* and *T. alalunga*).

These large-scale surveys conducted over seasonal cycles remain extremely rare in oceanographic research. The advantage of continuously sampling a specific area allows for the collection of the varying species throughout the year. It is evident that different scombrids spawn at different times throughout the year and under different environmental conditions; thus, these surveys provided information on the variance in the ecology of specific species that inhabit the dynamic GoM oceanic ecosystem. Long-term surveys, such as in this study, identify commonalities among years and can highlight typical and rare species occurrences in a region. Overall, all cruise series in this study collected the dominant scombrids occurring in the GoM.

4.3. Length-weight regressions of larval and juvenile scombrids in the northern Gulf of Mexico.

Length and weights vary among species based on their body shape and within species based on the condition or robustness of an individual. Condition is variable and dynamic, as it is dependent on food availability and growth prior to capture. Individuals within a sample can drastically vary, and this variability can be seen within a populations based on season and year (Schneider et al. 2000).

Collecting length-weight regression data is useful for calculating fish weights from length-frequency data, which eliminates the need for bulk weighing. These regressions can

also help determine changes in robustness and the health of a population related to past and future sampling in the similar locations and seasons. Length-weight regressions are helpful in determining the relative condition of small fish compared to large fish and comparing the condition of a localized population to a regional population. Thus, these data can be utilized for the comparison of populations, species, and life stages (Pauly 1993, Petrakis & Stergiou 1995, Schneider et al. 2000).

In this study, the length-weight regressions created for each species and/or taxa exhibited power relationships. The value of b of each species was relatively close to three, which represents isometric growth and is common for all fish species. If b is less than three, a fish grows faster in length than in weight, but if b is greater than three, a fish grows faster in weight than in length (Froese 2006).

At the species-level, *Acanthocybium solandri* and *T. atlanticus* had a b value less than three. However, a small range of lengths and weights were collected for *Acanthocybium solandri*, which explains why b was lower than expected ($b = 1.795$). *Auxis rochei*, *Auxis thazard*, *E. alletteratus*, *K. pelamis*, and *Scomber colias* had b values greater than three, indicating that these species grow faster in weight than in length as young scombrids. The majority of species collected an individual(s) that exceeded 100 mm SL, demonstrating a wide size range of larval and smaller juvenile specimens.

The following summary of known length-weight regressions are based on the collated data presented in the ICCAT Manual (2016a), although the regressions were based on FL instead of SL. The length-weight regressions for *Auxis rochei* were previously recorded from the Aegean Sea, eastern and western Mediterranean, and the Gibraltar Strait, with individuals ranging from 25.9 to 47.0 cm FL. *Auxis thazard* length-weight regressions were recorded from the Gibraltar Strait, South Africa, southwest Brazil, Mikomoto and Shionomisaki, Japan, and Sri Lanka. *Euthynnus alletteratus* length-weight regressions included specimens ranging from 20.0 to 101.0 cm FL from the Aegean Sea, Coasts of Senegal, and western and eastern Mediterranean Sea. *Katsuwonus pelamis* ranging from 32.0 to 78.0 cm FL were recorded in the Atlantic with an equation of $W = 7.480 \times 10^{-6} FL^{3.253}$, which is relatively similar to the curve in this study. *Thunnus atlanticus* length-weight regressions from specimens ranging from 18.5 to 87.0 cm FL were

recorded in Cuba, Brazil, and Martinique. All equations provided in the ICCAT Manual maintained a low a value and a b value close to three, which was similar to the results in this study. *Acanthocybium solandri* and *Scomber colias* were not included in the ICCAT Manual.

All species length-weight regressions in the ICCAT Manual were not from the GoM. Additionally, all individuals in this study were smaller than the size range of the length-weight regression data previously reported by ICCAT. Thus, this thesis adds length-weight regressions for seven species of smaller sizes in the GoM that were not previously reported.

4.4. Variation in the morphometrics of juvenile Euthynnus alletteratus and Thunnus atlanticus.

Larval and juvenile scombrids in the Tribe Thunnini are known for having large heads, large jaws, and short bodies (Richards 2005). Both *E. alletteratus* and *T. atlanticus* possessed these features as larvae and juveniles. It was observed that smaller individuals of both species have larger heads compared to their body length. In addition, smaller individuals of both species also have larger jaws, larger snouts, and larger eyes compared to their HL. As these species grow, these ratios decrease. Large heads, eyes, snouts, and upper jaws of scombrid early life stages are presumably important attributes for feeding. Larval and juvenile scombrids have high energy demands to ensure fast growth and survival. Thus, scombrid early life stages are likely constantly searching for food. These four features are essential search-and-capture structures in early ontogeny (Catalán et al. 2011).

As smaller individuals exist in a high Reynold's number environment, they are less able to move freely in the water in search of food, and therefore, their search volume is smaller relative to larger fishes. Smaller individuals need to maintain the ability to select high-energy prey in order to effectively support the energetic requirements for the development of advanced feeding structures. Larvae need to consume 70% of their body mass per day in order to maintain optimal growth (Reglero et al. 2009). As a result, scombrid early life stages have evolved large heads, jaws, snouts, and eyes that are used to optimize their feeding success by improving their ability to locate and capture prey, and in

turn increase survival (Llopiz et al. 2010). Catalán et al. (2011) observed an increase in prey size in relation to larval mouth or body size, indicating that large mouths allow for the consumption of larger, energy-rich, and nutritional prey. Gape size affects the food consumption by dictating the size range of prey that a predator can catch and the efficiency at which this food is collected; thus, a large gape enhances consumption success (Wainwright & Richard 1995).

Larval and juvenile scombrids are voracious, aggressive, and cannibalistic feeders. During the third week post-hatch, *T. albacares* larvae have these diagnostic features (e.g., large mouths, well-developed eyes and teeth) and begin the piscivorous stage. A 15-day post-hatch *T. albacares* larvae was recorded with another larvae in its gut (Benetti et al. 2015), demonstrating their cannibalistic and opportunistic feeding behaviors. Their aggressive and voracious behaviors as young drive the need for these feeding features.

As an individual scombrid grows in size, its search volume increases and feeding frequency increases. Increased swimming ability, reflected in the development of locomotive features and a decreased Reynold's number environment, is likely related to the size of the upper jaw and snout compared to HL. Therefore, as an individual grows, its upper jaw size becomes smaller compared to HL and the ratio asymptotes. Moreover, as an individual grows, the body size increases drastically, resulting in smaller eye and HL ratios.

Overall, *E. alletteratus* and *T. atlanticus* showed similar declining patterns for these critical feeding structures. However, there were two differences in these ratios for *E. alletteratus* and *T. atlanticus*: 1) *E. alletteratus* always maintained a larger snout compared to *T. atlanticus*, and 2) *T. atlanticus* had a larger eye compared to *E. alletteratus*. Larger eyes decrease the snout size, which correlates with both patterns in this study. However, these differences can also relate to the species-specific biological adaptations.

Larger snouts relate to an individual's ability to collect more prey. Developing the capacity to select larger prey occurs earlier for *E. alletteratus* than *T. atlanticus*. This early development was also noted by Morote et al. (2008) with larval *Auxis rochei* in the northwest Mediterranean Sea. High size selectivity and high competition for prey exists

among tuna species of the same larval size range (Catalán et al. 2011), indicating species-specific trophic niches (Llopiz et al. 2010). *Euthynnus alletteratus* exhibit a high degree of feeding selectivity for appendicularians, which are generally abundant and available in oligotrophic environments. Contrastingly, *Thunnus* spp. do not exhibit preferences for appendicularians, but rather for cladocerans and copepods. These niches reduce inter- and intraspecific competition for prey resources. Larval *E. alletteratus* and *T. atlanticus* have adapted their morphology and trophic ecology based on resource availability in order to maximize the feeding success and survival of their early life stages (Llopiz et al. 2010).

Feeding behaviors and larval distributions are reflective of larval and juvenile tuna morphology. Varying morphometric ratios between species indicate species-specific adaptations to their environment and individual niches. Specific features may be shared between species; however, differences highlight ecological variation between their life histories. It is critical to identify these differences, not only for taxonomic purposes, but also for understanding the development of a species and its ecology.

4.5. Spatiotemporal distributions of larval and juvenile scombrid fishes in the northern Gulf of Mexico.

4.5.1. Variations in vertical distributions.

Vertical distributions determined using MOCNESS derived data, as this gear allowed for discrete-depth sampling from the surface to 1500 m depth. On all MOCNESS cruises, scombrids were predominantly collected in the upper 200 m of the water column, confirming their epipelagic early life stages. This relates to their biology and ecology, in which tuna eggs are buoyant, larvae are pelagic, and both are typically found at the sea surface (Richards 2005). The occurrence of individuals at deeper depths (200 – 1500 m) in this study may be due to net contamination (i.e. some specimens were collected in deep nets that were not completely closed as the unit was lowered and retrieved through shallower strata). The lack of individuals collected at deeper depths from 2015-2017 further suggested that larvae are not residing at those depths and that this phenomenon was isolated to 2011.

Previous studies highlight the fine-scale differences among species' depth distributions within the epipelagic zone. Habtes et al. (2014) found that the largest abundances of larval scombrids were found in the upper 30 m of the water column in the GoM. Abundances decreased successively for all species to 50 m depth, except for *E. alletteratus*, which exhibited its highest abundances from 30 to 40 m depth. Overall, highest abundances of *T. thynnus*, *K. pelamis*, and other *Thunnus* spp. were found at shallower depths compared to *Auxis* spp. and *E. alletteratus*. *Katsuwonus pelamis* and other *Thunnus* spp. larvae were found at all depths (0 - 50 m, Habtes et al. 2014). As 75% of zooplankton biomass resides in the top 200 m (Hopkins 1982), it is important for planktivores, such as scombrid larvae, to live in these highly productive surface waters. The sampling methods in this thesis did not allow for the investigation of high-resolution vertical distribution differences within the upper 200 m of the water column. However, it was evident that early life stages of scombrids reside in the epipelagic zone.

4.5.2. Diel catch rates.

It is important to understand diel differences in day/night catch rates if quantitative data are used in scombrid stock assessments. In all sampling reported here, scombrid early life stages were collected at higher abundances and higher frequencies at night than during the day. Further, during the MOCNESS 2015-2017 survey, all specimens were collected at night, except for one *E. alletteratus* specimen.

The family Scombridae exhibited a significant difference in abundances by diel cycle (day vs. night catches), as higher abundances were caught at night than during the day. *Auxis thazard* and *K. pelamis* were caught at significantly higher abundances at night than during the day as well. However, *E. alletteratus* had no significant differences in the abundances caught based on diel cycle, and *T. atlanticus* exhibited marginal differences; although higher abundances were recorded at night for both species. Results from this study are similar to a study by Hare et al. (2001), which found that more *K. pelamis* larvae were collected at night, while larval *T. atlanticus* and *E. alletteratus* abundances were similar between day and night tows. Cornic and Rooker (2018) also noted an increase in abundances of *T. atlanticus* at crepuscular periods prior to sunset and after dawn. Previous

studies involving *Auxis* spp. also observed higher catches at night (Wade & Bravo 1951, Matsumoto 1959, Strasburg 1960, Klawe 1963).

Increased catches at night are most likely a result of net detection and avoidance during the daytime (Davis et al. 1990). Diel differences in feeding activity also influence catch rates. Most larval and juvenile scombrids feed during the day (Young & Davis 1990, Tanabe 2001, Morote et al. 2008), when they are more active. Sensing and swimming away from the net during the day is expected with increased daytime activity. Thus, high catches at night can be related to low activity levels and a decrease in swimming activity (Takashi et al. 2006).

This study showed that there are higher catch rates of scombrids at night than during the day in upper 200 m of the water column. Recognizing catch differences between day and night sampling is critical for fisheries management. Results from this study indicate that it is more appropriate to sample the epipelagic zone at night in order to collect quantitative abundance data that more accurately reflect the true abundance of scombrids in an area.

4.5.3. Seasonal and horizontal distributions of larval and juvenile scombrids in the northern Gulf of Mexico.

4.5.3.1. Scombridae larval and juvenile distributions.

GAMs and presence-absence models from the MOCNESS 2011 survey showed that Julian date, water body, and distance to the nearest 200-m isobath were related to scombrid abundances in the GoM.

Julian date was an important determinant, as abundances slightly increased in May and continued into a larger peak in August. These patterns were most likely caused by species-specific spawning preferences. For example, an increase in abundance around day 115 (April) was dominated by *Auxis thazard* specimens. *Auxis thazard* spawn at SSTs of 21.6 to 30.5 °C, with mass spawning between 25.0 and 26.0 °C (Rudomiotkina 1984, ICCAT 2016a). SSTs in April reached the massive spawning temperature range, which explains the high abundance of *Auxis thazard*. The second peak in August was driven by

the two most-abundant species, *E. alletteratus* and *T. atlanticus*, whose spawning preferences will be discussed in depth below.

Water body was also an important determinant, with more specimens collected in Common Water. Several studies have found similar results in which scombrid species prefer GoM Common Water (Lindo-Atichati et al. 2012, Domingues et al. 2016). Distance to the nearest 200-m isobath appeared to be an important variable with respect to scombrids abundance.

4.5.3.2. *Euthynnus alletteratus* larval and juvenile distributions.

During the MOCNESS 2011 survey, larvae and small juveniles were collected from March to September, with a peak in August. The MOCNESS 2015-2017 survey only collected larvae in August 2015 and 2016, with high schooling behavior and patchiness in the 2016 samples. Thus, it appeared that patchiness is more important than season in the MOCNESS 2015-2017 survey, but patches were more frequently observed in the fall. The high-speed rope trawl 2011 survey collected juveniles in June, July and September, with the highest peak in June. Juvenile abundances appeared to lag behind the larval abundances in 2011. *Euthynnus alletteratus* produces several spawning batches per reproductive season (Chur 1973, Rudomiotkina 1986, ICCAT 2016a), which explains the numerous peaks in abundances throughout the year. Abundances increased from June to September in 2011, with no sampling in August using the high-speed rope trawl. If sampling continued after September, it is predicted that more juveniles would be collected as their abundances lag behind the larvae.

All *E. alletteratus* specimens were collected in Common Water in the MOCNESS 2011 survey, and the distribution plots further identified higher abundances in Common Waters in addition to along frontal boundaries. Previous studies showed high abundances of *E. alletteratus* eggs outside cyclonic eddies in open waters near southern Brazil (Matsuura & Sato 1981) and in the eastern Pacific (Klawe 1963). Lindo-Atichati et al. (2012) found that larval *E. alletteratus* had similar abundances between Common Water and Loop Current Origin Water in the GoM. However, in this study, individuals were only collected in Common Water and only a few were sampled in Loop Current Origin Water; thus, these comparisons could not be investigated. Larval scombrids are typical along

frontal boundaries (Richards et al. 1993), as frontal boundaries concentrate scombrid larvae and other ichthyoplankton in addition to nutrients and food particles that are critical for survival. It has been reported that *T. thynnus* and *Auxis* spp. (Muhling et al. 2010, Habtes et al. 2014) reside along these boundaries as well. High abundances along the frontal boundaries in this study could also relate to the Mississippi River Plume that was being drawn offshore into the GoM into the in summer of 2011. Moreover, it is thought that variability in the abundances in Common Water can also relate to smaller-scale oceanographic features that were not considered in this analysis (e.g., cyclonic eddies) in addition to changes in environmental variables (e.g., temperature and salinity).

The results from the GAMs for the MOCNESS 2011 survey indicated that Julian date, minimum salinity and distance to the nearest 200-m isobath were important determinants of *E. alletteratus* abundances throughout the GoM. These results also related to larval abundances and distributions observed in the MOCNESS 2015-2017 survey.

Julian date was an important determinant, with more individuals caught later in the season, with a peak in August. As previously stated, spawning occurs when waters are the warmest in the GoM (preferably greater than 25 °C), from April to November. Surface temperatures reached about 25 °C in April, when spawning begins to occur for this species (Chur 1973, Rudomiotkina 1986, ICCAT 2016a). Thus, the temporal changes observed through this 9-month survey influenced the abundances of *E. alletteratus* in the GoM.

Higher abundances of *E. alletteratus* were also correlated with lower levels of minimum salinity. Catches occurred in salinities ranging from 29.47 to 36.19 (psu). A few specimens were collected at higher levels, but the majority were collected in salinities less than 34. The MOCNESS 2015-2017 survey also collected larvae at salinities ranging from 32.39 to 35.72, indicating that *E. alletteratus* can tolerate a wider range of salinities, but has a preference for lower levels (below 34). The distributions plots highlighted the association of abundances with lower salinity levels. Distributional plots from 2011 also showed that *E. alletteratus* was collected near areas of higher chlorophyll *a* concentrations along the Mississippi River Plume that protruded into the GoM in August 2011. However, some *E. alletteratus* specimens were also collected in lower chlorophyll *a* concentrated areas, likely due to the transient nature of surface chlorophyll plumes.

Being a coastal species, *E. alletteratus* appears to prefer lower salinity water masses, which are associated with nearshore environments and areas with high runoff. In the spring, freshwater discharges into the GoM from the Mississippi River. This plume is characterized by lower salinities and higher chlorophyll *a* concentrations. This suggests that areas with high freshwater inflow are suitable habitats for their larvae and small juveniles. As nutrients increase from runoff, primary and secondary production increase, and in turn provide food for larvae along the continental shelf regions (Le Fevre 1986, Grimes & Kingsford 1996). Thus, riverine discharge likely maximizes growth and survival of *E. alletteratus* early life stages.

The distance to the nearest 200-m isobath was also related to *E. alletteratus* horizontal distributions. More individuals were collected near the shelf break and along the continental slope, at distances ranging from 19.79 to 227.31 km from the 200-m isobath, through the majority of specimens were within 175 km. Results from the MOCNESS 2015-2017 survey indicated a similar pattern of distribution with individuals between 69.5 and 243.8 km from the shelf edge.

Juvenile abundances and distributions, derived from the high-speed rope trawl 2010-2011 survey mirrored those of the larvae. Juvenile abundances across the grid varied seasonally, inhabiting the northern stations in June, eastern stations in July, and both the northern and eastern stations in September. Similar to the larvae, juveniles were found in Common Waters with moderate chlorophyll *a* concentrations and moderate salinities. Specimens were also caught above the same depths, ranging from 200- to 2700-m isobaths. It appeared that juveniles may reside in a slightly wider range of salinity and chlorophyll *a* concentrations. This could be due to juveniles developing advanced locomotive capacity that allows for greater search and capture abilities. In all, adult spawning preferences guide larval *E. alletteratus* distributions. Juvenile *E. alletteratus* remain in these areas, but also can move to areas not typical of their larval stage (moderate levels of salinity and chlorophyll *a* concentrations) most likely due to the development of their swimming and feeding structures.

4.5.3.3. *Thunnus atlanticus* larval and *Thunnus* spp. juvenile distributions.

During the MOCNESS 2011 survey, larvae and small juveniles were collected in March and from May to September. Abundances remained high from May to September, with a peak occurring in June and the highest catches in August. The MOCNESS 2015-2017 survey only collected larvae in August 2016. The high-speed rope trawl 2011 survey collected juvenile *Thunnus* spp. in June, July and September, with the highest peak in June. High abundances in June and July were similar to those of their larvae, however, species-level identifications would identify whether a lag exists between the assemblages of these two life stages. For example, *T. thynnus* spawns from April to June in the GoM; thus, their juvenile abundances would not be expected to increase until later in the season (e.g., June), which was observed in the *Thunnus* spp. data. Moreover, juvenile abundances were still high in September, indicating a lag and the potential of *T. atlanticus* specimens dominating the generic assemblage.

Thunnus atlanticus spawns from June to September in the GoM (Collette 2010), indicating that juvenile abundances would persist after September. Cornic and Rooker (2018) found that spawning during both late spring and summer in the northern GoM, explaining the high abundances of larvae in this study and the increase in juveniles later in the season. High abundances of *Thunnus* juveniles can also be related to *T. thynnus*, *T. albacares*, *T. obesus*, and *T. alalunga* contributions. For example, *T. thynnus* spawns from April to June in the GoM (Richards 1975), which would indicate that juvenile abundances would be increasing during our sampling time period and potentially appear in the catch records (June to September).

Thunnus atlanticus larvae were collected in Common Water and Loop Current Origin Water during the MOCNESS 2011 survey. The distribution plots further identified higher abundances in Common Waters as well as along frontal boundaries with higher SSHAs than the surrounding areas. Previous studies showed that *Thunnus* spp. and *T. thynnus* larvae were higher in the boundaries of anticyclonic features in the GoM (Lindo-Atichati et al. 2012). Cornic and Rooker (2018) found that *T. atlanticus* larvae strongly associated with convergent zones near the Loop Current and anticyclonic eddies. Moreover, *Thunnus* spp. (presumably *T. atlanticus* and *T. albacares*) were found at higher

abundances in the boundaries of anticyclonic features and inhabit broader distributions and SSHA ranges than *T. thynnus*. It has been proposed that year-round inhabitant species have broader habitat preferences in the GoM than *T. thynnus* and are better able to tolerate warm features, such as the Loop Current and warm eddies (Muhling et al. 2010, Teo & Block 2010, Lindo-Atichati et al. 2012).

The results from the GAMs for the MOCNESS 2011 survey indicated that Julian date, minimum salinity and diel cycle were important variables relating to *E. alletteratus* abundances throughout the GoM. These results also related to larval abundances from the MOCNESS 2015-2017 survey.

Julian date was an important correlate of *T. atlanticus* larval abundances in the GoM. Abundances increased throughout the year from June to September. *Thunnus atlanticus* typically spawn in the GoM between June and September (Collette 2010), particularly when the SSTs reach 27 °C (Juarez & Frías 1986). In this study, individuals were caught in late May, with a strong increase in June when water temperatures reached 27 °C, aligning with previously reported spawning preferences. Abundances increased until August and a few specimens were collected throughout September, as temperatures began to drop. These patterns relate to the high abundances noted in the ichthyoplankton surveys conducted by Cornic and Rooker (2018) from June to July in 2011.

Higher abundances of *T. atlanticus* were also correlated with higher levels of minimum salinity, with catches in salinities ranging from 33.82 to 36.13. The majority of specimens caught between 35 and 36, suggesting a preference for oceanic waters. The MOCNESS 2015-2017 survey also collected larvae at salinities ranging from 34.04 to 34.97. The distribution plots also identified the correlation of higher *T. atlanticus* abundances with higher salinity levels and lower chlorophyll *a* concentrations.

This oceanic species spawns in offshore waters, which typically exhibit higher salinity and low to moderate chlorophyll *a* concentrations. Cornic and Rooker (2018) also found that *T. atlanticus* larvae preferred intermediate to high salinities, ranging from 31 to 36. Spawning in these open-ocean environments can facilitate the survival of their larvae

owing to the reduction in ichthyoplankton predators compared to the coastal waters, thus reducing predation on eggs and larvae.

Adult *T. thynnus* also spawn in waters with lower surface chlorophyll *a* concentrations (0.10 - 0.16 mg m⁻³) and higher salinities (35.5 - 37.0, Teo et al. 2007). This pattern of environmental preference has been observed in other pelagic fishes that utilize warm, oligotrophic waters for spawning (e.g., swordfish, *Xiphias gladius*; (Teo et al. 2007). Several tuna species have larvae adapted to living in these nutrient-poor environments, utilizing appendicularians for food beginning piscivory at an early stage (Llopiz et al. 2010).

Due to the lack of diagnostic features for discriminating juvenile *Thunnus* spp., the genus was treated as a single taxonomic unit in the analysis of the high-speed rope trawl data. Juvenile *Thunnus* spp. assemblages were wide spread across the northern GoM, covering the entire sampling grid. They were collected in waters with bottom depths between 1200 and 2700 m. Larval *T. atlanticus* were collected over a wider range, in water depths between 700 and greater than 3300 m. Cornic and Rooker (2018) found that smaller larvae were found in the GoM from the outer continental shelf region into oceanic waters (areas seaward of the 100-m isobath). Based on larval *T. atlanticus* distributions, it appeared that juvenile *Thunnus* spp. move and concentrate in waters further offshore compared to their early life stages. Additionally, *Thunnus* spp. juveniles were found in areas of higher salinities and lower chlorophyll *a* concentrations, which correlates with larval distributions and adult spawning preferences.

4.5.3.4. *Auxis thazard* larval and juvenile distributions.

During the MOCNESS 2011 survey, larvae and small juveniles were collected relatively consistently from February to September, with a large peak occurring in April. The MOCNESS 2015-2017 survey only collected larvae in August in 2016. Due to low taxonomic resolution of the genus *Auxis*, juvenile seasonality and horizontal distributions were not examined. *Auxis thazard* spawns at surface water temperatures between 20 and 32 °C, which is the broadest larvae temperature range tolerance of all GoM scombrids (Muhling et al. 2017) and has mass spawning between 25 and 26 °C (Rudomiotkina 1984, ICCAT 2016a). Surface waters in April reached the massive spawning temperature range,

which explains the high abundance of *A. thazard* larvae. *Auxis thazard* has an extended spawning season in the North Atlantic, from February to November (Rudomiotkina 1984, ICCAT 2016a). It is evident that spawning occurs throughout the majority of the year in the GoM.

Auxis thazard larvae were only collected in Common Water during the MOCNESS 2011 and 2015-2017 surveys. The distribution plots further identified higher abundances in Common Water in addition to along frontal boundaries with higher SSHAs than the surrounding areas. Lindo-Atichati et al. (2012) found larval *Auxis* spp. along the boundaries of anticyclonic features and within GoM Common Water as well. Probabilities of occurrence of *Auxis* spp. in Common Water was higher than in anticyclonic regions, cyclonic boundaries, or cyclonic regions and also higher in anticyclonic boundaries than anticyclonic regions (Lindo-Atichati et al. 2012).

The distributional plots from the MOCNESS 2011 survey data highlighted other environmental drivers of *A. thazard* larval distributions. Individuals were collected along the shelf break and slope and in the southern portion of the grid. *Auxis thazard* also were caught in areas of moderate chlorophyll *a* concentrations (along the edges of the plume), moderate salinity levels, and low SSHA (Common Water and also frontal boundaries). The MOCNESS 2015-2017 survey collected individuals in moderate salinities (34.04 to 34.97) and moderate chlorophyll *a* concentrations (0.54 to 1.14 mg m⁻³). In the southern GoM, Espinosa-Fuentes and Flores-Coto (2004) categorized larval *Auxis thazard* as an outer neritic species (species occupying the outer shelf and potentially mid-shelf areas) that preferred intermediate temperatures (24.36 to 28.95 °C) and salinity values (35.82 to 36.43). In Hawaii, *Auxis* spp. larvae were found in salinities ranging from 34.69 to 35.32 (Boehlert & Mundy 1994), which is relatively close to the levels and preferences in the GoM. These larval preferences of moderate levels of environmental variables may relate to their widespread prevalence in the GoM and their adult spawning habits.

4.5.3.5. *Katsuwonus pelamis* larval and juvenile distributions.

During the MOCNESS 2011 survey, larvae and small juveniles were collected from May – September, with fluctuating abundances throughout the year. Lower abundances occurred in May, July, and September, while higher abundances occurred in June and July.

The highest abundances were recorded in June. The MOCNESS 2015-2017 survey collected larvae in May and August of 2016 and May 2017. The high-speed rope trawl 2011 survey collected juveniles in June, July and September, with the highest peak in July and a few individuals collected in June and September. Juvenile abundances appear to lag behind the larval abundances in the spring and summer 2011. For example, larval abundances were low in May, and juveniles started to be collected in low abundances in June. Also, larval abundances were high in June and juveniles were high in July. *Katsuwonus pelamis* spawns several times a season when SSTs are between 24 and 29 °C in the Caribbean Sea and equatorial waters (Erdman 1977, Collette 2010). In the tropics, spawning occurs almost daily (Collette 2010). *Katsuwonus pelamis* are opportunistic breeders throughout the year in the Atlantic (ICCAT 2016a). This explains the numerous peaks in abundances throughout the year. If sampling continued past September, it is predicted that more juveniles would be collected, as their abundances lagged behind the larvae.

Katsuwonus pelamis larvae were collected in Common Water and one specimen was collected in Mixed Water in the MOCNESS 2011 survey. Specimens were caught in only Common Water during the MOCNESS 2015-2017 survey. *Katsuwonus pelamis* inhabits open waters in aggregations associated with convergences, boundaries between water masses, outcrops and hydrographic discontinuities (Collette & Nauen 1983). This pattern is reflected in their larval distributions, which favor Common Water or water in between boundaries of mesoscale features. Larvae were also collected in waters with moderate to higher salinities (33.90 – 36.08) and lower chlorophyll *a* concentrations (0.07 – 0.50 mg m⁻³) during the MOCNESS 2011 survey. Similarly, *K. pelamis* larvae were collected in waters with moderate to high salinities (34.04 - 36.16) and lower chlorophyll *a* concentrations (0.11 – 0.54 mg m⁻³) during the MOCNESS 2015-2017 survey. Boehlert and Mundy (1994) found larval *K. pelamis* in deeper waters compared to other scombrids. *Katsuwonus pelamis* had low abundances nearshore that increased offshore, and it was only abundant when temperatures were relatively warm, ranging from 22 to 27.2 °C. Boehlert and Mundy (1994) also found that *K. pelamis* larvae prefer salinities between 34.74 and 35.31. Higher recruitment was reported during El Niño years, when the surface waters were

warm and less productive, providing an increase in spawning habitat and improving conditions for larval survival and growth for this species (Lehodey et al. 2011).

Juveniles were collected in offshore waters with bottom depths between of 2200 and 2700 m, demonstrating that this oceanic species resides in offshore waters as juveniles. Similar to the larval distributions, juvenile *K. pelamis* preferred Common Water with moderate salinity and moderate chlorophyll *a* concentrations. In Oahu, juveniles were 11-fold more abundant at 56 km offshore compared to 7 km offshore (Higgins 1970), relating to the ecology of this oceanic species. It is evident that larval and juvenile distributions are similar in the GoM and are related to adult preferences.

4.6. Caveats and suggestions for future research.

In this study, the sampling methods were not equal among surveys in terms of gear and temporal scales, which complicated the comparisons among cruise series. Additionally, sampling methods in this study were not designed specifically to catch scombrid early life stages. A MOCNESS with a smaller mesh size may be more appropriate for sampling larval scombrids. Additionally, sampling the upper 200 m in discrete depths with the MOCNESS would be ideal for understanding the vertical distributions of larvae in the GoM.

The high-speed rope trawl caught juvenile scombrids that have not been assessed in the GoM; however, trawling a large, midwater trawl behind the boat at deeper depths (maximum 1500 m) is not an ideal method for sampling juvenile tuna that most likely do not reside that deep in the water column. In order to properly collect these smaller juvenile specimens, it may be more useful to use pair-trawling at night, as we saw more individuals are collected during nighttime sampling. Pair-trawling samples the water column with two vessels, with one towing each warp. The mouth is opened by a lateral pull from both vessels and doors are not necessary. Using two vessels allows for a larger net to be towed behind the boat at faster speeds to target fast-swimming pelagic species. This method is often used to sample cod off the New England coast. Creating a specific sampling method for juvenile scombrids will increase our knowledge regarding the faunal composition, distributions, and

ecology of early life stages in the GoM, which is necessary for population dynamic studies and fisheries management and conservation efforts.

Lastly, juvenile specimens need to be preserved for genetic analyses in order to be able to use them as guides or as “voucher” specimens for identifying key morphological features that can distinguish different species. In this study, the range of individuals preserved for genetic analysis was skewed, with *E. alletteratus* as the most-sampled species and several species only having one to four representatives (e.g., *K. pelamis* and *T. thynnus*). Increasing the sample size in addition to the number of individuals per size class will provide a greater opportunity to find the features that vary among species. Identifying the size at which gill raker counts and liver morphology (i.e. *Thunnus* spp.) become useful is critical, as these features assist in adult identifications. Investigating the ratios that were identified in this study with a larger sample size will help determine which ratios are most informative.

5. CONCLUSION

The taxonomy of larval scombrids is fairly well-described, owing to species-specific pigmentation patterns. Genetic analyses can aid larval identifications when there is low taxonomic resolution due to the lack of pigmentation. However, juvenile scombrid taxonomy is unresolved and still needs work. The juvenile body ratios analyzed in this study indicate that body ratios vary substantially as juvenile fish grow in length. Since the ratios change ontogenetically, the best method for identifying morphological differences between juvenile scombrids is comparing fishes of similar sizes. This finding also pertains to gill raker counts, since scombrids develop more gill rakers as they grow until they obtain adult counts. Meristics provide a constant character trait to compare among certain scombrid species, but not all (e.g., *Thunnus* spp.). Therefore, a combination of diagnostic features by life stage and size class is needed in order to properly identify juvenile tunas. Genetic analyses, larger sample size per species, and more individuals per size class are needed to further develop diagnostic keys for these intermediate fauna.

Using multiple gears to sample different temporal and spatial scales is highly desirable for faunal surveys. For example, bongo nets have proven effective at catching smaller larvae, neuston nets effectively catch larger larvae, and hook-and-line sampling catches adults. However, an effective sampling method does not currently exist for sampling small juveniles. In this study, larvae were only caught with the MOCNESS, while the high-speed rope trawl only collected juveniles. If these nets were not used together, the scombrid early life stages in the GoM would have been undersampled. Thus, using multiple gear types is critical for sampling varying life stages and size classes and identifying changes in spatiotemporal distributions.

Scombrids have a wide variety of life history strategies and spatiotemporal distributions that are often dictated by adult spawning and migratory behaviors. Through spawning, adults establish the initial broad distribution of eggs and small larvae, and the larger larvae and small juveniles modify these distributions through their own behavior. Different vertical, seasonal, and horizontal distributional patterns existed among the species examined over the three cruise series. Horizontal distributions are closely linked with physical characteristics of the water column and mesoscale oceanographic features.

Oceanic species (*Thunnus atlanticus* and *Katsuwonus pelamis*) preferred more oligotrophic spawning habitats (moderate to high salinity, low chlorophyll *a* concentrations, further distance from shelf break), while coastal species (*Euthynnus alletteratus* and *Auxis thazard*) spawned in more productive continental shelf and slope environments (low to moderate salinity, moderate to high chlorophyll *a* concentrations, nearer to shelf break). It is evident that the time and place of spawning provides optimal conditions for the growth and survival of larvae and juveniles.

Overall, this study quantified the habitat preferences of larval and juvenile scombrids in the northern GoM. Results from this study can help develop a more detailed model of habitat use of larval and juvenile scombrids, and in turn assist in managing and conserving adult populations, specifically for small tuna species that do not have any current stock assessments or management plans (e.g., *E. alletteratus* and *T. atlanticus*). By understanding habitat preferences of tuna early life stages, we can protect critical spawning grounds and nursery habitats and aim to improve management and conservation efforts regarding scombrid populations in the GoM.

APPENDIX

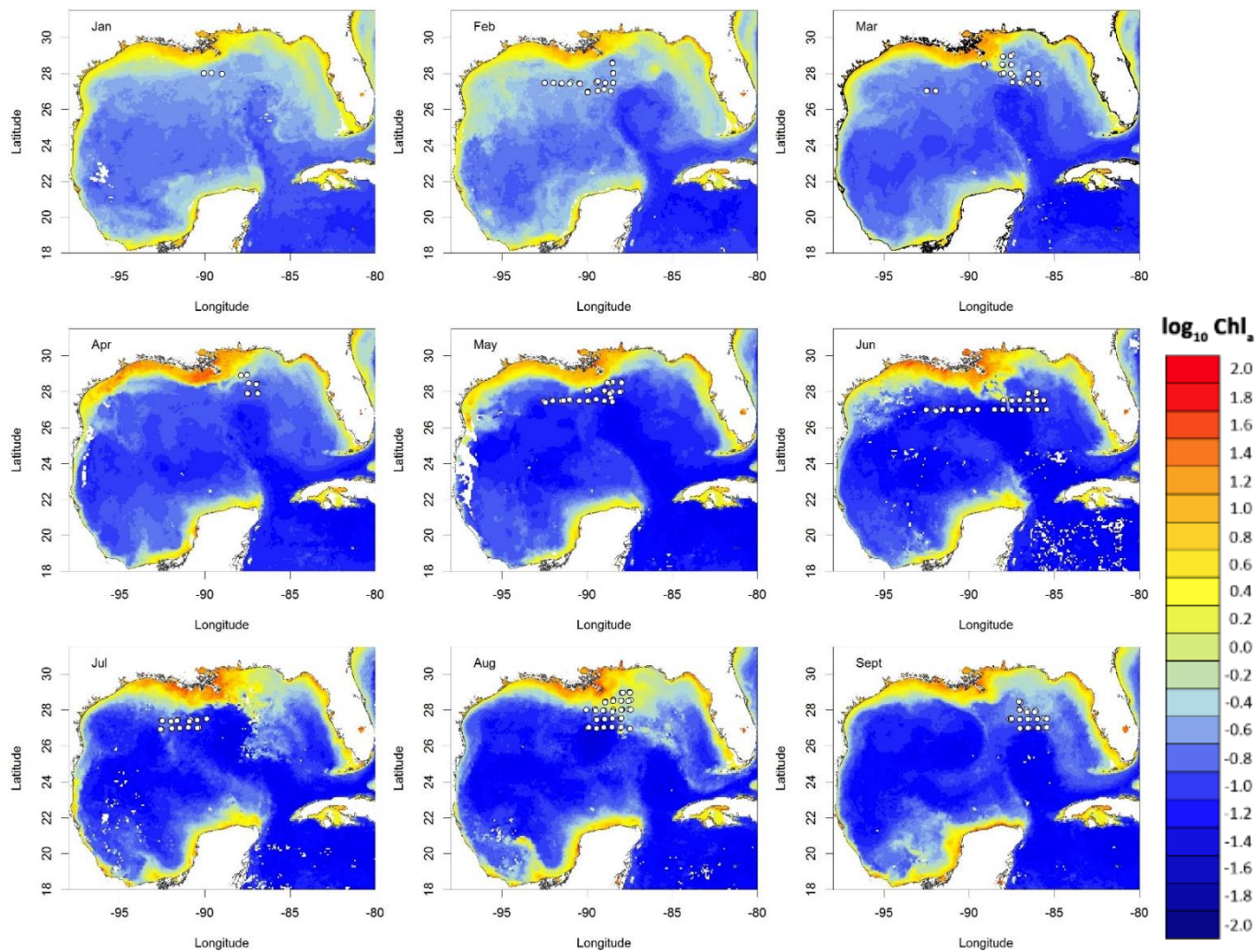
Appendix Table 1. Stations sampled per cruise series. An “X” indicates that quantitative sample(s) were taken at that specific station.

Station	MOCNESS 2011	MOCNESS 2015-2017	High-speed rope trawl 2010-2011
B001	X	X	
B003	X	X	
B016	X		
B061	X		
B064	X	X	X
B065	X	X	
B078	X		
B079	X	X	
B080	X		
B081	X	X	X
B082	X	X	X
B083	X		X
B162	X		
B163	X		
B175	X	X	
B184	X		X
B185	X		
B245	X		
B246	X		
B247	X		
B248	X		X
B249	X		X
B250	X		
B251	X		X
B252	X	X	X
B254	X		
B255	X	X	
B286	X	X	
B287	X	X	X
SE-1	X	X	
SE-2	X	X	
SE-3	X	X	
SE-4	X	X	
SE-5	X	X	
SE-6	X		
SW-1	X		
SW-2	X		
SW-3	X	X	

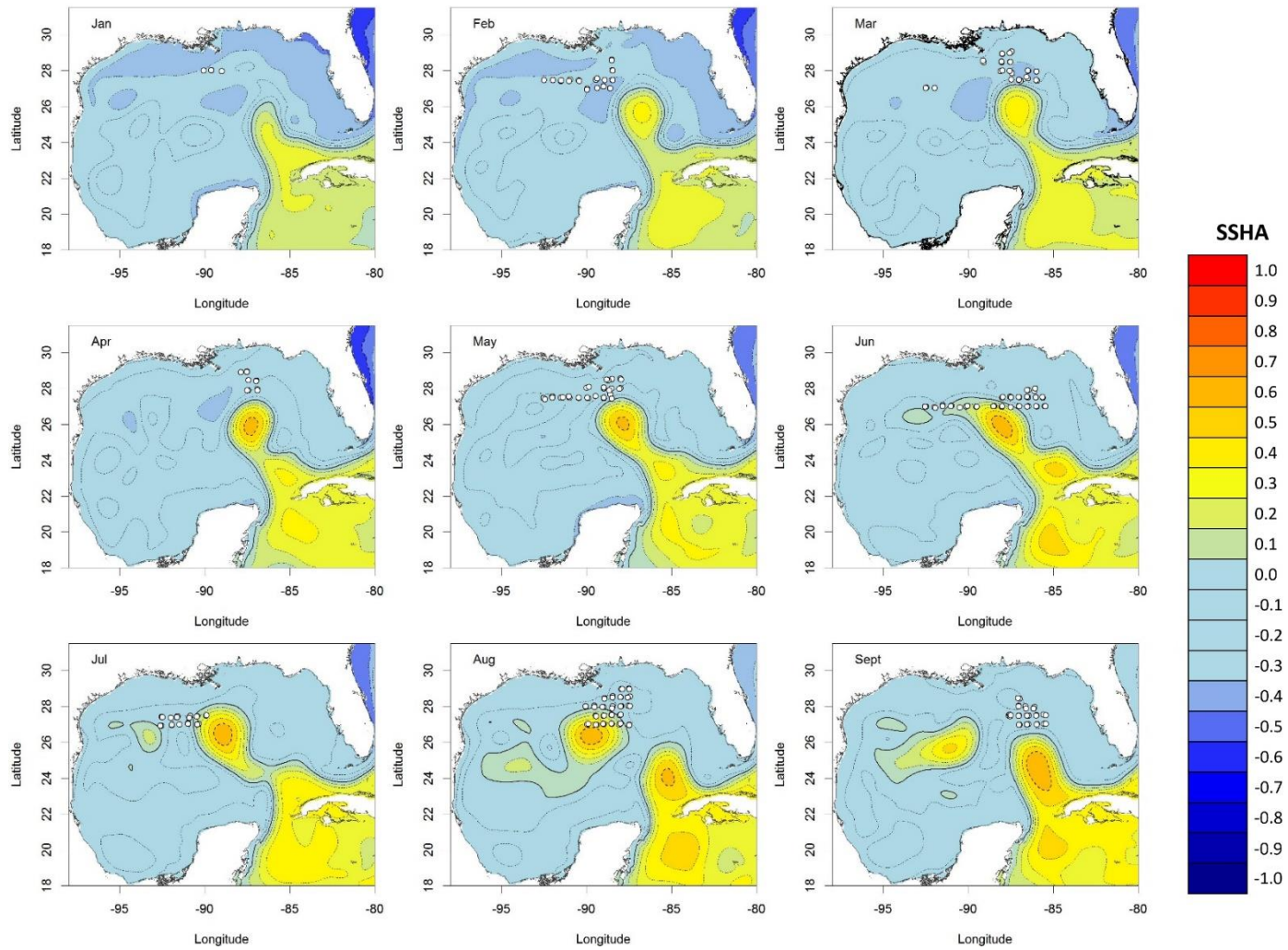
SW-4	X	X	
SW-5	X	X	X
SW-6	X	X	X
SW-7	X		X
SW-8	X		X
SW-9	X		
SW-10	X		
SW-11	X		

Appendix Table 2. Meristics for the 16 scombrid species found in the Western Central North Atlantic, with tribes separated by heavy black lines (Richards 2005)

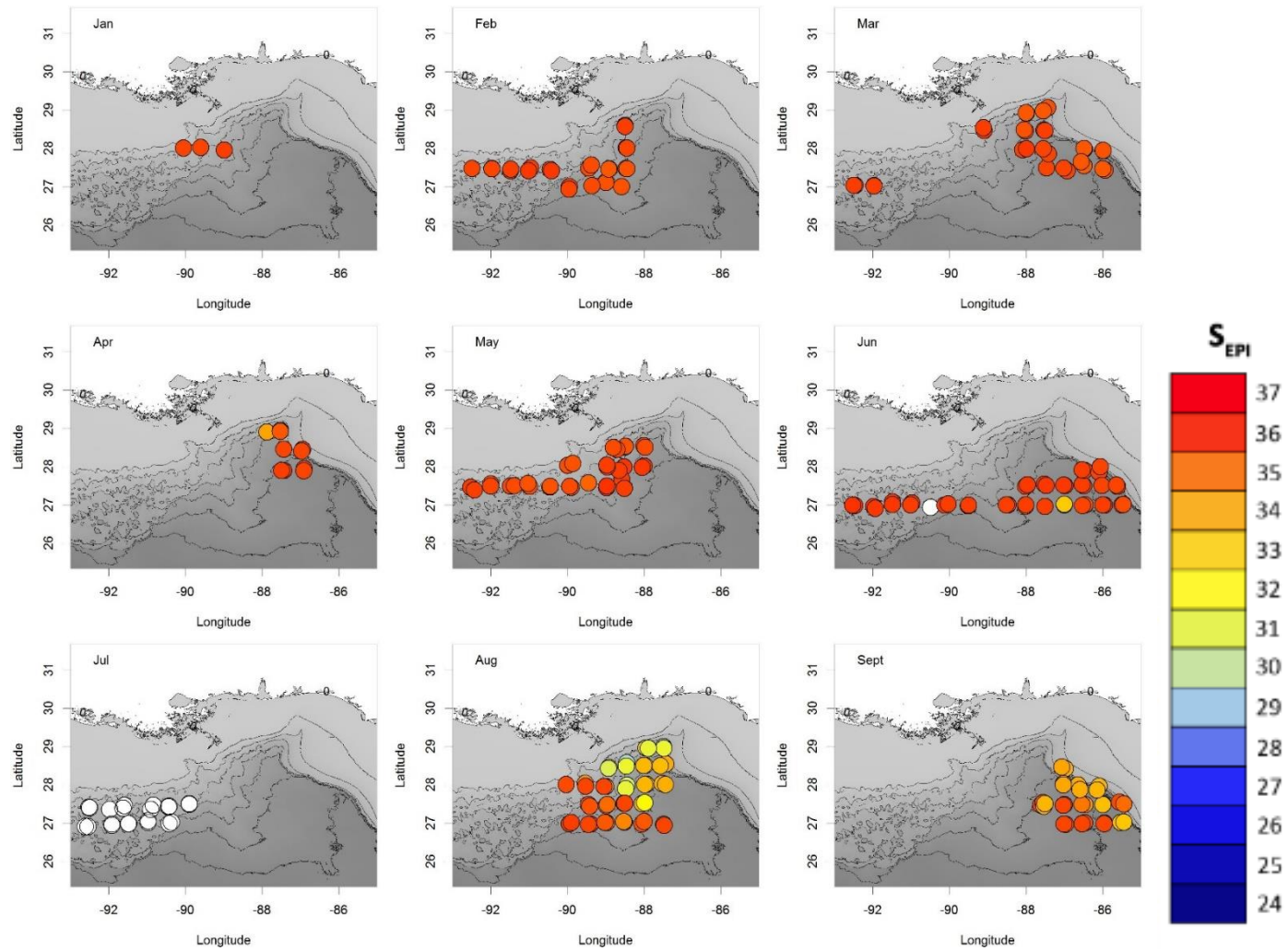
Taxa	First Dorsal Fin	Second Dorsal Fin	Dorsal Finlets	Anal Fin	Ventral Finlets	Pectoral Fin	Pelvic Fin	Caudal Fin
<i>Auxis rochei</i>	10-12	10-12	7-9	11-14	7	23-25	I, 5	48
<i>Auxis thazard</i>	10-12	10-12	7-9	11-14	7	23-25	I, 5	48
<i>Euthynnus alletteratus</i>	13-17	11-13	8-9	11-15	7-8	25-29	I, 5	47-49
<i>Katsuwonus pelamis</i>	14-16	14-16	7-8	14-16	6-8	26-28	I, 5	50-51
<i>Thunnus alalunga</i>	14 (11-14)	15 (12-16)	8 (7-10)	14 (11-16)	7 (7-10)	30-36	I, 5	47-51
<i>Thunnus albacares</i>	14 (11-14)	15 (12-16)	8 (7-10)	14 (11-16)	7 (7-10)	30-36	I, 5	47-51
<i>Thunnus atlanticus</i>	14 (11-14)	15 (12-16)	8 (7-10)	14 (11-16)	7 (7-10)	30-36	I, 5	47-51
<i>Thunnus obesus</i>	14 (11-14)	15 (12-16)	8 (7-10)	14 (11-16)	7 (7-10)	30-36	I, 5	47-51
<i>Thunnus thynnus</i>	14 (11-14)	15 (12-16)	8 (7-10)	14 (11-16)	7 (7-10)	30-36	I, 5	47-51
<i>Sarda sarda</i>	21 (20-23)	15-16 (13-18)	7-9	14-16	6-8	23-26	I, 5	-
<i>Scomber colias</i>	9-13	11-12	4-5	I, 11-14	5	19-22	I, 5	37-39
<i>Acanthocybium solandri</i>	23-27	13 (11-16)	7-10	11-14	7-10	22-26	I, 5	-
<i>Scomberomorus brasiliensis</i>	17-19	17-18 (15-19)	8-10	16-20	7-10	21-24	I, 5	39-43
<i>Scomberomorus cavalla</i>	15 (12-18)	15-18	7-10	16-20	7-10	21-23	I, 5	39-43
<i>Scomberomorus maculatus</i>	17-19	17-20	7-9	17-20	7-10	20-23	I, 5	39-43
<i>Scomberomorus regalis</i>	16-18	16-19	7-9	18-19 (15-20)	7-10	20-24	I, 5	39-43



Appendix Figure 1. Chlorophyll *a* concentrations across the GoM from January to September 2011. Red represents high concentrations, and blue represents low concentrations. Stations are designated with white dots.



Appendix Figure 2. SSHA across the GoM from January to September 2011. Red represents positive values, and blue represents negative values. Stations are designated with white dots.



Appendix Figure 3. Minimum salinity of the epipelagic zone across the GoM from January to September 2011. High values (37) are represented by red, and low values (24) are represented by blue. White are missing data

Appendix Table 3. Morphometric ratios vs. the comparable variable (HL/SL) used for the genetically identified scombrid species. Each ratio was ranked on how informative it was and comments were included

Ratio	HL and/or SL	Informative character?	Comments
HL : SL	SL	Not informative	-
Pectoral fin length : SL	SL	Not informative	Pectoral fins often damaged due to preservation
First dorsal fin length : SL	SL	Not informative	-
Second dorsal fin length : SL	SL	Not informative	-
Interdorsal length: SL	SL	Informative	<i>Auxis</i> spp.
Interdorsal length : HL	HL	Slightly informative	<i>Auxis</i> spp.
Anal fin length : SL	SL	Not informative	Anal fins often damaged due to preservation
Pelvic fin length: SL	SL	Not informative	-
Interdorsal length : eye diameter	SL	Not informative	-
Interdorsal length : first dorsal fin length	SL	Slightly informative	<i>Auxis</i> spp.
Eye diameter : snout length	SL	Informative	<i>Euthynnus alletteratus</i> <i>Thunnus</i> spp. <i>Acanthocybium solandri</i>
Eye diameter : HL	HL	Informative	<i>Euthynnus alletteratus</i> <i>Thunnus</i> spp.
Snout length : HL	HL	Informative	<i>Acanthocybium solandri</i>
Upper jaw length : HL	HL	Slightly informative	<i>Auxis</i> spp.

REFERENCES

- Addis P, Secci M, Pischedda M, Laconcha U, Arrizabalaga H (2014) Geographic variation of body morphology of the Atlantic bluefin tuna, *Thunnus thynnus* (Linnaeus, 1758). *J Appl Ichthyol* 30:930-936
- Anonymous (1984) Meeting of the Working Group on Juveniles Tropical Tunas. Coll Vol Sci Pap, ICCAT 21:1-289
- Bakun A (2006) Fronts and eddies as key structures in the habitat of marine fish larvae: opportunity, adaptive response and competitive advantage. *Sci Mar* 70:105-122
- Bane JM, Brooks DA, Lorenson KR (1981) Synoptic observations of the three-dimensional structure and propagation of Gulf Stream meanders along the Carolina continental margin. *J Geophys Res (Oceans)* 86:6411-6425
- Bard FX, Cayré P, Diouf T (1991) Migrations. In: Fonteneau AJM (ed) Resources, fishing and biology of the tropical tunas of the Eastern Central Atlantic, FAO Fisheries Technical Paper No. 292
- Bayliff WH (1988) Integrity of schools of skipjack tuna, *Katsuwonus pelamis*, in the eastern Pacific Ocean, as determined from tagging data. *Fish Bull* 86:631-643
- Benetti D, Partridge G, Buentello A (2015) Advances in tuna aquaculture: From hatchery to market. Academic Press
- Betancurr R, Broughton RE, Wiley EO, Carpenter K, López JA, Li C, Holcroft NI, Arcila D, Sanciangco M, Cureton J (2013) The tree of life and a new classification of bony fishes. *PLoS Curr* 5:1-33
- Blank JM, Morrisette JM, Landeira-Fernandez AM, Blackwell SB, Williams TD, Block BA (2004) *In situ* cardiac performance of Pacific bluefin tuna hearts in response to acute temperature change. *J Exp Biol* 207:881-890
- Block BA, Dewar H, Williams T, Prince ED (1998) Archival tagging of Atlantic bluefin tuna (*Thunnus thynnus*). *Mar Technol Soc J* 32:37
- Block BA, Finnerty JR, Stewart AF, Kidd J (1993) Evolution of endothermy in fish: mapping physiological traits on a molecular phylogeny. *Science* 260:210-214
- Block BA, Teo SL, Walli A, Boustany A, Stokesbury MJ, Farwell CJ, Weng KC, Dewar H, Williams TD (2005) Electronic tagging and population structure of Atlantic bluefin tuna. *Nature* 434:1121
- Boehlert GW, Mundy BC (1994) Vertical and onshore-offshore distributional patterns of tuna larvae in relation to physical habitat features. *Mar Ecol Prog Ser*:1-13

- Brill RW (1994) A review of temperature and oxygen tolerance studies of tunas pertinent to fisheries oceanography, movement models and stock assessments. *Fish Oceanogr* 3:204-216
- Cadrin SX (2000) Advances in morphometric identification of fishery stocks. *Rev Fish Biol Fish* 10:91-112
- Capurro LR, Reid JL (1972) Contributions on the Physical Oceanography of the Gulf of Mexico, Vol 2. Texas A&M University Oceanographic Studies, Gulf Publishing Company, Houston, Texas
- Carey FG, Lawson KD (1973) Temperature regulation in free-swimming bluefin tuna. *Comp Biochem Physiol A* 44:375-392
- Catalán IA, Tejedor A, Alemany F, Reglero P (2011) Trophic ecology of Atlantic bluefin tuna *Thunnus thynnus* larvae. *J Fish Biol* 78:1545-1560
- Cayré P, Farrugio H Biologie de la reproduction du listao (*Katsuwonus pelamis*) de l'océan Atlantique. Proc ICCAT Intl Skipjack Yr Prog
- Center for Biological Diversity (2010) Petition to list the Atlantic bluefin tuna (*Thunnus thynnus*) as Endangered under the United States Endangered Species Act. www.nmfs.noaa.gov/pr/pdfs/species/cbd_bluefintunapetition_5242010.pdf
- Chur V (1973) Some biological characteristics of little tuna (*Euthynnus alletteratus*, Rafinesque, 1810) in the eastern part of the tropical Atlantic. *Coll Vol Sci Pap, ICCAT* 1:489-500
- Collette B, Nauen CE (1983) FAO species catalogue. Vol 2. Scombrids of the world. An annotated and illustrated catalogue of tunas, mackerels, bonitos and related species known to date, Vol 2. FAO Fish Synop, Rome, Italy
- Collette BB (1978) Adaptations and systematics of the mackerels and tunas. In: Sharp GD, Dizon AE (Eds.) *The Physiological Ecology of Tunas*. Academic Press, New York
- Collette BB (1995) Scombridae, atunes, bacoretas, bonitos, caballas, estorninos, melva, etc: Guia FAO para identificación de especies para los fines de la pesca. FAO
- Collette BB (2010) Reproduction and Development in Epipelagic Fishes. In: Cole KS (ed) *Reproduction and sexuality in marine fishes: patterns and processes*. University of California Press, Berkeley
- Collette BB, Potthoff T, Richards WJ, Ueyanagi S, Russo JL, Nishikawa Y (1984) Scombroidei: Development and relationships. In: Moser HG *et al.* (eds) *Ontogeny and Systematics of Fishes*. *Am Soc Ichthyol Herpetol Spec Publ* 1:591-620
- Cooper P (2011) Essential Fish Habitats - Highly Migratory Species - Atlantic Bluefin Tuna In Gulf of Mexico Data Atlas. <https://gulfatlas.noaa.gov/>

- Cornic M, Rooker JR (2018) Influence of oceanographic conditions on the distribution and abundance of blackfin tuna (*Thunnus atlanticus*) larvae in the Gulf of Mexico. Fish Res 201:1-10
- Cornic M, Smith BL, Kitchens LL, Bremer JRA, Rooker JR (2018) Abundance and habitat associations of tuna larvae in the surface water of the Gulf of Mexico. Hydrobiologia 806:29-46
- Dagg MJ, Whitlege TE (1991) Concentrations of copepod nauplii associated with the nutrient-rich plume of the Mississippi River. Cont Shelf Res 11:1409-1423
- Davis TL, Jenkins GP, Young JW (1990) Diel patterns of vertical distribution in larvae of southern bluefin, *Thunnus maccoyii*, and other tuna in the East Indian Ocean. Mar Ecol Prog Ser:63-74
- De Vries DA, Grimes CB, Lang KL, White BDW (1990) Age and growth of king and Spanish mackerel larvae and juveniles from the Gulf of Mexico and U.S. South Atlantic Bight. Environ Biol Fish 29:135-143
- Dietrich DE, Lin CA (1994) Numerical studies of eddy shedding in the Gulf of Mexico. J Geophys Res (Oceans) 99:7599-7615
- Dinnel S, Bratkovich A (1993) Water discharge, nitrate concentration and nitrate flux in the lower Mississippi River. J Mar Syst 4:315-326
- Domingues R, Goni G, Bringas F, Muhling B, Lindo-Atichati D, Walter J (2016) Variability of preferred environmental conditions for Atlantic bluefin tuna (*Thunnus thynnus*) larvae in the Gulf of Mexico during 1993–2011. Fish Oceanogr 25:320-336
- Eilers PH, Marx BD (1996) Flexible smoothing with B-splines and penalties. Stat Sci 11:89-102
- Eilers PH, Marx BD, Durbán M (2015) Twenty years of P-splines. SORT 39:149-186
- Elliott BA (1982) Anticyclonic rings in the Gulf of Mexico. J Phys Oceanogr 12:1292-1309
- Erdman DS (1977) Spawning patterns of fish from the northeastern Caribbean. FAO Fish Rep 200
- Eschmeyer W, Fricke R, van der Laan R (2018) Catalog of Fishes: Genera, Species, References
- Eschmeyer WN, Fricke R, van der Laan R (2016) Catalog of Fishes: Genera, Species, References.

- Espinosa-Fuentes M, Flores-Coto C (2004) Cross-shelf and vertical structure of ichthyoplankton assemblages in continental shelf waters of the Southern Gulf of Mexico. *Estuar Coast Shelf Sci* 59:333-352
- Frade F (1931) Données biométriques sur trois espèces de Thon de l'Atlantique orientale. *Rapp Comm Int Mer Medit* 1:117-120
- Froese R (2006) Cube law, condition factor and weight–length relationships: history, meta-analysis and recommendations. *J Appl Ichthyol* 22:241-253
- Grimes CB, Finucane JH (1991) Spatial distribution and abundance of larval and juvenile fish, chlorophyll and macrozooplankton around the Mississippi River discharge plume, and the role of the plume in fish recruitment. *Mar Ecol Prog Ser* 75:109-119
- Grimes CB, Kingsford MJ (1996) How do riverine plumes of different sizes influence fish larvae: do they enhance recruitment? *Mar Freshw Res* 47:191-208
- Gunn J, Block B (2001) Advances in acoustic, archival, and satellite tagging of tunas. *Fish Physiol* 19:167-224
- Habtes S, Muller-Karger FE, Roffer MA, Lamkin JT, Muhling BA (2014) A comparison of sampling methods for larvae of medium and large epipelagic fish species during spring SEAMAP ichthyoplankton surveys in the Gulf of Mexico. *Limnol Oceanogr-Meth* 12:86-101
- Hajjej G, Hattour A, Hajjej A, Allaya H, Jarboui A, Bouain A (2011) Biometry, length-length and length-weight relationships of little tuna *Euthynnus alletteratus* in the Tunisian waters. *J Fish Aquat Sci* 6:256
- Hajjej G, Hattour A, Hajjej A, Allaya H, Jarboui O, Bouain A (2013) Morphological variation of little tuna *Euthynnus alletteratus* in Tunisian waters and Eastern Atlantic. *Pan-Am J Aquat Sci* 8:1-9
- Hammond DL, Cupka DM (1975) *A Sportsman's Field Guide to the Billfishes, Mackerels, Little Tunas and Tunas of South Carolina*. SC Wildlife and Marine Resources Department, Marine Resources Division, Office of Conservation and Management, Recreational Fisheries Section
- Hare JA, Hoss DE, Powell AB, Konieczna M, Peters DS, Cummings SR, Robbins R (2001) Larval distribution and abundance of the family Scombridae and Scombrolabracidae in the vicinity of Puerto Rico and the Virgin Islands. *Bull Sea Fish Inst* 2:13-29
- Higgins BE (1970) Juvenile tunas collected by midwater trawling in Hawaiian waters, July-September 1967. *Trans Am Fish Soc* 99:60-69

- Hilborn R (1991) Modeling the stability of fish schools: exchange of individual fish between schools of skipjack tuna (*Katsuwonus pelamis*). Can J Fish Aquat Sci 48:1081-1091
- Hopkins TL (1982) The vertical distribution of zooplankton in the eastern Gulf of Mexico. Deep-Sea Res Part A Oceanogr Res Pap 29:1069-1083
- Ibañez AL, Cowx IG, O'higgins P (2007) Geometric morphometric analysis of fish scales for identifying genera, species, and local populations within the Mugilidae. Can J Fish Aquat Sci 64:1091-1100
- ICCAT (2016a) ICCAT Manual. International Commission for the Conservation of Atlantic Tuna. In: ICCAT Publications. Accessed July. <http://www.iccat.int/en/ICCATManual.asp>
- ICCAT (2016b) Report of the Standing Committee on Research and Statistics (SCRS).1-426
- IUCN (2018) International Union for Conservation of Nature.
- Johnson GD (1986) Scombroid phylogeny: an alternative hypothesis. Bull Mar Sci 39:1-41
- Johnston M, RJ M, Easson C, deRada S, Penta B, Sutton TT (submitted) Characterizing Pelagic Habitats in the Gulf of Mexico Using Model, Empirical, and Remotely-Sensed Data. Journal of Marine Systems
- Juan-Jordá MJ, Mosqueira I, Cooper AB, Freire J, Dulvy NK (2011) Global population trajectories of tunas and their relatives. Proc Natl Acad Sci USA 108:20650-20655
- Juarez M, Frías P Distribución de las larvas de bonito (*Kasuwonus pelamis*) y falsa albacora (*Thunnus atlanticus*)(Pisces: Scombridae) en la zona económica de Cuba. Actas de la Conferencia ICCAT sobre el Programa del Año Internacional del Listado
- Karakulak F, Oray I, Addis P, Yildiz T, Uzer U (2016) Morphometric differentiation between two juvenile tuna species [*Thunnus thynnus* (Linnaeus, 1758) and *Euthynnus alletteratus* (Rafinesque, 1810)] from the Eastern Mediterranean Sea. J Appl Ichthyol 32:516-522
- Kashkin NI, Parin NV (1983) Quantitative assessment of micronektonic fishes by nonclosing gear (a review). Biol Oceanogr 2:263-287
- Klawe WL (1963) Observations on the spawning of four species on tuna (*Neothunnus macropterus*, *Katsuwonus pelamis*, *Auxis thazard* and *Euthynnus lineatus*) in the Eastern Pacific Ocean, based on the distribution of their larvae and juveniles. Inter-Am Trop Tuna Comm Bull 6:447-540
- Le Fevre J (1986) Aspects of the biology of frontal systems. Adv Mar Biol 23:163-299

- Lehodey P, Hampton J, Brill R, Nicol S, Senina I, Calmettes B, Pörtner H-O, Bopp L, Ilyina R, Bell J (2011) Chapter 8: Vulnerability of oceanic fisheries in the tropical Pacific to climate change. Vulnerability of tropical Pacific fisheries and aquaculture to climate change. Secretariat of the Pacific Community, Noumea, New Caledonia
- Lindo-Atichati D, Bringas F, Goni G, Muhling B, Muller-Karger FE, Habtes S (2012) Varying mesoscale structures influence larval fish distribution in the northern Gulf of Mexico. *Mar Ecol Prog Ser* 463:245-257
- Llopiz JK, Richardson DE, Shiroza A, Smith SL, Cowen RK (2010) Distinctions in the diets and distributions of larval tunas and the important role of appendicularians. *Limnol Oceanogr* 55:983-996
- Lutcavage ME, Brill RW, Skomal GB, Chase BC, Howey PW (1999) Results of pop-up satellite tagging of spawning size class fish in the Gulf of Maine: do North Atlantic bluefin tuna spawn in the mid-Atlantic? *Can J Fish Aquat Sci* 56:173-177
- MacLennan DN (1992) Fishing gear selectivity: an overview. *Fish Res* 13:201-204
- Majkowski J (2007) Global fishery resource of tuna and tuna-like species. FAO Fish Tech Pap 54 FAO Rome, (No 483)
- Marcek BJ, Fabrizio MC, Graves JE (2016) Short-term habitat use of juvenile Atlantic bluefin tuna. *Mar Coast Fish* 8:395-403
- Matsumoto WM (1959) Descriptions of *Euthynnus* and *Auxis* larvae from the Pacific and Atlantic Oceans and adjacent seas. *Fish Bull*, Book 50. Copenhagen: Carlsberg Foundation
- Matsumoto WM, Ahlstrom EH, Jones S, Klawe W, Richards W, Ueyanagi S (1971) On the clarification of larval tuna identification. *Fish Bull* 70:1-12
- Matsuura Y, Sato G (1981) Distribution and abundance of scombrid larvae in southern Brazilian waters. *Bull Mar Sci* 31:824-832
- Matthews FD, Damaker DM, Knapp LW, Collette B (1977) Food of western North Atlantic tunas (*Thunnus*) and lancetfishes (*Alepisaurus*). Department of Commerce, National Oceanic and Atmospheric Administration, National Marine Fisheries Service
- McEachran JD, Fechhelm JD (1998) Fishes of the Gulf of Mexico, Vol. 1: Myxiniiformes to Gasterosteiformes. University of Texas Press, Austin, Texas
- Millar RB (1992) Estimating the size-selectivity of fishing gear by conditioning on the total catch. *J Am Stat Assoc* 87:962-968

- Milligan R (unpub. data) Classifying the Gulf of Mexico stations using CTD & MOCNESS sensor data (MS6, MS7, MS8, & DP01-DP04).
- Miya M, Friedman M, Satoh TP, Takeshima H, Sado T, Iwasaki W, Yamanoue Y, Nakatani M, Mabuchi K, Inoue JG (2013) Evolutionary origin of the Scombridae (tunas and mackerels): members of a paleogene adaptive radiation with 14 other pelagic fish families. *PLoS One* 8:e73535
- Miyashita S, Sawada Y, Okada T, Murata O, Kumai H (2001) Morphological development and growth of laboratory-reared larval and juvenile *Thunnus thynnus* (Pisces: Scombridae). *Fish Bull* 99:601-617
- Miyashita S, Tanaka Y, Sawada Y, Murata O, Hattori N, Takii K, Mukai Y, Kumai H (2000) Embryonic development and effects of water temperature on hatching of the bluefin tuna, *Thunnus thynnus*. *Aquaculture Science* 48:199-207
- Molinari RL (1980) Current variability and its relation to sea-surface topography in the Caribbean Sea and Gulf of Mexico. *Mar Geod* 3:409-436
- Morote E, Olivar MP, Pankhurst PM, Villate F, Uriarte I (2008) Trophic ecology of bullet tuna *Auxis rochei* larvae and ontogeny of feeding-related organs. *Mar Ecol Prog Ser* 353:243-254
- Muhling BA, Lamkin JT, Alemany F, García A, Farley J, Ingram GW, Berastegui DA, Reglero P, Carrion RL (2017) Reproduction and larval biology in tunas, and the importance of restricted area spawning grounds. *Rev Fish Biol Fish* 27:697-732
- Muhling BA, Lamkin JT, Roffer MA (2010) Predicting the occurrence of Atlantic bluefin tuna (*Thunnus thynnus*) larvae in the northern Gulf of Mexico: building a classification model from archival data. *Fish Oceanogr* 19:526-539
- Muhling BA, Reglero P, Ciannelli L, Alvarez-Berastegui D, Alemany F, Lamkin JT, Roffer MA (2013) Comparison between environmental characteristics of larval bluefin tuna *Thunnus thynnus* habitat in the Gulf of Mexico and western Mediterranean Sea. *Mar Ecol Prog Ser* 486:257-276
- Nakata H, Kimura S, Okazaki Y, Kasai A (2000) Implications of meso-scale eddies caused by frontal disturbances of the Kuroshio Current for anchovy recruitment. *ICES J Mar Sci* 57:143-152
- Near TJ, Eytan RI, Dornburg A, Kuhn KL, Moore JA, Davis MP, Wainwright PC, Friedman M, Smith WL (2012) Resolution of ray-finned fish phylogeny and timing of diversification. *Proc Natl Acad Sci USA* 109:13698-13703
- Nishikawa Y, Rimmer DW (1987) Identification of larval tunas, billfishes and other scombroid fishes (suborder Scombroidei): an illustrated guide, CSIRO Marine Laboratories

- NMFS (2006) Final Consolidated Atlantic Highly Migratory Species Fisheries Management Plan. National Oceanic and Atmospheric Administration, National Marine Fisheries Service, Office of Sustainable Fisheries, Highly Migratory Species Management Division.1-1600
- Olson DB (1991) Rings in the ocean. *Annu Rev Earth Planet Sci* 19:283
- Olson DB, Backus RH (1985) The concentrating of organisms at fronts: a cold-water fish and a warm-core Gulf Stream ring. *J Mar Res* 43:113-137
- Orrell TM, Collette BB, Johnson GD (2006) Molecular data support separate scombroid and xiphioid clades. *Bull Mar Sci* 79:505-519
- Pante E, Simon-Bouhet B (2013) marmap: a package for importing, plotting and analyzing bathymetric and topographic data in R. *PLoS ONE* 8:e73051
- Pauly D (1993) Fishbyte section. Editorial *Naga ICLARM Quart* 16:26
- Peterson WT, Ausubel SJ (1984) Diets and selective feeding by larvae of Atlantic mackerel *Scomber scombrus* on zooplankton. *Mar Ecol Prog Ser* 17:65-75
- Petrakis G, Stergiou K (1995) Weight-length relationships for 33 fish species in Greek waters. *Fish Res* 21:465-469
- Polovina JJ, Abecassis M, Howell EA, Woodworth P (2009) Increases in the relative abundance of mid-trophic level fishes concurrent with declines in apex predators in the subtropical North Pacific, 1996-2006. *Fish Bull* 107:523-531
- Puncher GN, Alemany F, Arrizabalaga H, Cariani A, Tinti F (2015) Misidentification of bluefin tuna larvae: a call for caution and taxonomic reform. *Rev Fish Biol Fish* 25:485-502
- Regan CT (1909) XI. On the anatomy and classification of the Scombroid fishes. *J Nat Hist* 3:66-75
- Reglero P, Urtizberea A, Fiksen Ø, Catalán I, Pérez-Torres A, Alemany F (2009) Size dependent predation in piscivorous larval stages of three tuna species. *ICES CM* 2009
- Richards WJ (1975) Spawning of bluefin tuna (*Thunnus thynnus*) in the Atlantic Ocean and adjacent seas. *ICCAT Coil Vol Sci Paps* 5:267-278
- Richards WJ (2005) Early Stages of Atlantic Fishes: An Identification Guide for the Western Central North Atlantic, Two Volume Set, Vol 2. CRC Press, Boca Raton, FL

- Richards WJ, McGowan MF, Leming T, Lamkin JT, Kelley S (1993) Larval fish assemblages at the Loop Current boundary in the Gulf of Mexico. *Bull Mar Sci* 53:475-537
- Richards WJ, Potthoff T, Kelley S, McGowan MF, Ejsymont L, Power JH, Olvera LRM (1984) Larval distribution and abundance of Engraulidae, Carangidae, Clupeidae, Lutjanidae, Serranidae, Coryphaenidae, Istiophoridae, Xiphiidae and Scombridae in the Gulf of Mexico. *NOAA Tech Mem NMFS SEFC* 144:1-51
- Riley GA (1937) The significance of the Mississippi River drainage for biological conditions in the northern Gulf of Mexico. *J Mar Res* 1:60-74
- Rooker JR, Alvarado Bremer JR, Block BA, Dewar H, De Metrio G, Corriero A, Kraus RT, Prince ED, Rodríguez-Marín E, Secor DH (2007) Life history and stock structure of Atlantic bluefin tuna (*Thunnus thynnus*). *Rev Fish Sci* 15:265-310
- Rooker JR, Kitchens LL, Dance MA, Wells RD, Falterman B, Cornic M (2013) Spatial, temporal, and habitat-related variation in abundance of pelagic fishes in the Gulf of Mexico: Potential implications of the Deepwater Horizon Oil Spill. *PloS one* 8:e76080
- Rudomiotkina G (1984) New data on reproduction of *Auxis* spp. In the Gulf of Guinea. *Collect Vol Sci Pap ICCAT* 20:465-468
- Rudomiotkina G (1986) Data on reproduction of Atlantic black skipjack in the tropical West African water. *Collect Vol Sci Pap ICCAT* 25:258-261
- Schneider JC, Laarman PW, Howard Gowing JC, Laarman P, Schneider JC, Laarman PW, Gowing H (2000) Chapter 17: Length-weight relationships. In: Schneider JC (ed) *Manual of fisheries survey methods II: with periodic updates*, Book Fisheries Special Report 25. Michigan Department of Natural Resources, Ann Arbor
- Schulze-Haugen M, Corey T, Kohler NE (2003) *Guide to sharks, tunas and billfishes of the US Atlantic & Gulf of Mexico*. Rhode Island Sea Grant, University of Rhode Island, Narragansett, Rhode Island
- Scott EL, Prince ED, Goodyear CD History of the cooperative game fish tagging program in the Atlantic Ocean, Gulf of Mexico, and Caribbean Sea, 1954–1987. *Am Fish Soc Symp*
- Strasburg DW (1960) Estimates of larval tuna abundance in the central Pacific. *Fish Bull* 60:231-255
- Takashi T, Kohno H, Sakamoto W, Miyashita S, Murata O, Sawada Y (2006) Diel and ontogenetic body density change in Pacific bluefin tuna, *Thunnus orientalis* (Temminck and Schlegel), larvae. *Aquac Res* 37:1172-1179

- Tanabe T (2001) Feeding habits of skipjack tuna *Katsuwonus pelamis* and other tuna *Thunnus* spp. juveniles in the tropical western Pacific. *Fish Sci* 67:563-570
- Teo SL, Block BA (2010) Comparative influence of ocean conditions on yellowfin and Atlantic bluefin tuna catch from longlines in the Gulf of Mexico. *PLoS One* 5:e10756
- Teo SL, Boustany AM, Block BA (2007) Oceanographic preferences of Atlantic bluefin tuna, *Thunnus thynnus*, on their Gulf of Mexico breeding grounds. *Mar Biol* 152:1105-1119
- Tičina V, Grubišić L, Šegvić Bubić T, Katavić I (2011) Biometric characteristics of small Atlantic bluefin tuna (*Thunnus thynnus*, Linnaeus, 1758) of Mediterranean Sea origin. *J Appl Ichthyol* 27:971-976
- Turner RE, Rabalais NN (1991) Changes in Mississippi River water quality this century. *BioScience* 41:140-147
- Van der Leeden F (1990) *The water encyclopedia*. CRC Press, Chelsea, Michigan
- Vilela M, Castello J (1993) Dinámica poblacional del barrilete (*Katsuwonus pelamis*) explotado en la región sudeste-sur del Brasil en el período 1980-1986. *Frente Marit* 14:111-124
- Vukovich FM, Crissman BW, Bushnell M, King WJ (1979) Some aspects of the oceanography of the Gulf of Mexico using satellite and *in situ* data. *J Geophys Res (Oceans)* 84:7749-7768
- Vukovich FM, Maul GA (1985) Cyclonic eddies in the eastern Gulf of Mexico. *J Phys Oceanogr* 15:105-117
- Wade CB, Bravo P (1951) Larvae of tuna and tuna-like fishes from Philippine waters. *Fish Bull* 51:455-485
- Wainwright PC, Richard BA (1995) Predicting patterns of prey use from morphology of fishes. *Environ Biol Fish* 44:97-113
- Ward RD, Hanner R, Hebert PD (2009) The campaign to DNA barcode all fishes, FISH-BOL. *J Fish Biol* 74:329-356
- Wiebe P, Morton A, Bradley A, Backus R, Craddock J, Barber V, Cowles T, Flierl Gd (1985) New development in the MOCNESS, an apparatus for sampling zooplankton and micronekton. *Mar Biol* 87:313-323
- Willis TJ, Millar RB, Babcock RC (2000) Detection of spatial variability in relative density of fishes: comparison of visual census, angling, and baited underwater video. *Mar Ecol Prog Ser*:249-260

- Wilson S, Lutcavage M, Brill R, Genovese M, Cooper A, Everly A (2005) Movements of bluefin tuna (*Thunnus thynnus*) in the northwestern Atlantic Ocean recorded by pop-up satellite archival tags. *Mar Biol* 146:409-423
- Yagishita N, Miya M, Yamanoue Y, Shirai SM, Nakayama K, Suzuki N, Satoh TP, Mabuchi K, Nishida M, Nakabo T (2009) Mitogenomic evaluation of the unique facial nerve pattern as a phylogenetic marker within the perciform fishes (Teleostei: Percomorpha). *Mol Phylogenet Evol* 53:258-266
- Young JW, Davis TL (1990) Feeding ecology of larvae of southern bluefin, albacore and skipjack tunas (Pisces: Scombridae) in the eastern Indian Ocean. *Mar Ecol Prog Ser*:17-29
- Zuur AF, Ieno EN, Elphick CS (2010) A protocol for data exploration to avoid common statistical problems. *Methods Ecol Evol* 1:3-14
- Zuur AFI, Elena N; Walker, Neil J; Saveliev, Anatoly A; Smith, Graham M (2009) *Mixed effects models and Extensions in Ecology with R*. Springer